Effect of Voltage Pulsation Generated by Solargizer® on Charging/Discharging Processes of Lead/Acid Batteries

Also referred to as "The Mailnski Report"

Report prepared for
Pulse Tech Products Corporation
by
Professor Tadeusz Malinski Ph.D.
Department of Chemistry
Oakland University
Rochester, MI 48309-4477

INTRODUCTION

The main objective of this project was to perform electrochemical studies on the influence of voltage pulsation generated by Solargizer (pulse generator) on the charging/discharging processes of lead/acid batteries. For the evaluation of electrochemical properties we distinguished between the following:

1. Cells and batteries as complete technical units.
2. Active masses and plates as components.

The approach to the evaluation of these two groups is generally different, even though in both cases measurements of the influence of external parameters on similar electrochemical properties are made. The reasons for the failure of a battery in the field depend on the type of load and maintenance. Batteries that have been tested in the laboratory following special controlled methods show a smaller spectrum of failure modes than the batteries in the field. In the following report only failures caused by active components (plates consisting of the active mass and the grid or mass carrier) are discussed. Other reasons such as mechanical destruction or maintenance failure are not considered.

The most frequent reasons for failure are the following:

1. Sludging of the positive mass.
2. Destruction of the positive grid.

3. Defects in the negative mass.

4. Combination of these causes.

In order to limit the variables in the basic studies of positive mass (PbO_2) we prepared standard lead oxide electrodes. These electrodes have been made to have a reproducible surface area, dimension, weight, and composition. These electrodes were prepared according to procedure described in the experimental portion of the report. The process of the preparation of electrodes was crucial in obtaining reproducible results. These electrodes were used in the initial phase of the project to obtain basic data concerning the role of Solargizer in the charging/discharging process. In the second phase of the project, commercially available lead-acid batteries of different capacity (15-60 Ah) were used. In these studies a large number of batteries were studied in order to acquire statistically significant data. Electrodes were studied using several electrochemical, optical and x-ray spectroscopy methods which include galvanostatic charge/discharge, reflectance spectroscopy imaging, electron scanning microscopy and x-ray diffraction.

The most frequent reason for the failure of lead/acid batteries is deactivation of the positive electrode (lead dioxide, PbO_2 electrode). Therefore, the electrochemical and morphological characterization of this electrode was especially extensive. However, the studies of negative (lead, Pb electrode) were also performed.

A kinetics of lead-acid battery reactions

The charged lead-acid battery uses metallic lead (Pb) as the negative electrode and lead dioxide (PbO_2) as the positive electrode. The positive electrode contains two different crystallographic structures: α - PbO_2 (orthorombotic) and β - PbO_2 (tetragonal). The α form is larger, less active electrochemically, has more compact crystals and promotes a longer cycle life of the battery. Neither of the two forms is fully stoichiometric (their compositions can be presented by PbO_x with x varying between 1.85 and 2.05). The electrolyte in a lead-acid battery is a sulfuric acid solution, about 1.28 g/cm^3 specific gravity or 37% acid by weight in a fully charged condition.

The fundamental chemical reactions occurring in a lead-acid battery as well as concentration changes during the discharge of the electrodes of a lead-acid storage battery are shown in Figure 1.

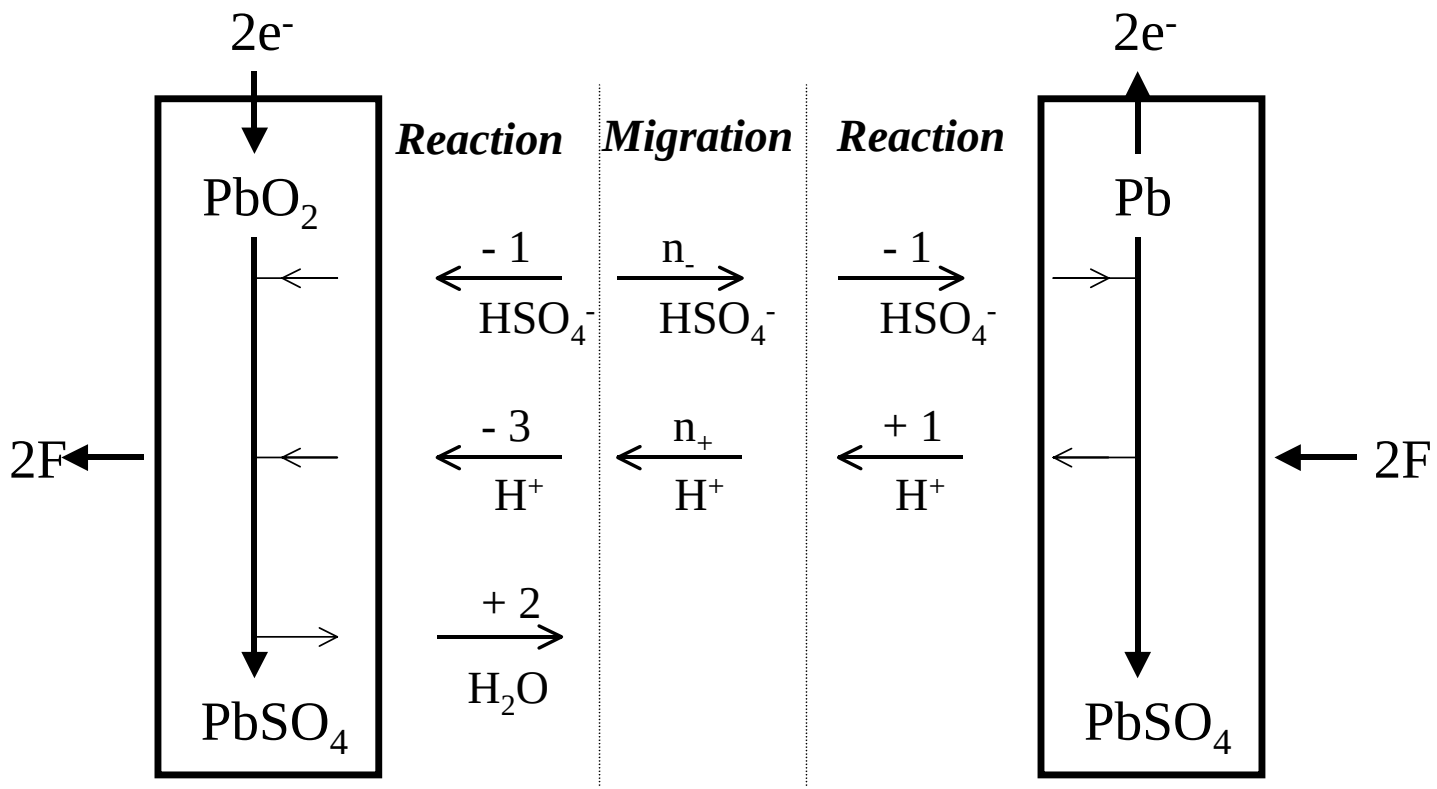

Cathode: $PbO_2 + 3H^+ + HSO_4^- + 2e \rightarrow PbSO_4 + 2H_2O$

Anode: $Pb + HSO_4^- \rightarrow PbSO_4 + H^+ + 2e$

Total: $PbO_2 + Pb + 2H^+ + 2HSO_4^- \rightarrow 2PbSO_4 + 2H_2O$

Figure 1

The overall charge/discharge reactions are as follows:

$$PbO_2 + 3H^+ + HSO_4^- \underset{\text{charge}}{\overset{\text{discharge}}{\rightleftharpoons}} PbSO_4 + 2H_2O \qquad (1)$$

$$Pb + H_2SO_4 \underset{\text{charge}}{\overset{\text{discharge}}{\rightleftharpoons}} PbSO_4 + 2H^+ \qquad (2)$$

As the cell approaches full charge and the majority of the $PbSO_4$ has been converted to Pb (negative electrode) or PbO_2 (positive electrode), the cell voltage on charge becomes greater than the gassing voltage (about 2.39 – 2.40 V per cell) and an overcharge reaction begins, resulting in the production of hydrogen and oxygen (gassing) and the resultant loss of water.

Negative electrode: $2H^+ + 2e \longrightarrow H_2$ (3)

Positive electrode: $H_2O - 2e \longrightarrow \frac{1}{2} O_2 + 2H^+$ (4)

Overall reaction: $H_2O \longrightarrow H_2 + \frac{1}{2} O_2$ (5)

In the sealed lead-acid batteries, this reaction is controlled to prevent hydrogen evolution and the loss of water by catalytic recombination of the evolved oxygen with the negative plate. As the cell is discharged, the voltage decreases due to depletion of material, increasing resistance and polarization.

The reactions that govern the charge/discharge of the active masses in a lead-acid battery constitute in addition to the electrochemical exchange reaction steps, a series of pre- and post- processes that can be measured as "total overvoltage". The formation and dissolution of lead sulfate, determines the electrochemical reactions and in some limited cases decides them. During charge the problems of lead sulfate dissolution include a cathodic limiting current on the negative electrode and the influence by absorbed inhibitors on the speed of the dissolution and disassociation. If the crystals that dissolved are not in proximity to the electrode surface, as for example, in the pores of the electrodes, the transport of Pb^{2+} ions form by migration and diffusion must be considered.

During discharge the formation of lead sulfate crystals from ions is decisive. Problems of nuclei formation can appear. For example in the induction period "critical seed", crystallization overvoltage, super saturated solution and voltage sagging may be observed. Crystal growth depends on the speed of replenishing Pb^{2+} ions by current and by migration and diffusion. The latter also applies to SO_4^{2-} ions. The formation of lead sulfate crystals depends on the concentration of ions in the preservation region. The formation and the disappearance of lead sulfate crystals is influenced by their own crystallization kinetics and by a more or less extended surface coverage of the electrode, which influences the kinetics of the actual electrochemical exchange reaction and changes in the current density. Therefore it is understandable that the elicitation of the kinetics of lead acid battery reaction has not been possible. Therefore, the electrode systems with soluble lead salts and the noble metal electrodes are used for the study of the kinetics of charge/discharge reactions. In these systems only the crystallization problems of PbO_2 and metallic Pb must be considered.

Charging and Discharging Process of Lead-Acid Batteries

Batteries can be recharged at constant current of constant potential (galvanostatic method). Constant current recharging, at one or more current rates, is not widely used for lead-acid batteries for practical reasons. This is because of the need for current adjustment unless the charging current is kept at a low level throughout the charge which will result in long charge times (12 hrs or longer). However, galvanostatic method appears to be superior (better reproducibility) for battery testing under laboratory conditions. In normal industrial application, modified constant-potential charging methods are used. Modified constant-potential

charging is used for on-the-road vehicles and utilities, telephone, and uninterruptible power system applications where the charging circuit is tied to the battery.

The following is a list of constant-potential charging methods, which can be used for battery charging:

1. Constant potential.
2. Modified constant potential with constant initial or/and finish rate.
3. Taper charge
4. Pulse charge
5. Trickle Charging
6. Float charging

Constant potential charging circuit has a current limit, and this value is maintained until a predetermined voltage is reached. Then the voltage is maintained constant until the battery is called on to discharge. The current limit and the constant-voltage value are influenced by the time interval when the battery is at the constant voltage and in a 100% state of charge. For this "float" type operation with the battery always on charge, a low charge current is desirable to minimize overcharge, grid corrosion associated with overcharge, water loss by electrolysis of the electrolyte, and maintenance to replace this water. To achieve a full recharge with a low constant potential, the proper selection of the starting current is required.

The modified constant potential charge with a constant start and finish rate is common for deep cycling batteries, which are typically discharged at the 6-hour rate

to a depth of 80%. The recharge is normally completed in an 8 hour period with the charge set for the constant potential of 2.39 V per cell, and the starting current is limited to 16 - 20 A. The time of charge is selected to ensure a recharge input capacity of a predetermined percent of the ampere-hour output of the previous discharge, normally 110 to 120%, or 10 - 20% overcharge.

Taper charging is a variation of a modified constant potential method using less sophisticated controls to reduce equipment cost. In this method of charging, the taper of voltage and current is such that the 2.39 V per cell is exceeded prior to the critical point of recharge, and cell temperature is increased. The end of the charge is often controlled by a fixed voltage rather than a fixed current. Therefore, when a new battery has a high EMF, this final charge rate is low and the battery often does not receive sufficient charge within the time period allotted to maintain the optimum charge state. Thus, the taper charge does degrade battery life.

In pulse charging, the charge is periodically isolated from the battery terminals and the open-circuit voltage of battery is measured (an impedance free measurement of the battery voltage). If the open-circuit voltage is above a preset value, the charger does not deliver energy. When the open-circuit voltage decays below that limit, the charger delivers a pulse for a fixed time period. When the battery state of charge is very low, charging current is connected almost 100% of the time because the open-circuit voltage is below the preset level or rapidly decays to it. The duration of the open-circuit and charge pulses is chosen so that when the battery is fully charged, the time for the open-circuit voltage to decay is exactly the same as the pulse duration.

When the charger controls sense this condition, the charger is automatically switched over to the finish rate current and shot charging pulses are delivered periodically to the battery to maintain it at full charge. In many applications, high voltage batteries may be used and difficulty can be encountered in keeping the cells in a balanced condition. This is particularly true when the cells have long periods of standby use with different rates of self-decay. In these applications, the batteries are completely discharged and recharged periodically in what is called "an equalizing charge", which brings the whole string of cells back to the complete charge state. The name of this method of charging-pulse charging is somewhat misleading because what we have really is a sampling of the charge (current) of the battery at open circuit and if needed a subsequent recharging at constant potential. Therefore "pulses" applied in this method have very small frequency (about 10^{-4} Hz) and very large amplitude (volts). Therefore, this method has no resemblance to the method of charging/discharging described in this report where high frequency ($10^3 – 10^4$ Hz), low amplitude (milivolts) pulses generated by Solargizer are superimposed on the constant potential (volts) used during the battery charging.

The trickle charging is based on continuous constant-current charge at low (about 1/100) cell capacity which is used to maintain the battery in a full charged condition, recharging it for losses due to self-discharge as well as to restore the energy discharged during intermittent use of the battery. This method is used mainly for small stationary type batteries when the battery is removed from the vehicle or when its regular source of charging is dysfunctional.

Float charging is a low-rate constant-potential charge. This method is mainly used to maintain the battery in a fully charged condition. The stationary batteries (charged from a DC bus) are usually charged by this method. The float voltage for a 1.210 specific gravity nonantimonial grid battery containing an electrolyte and having an open-circuit voltage of 2.059 V per cell at 25°C is 2.17 to 2.25 V per cell.

EXPERIMENTAL

Plates of dimensions 140 x 125 x 2.5 mm or 20 x 10 x 2.5 mm were formed. The paste was prepared by mixing a typical Barton pot with lead oxide, sulfuric acid and water. Barton pot leady oxide contained 21% free lead. Free lead was a core of each fine lead oxide spherical-shaped particle. The proportions of the different components are listed in Table 1. The paste density was 3.7 – 3.8 g/cm^3 and it was applied by hand to positive grid (lead/calcium grid). Plates were cured at 55°C with 100% of relative humidity for 48 hrs. Under these conditions 30 – 35 wt% of $3PbO \cdot PbSO_4 \cdot H_2O$ was formed. Following the curing process, plates were dried at 70°C until the moisture decreased below 0.2 wt%. The cured plates were stored until use. The shelf life of stored plates was not critical, and good reproducibility of measurements was observed even after 6 weeks of storage.

A typical cell used in these studies consisted of one positive plate ($PbO_2/PbSO_4$ electrode), two negative electrodes, and two separators in between (Figure 2). A noble metal (platinum mesh) was used as a negative electrode.

A microporous polyethylene separator with pore size 0.03 μm, backward thickness 0.3 mm, porosity 60% and electrical resistance 1.86 mOhm/cm^2 was used to separate platinum mesh from positive plate.

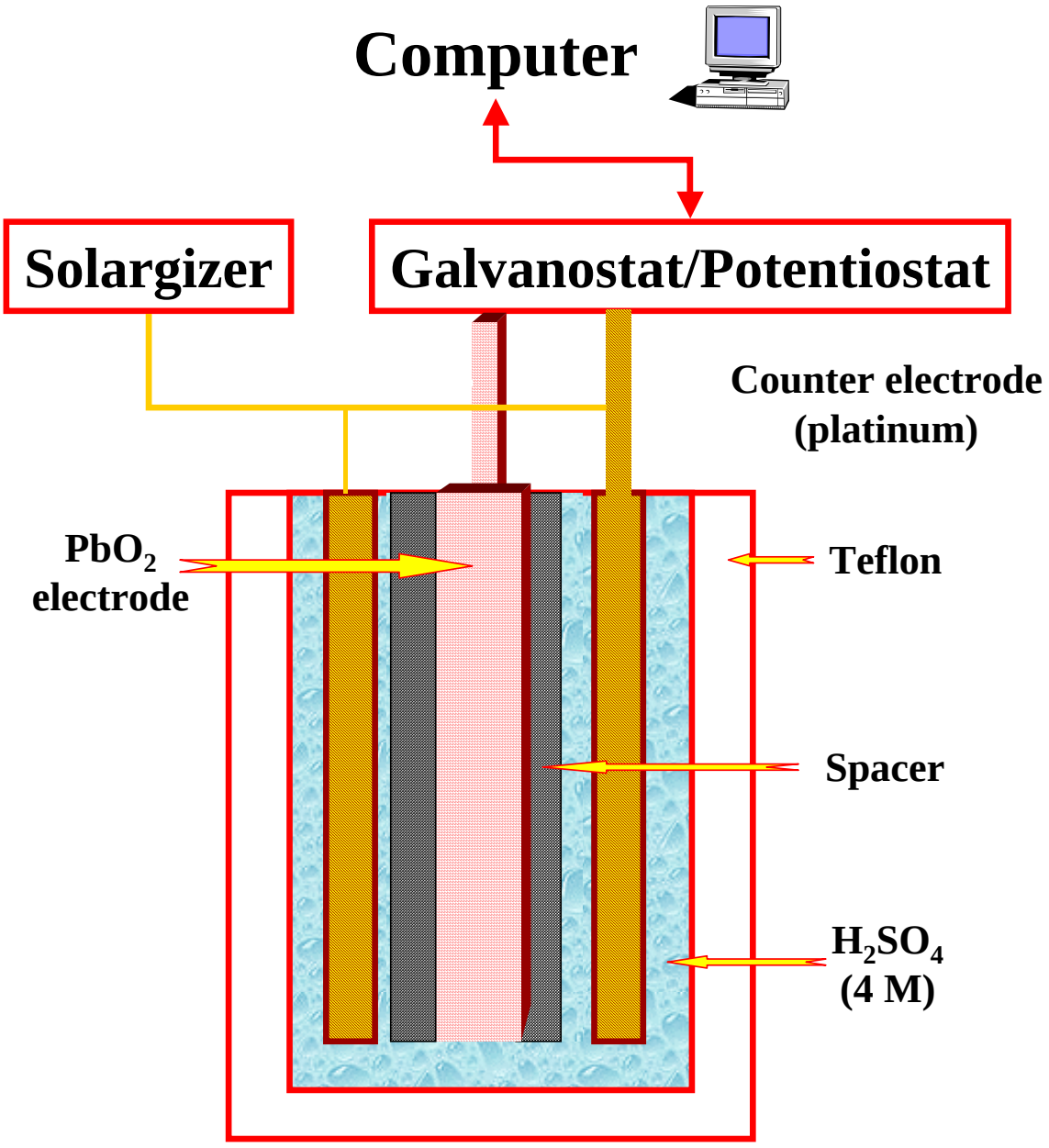
Computer
Solargizer
Galvanostat/Potentiostat
Counter electrode
(platinum)
PbO2
electrode
Teflon
Spacer
H2SO4
(4 M)

Figure 2

An assembly of Pt electrode, positive electrode and separator was placed in a specially designed Teflon electrolytic/galvanic container filled with sulfuric acid solution (d = 1.25 g/cm^3). The plates were allowed to stand in the sulfuric acid solution for 60 min at 25°C. DC current 0.5 or 1.5 A was used to form small and large plates, respectively. The formation process took about 5 – 20 hrs depending on cell size. After formation each cell was kept on open circuit for one hour at 25°C. For galvanostatic, voltammetric or coulometric studies, the Teflon container with cells was placed in a water bath maintained at 25°C. A computerized electrochemical analyzer PAR 283 with standard software was used for most of the electrochemical measurements. Galvanostatic, amperometric, voltammetric or coulometric measurements were performed by using a three-electrode system. The three electrode system consisted of PbO_2 (positive electrode), platinum mesh counter (negative electrode) and cadmium rod (reference electrode). A current flow was measured between the PbO_2 and platinum electrode while potential was measured between the PbO_2 and cadmium electrode. The electrochemical system was controlled by an IBM-compatible computer (Pentium II, 450 MHz) with standard software (PAR 283). In these studies a broad range of current density was used in a charging/discharging process including high-density current which is not normally use in commercial lead acid batteries (due to overheating). The high current was use in the experiments to decrease the time needed for deterioration of the PbO_2 electrode. X-ray diffraction spectra were obtained using Simens-5000 diffraction

spectrometer with a copper X-ray source. A Hitachi scanning Electron Microscope operated in Field Emission Mode was used to record microscopic images. The images of the surface of electrodes (reflected light) were obtained by using a Tracor Northern Spectrograph TN-6050, spectroscopic Leica Stereozoom microscope, and a high resolution digital camera (iMicroVision Electric Eyepiece V.I.S.). The commercially available batteries of different capacity (15 Ah, 20 Ah, 40 Ah, and 60 Ah) were used in these studies. A battery test system model; Series 4000, was used to charge/discharge of the batteries under the set of different experimental conditions. The eight channels were used simultaneously. The system has six operating modes: constant current, constant voltage, constant power, constant resistance, voltage or current. Most of the experiments reported here were performed at constant current mode. After electrochemical testing the electrodes were recorded from batteries and analyzed using x-ray diffraction, surface reflection microscopy and electron scan microscopy. About 180 batteries of different capacity were used in these studies. A statistical significance was achieved by analyzing 7- 12 batteries operating under identical conditions. Data are given as means $\pm$ SEM. In each set of experiments, n=7-12 is the number of measurements. Statistical analysis was performed using one-way ANOVA.

Table 1. Components of paste for positive (lead dioxide) electrode

Lead oxide (kg)	1.0
H_2SO_4 (d = 1.4 g/cm^3) (ml)	98
Water (ml)	156
Paste density g/cm^3	3.8 – 3.9

RESULTS

Effect of pulsation on the charging/discharging process of the lead oxide electrode

The studies of the influence of pulses applied during a charge/discharge of the positive electrode (PbO_2) were done using the instrumental set-up shown in Figure 2. The fundamental data characterizing the influence of pulsation on the electrochemical and structural properties of lead oxide electrode were acquired. In order to limit the number of variables, the reproducible electrodes of the same composition and morphology were prepared for each experiment. The conditions of the experiments were chosen to accelerate a process of changes of the PbO_2 electrode under multiple charge/discharge cycles. Under these specially designed, reproducible laboratory conditions the electrodes were tested to answer a fundamental question: does high frequency low amplitude pulsation have any influence on the electrochemical characteristics and morphology of lead oxide electrodes?

A typical pulse (potential versus time) generated by the Solargizer is shown in Figure 3. The amplitude of the peak is in the 130-150 mV and frequency of pulsation is 10-15 KHz.

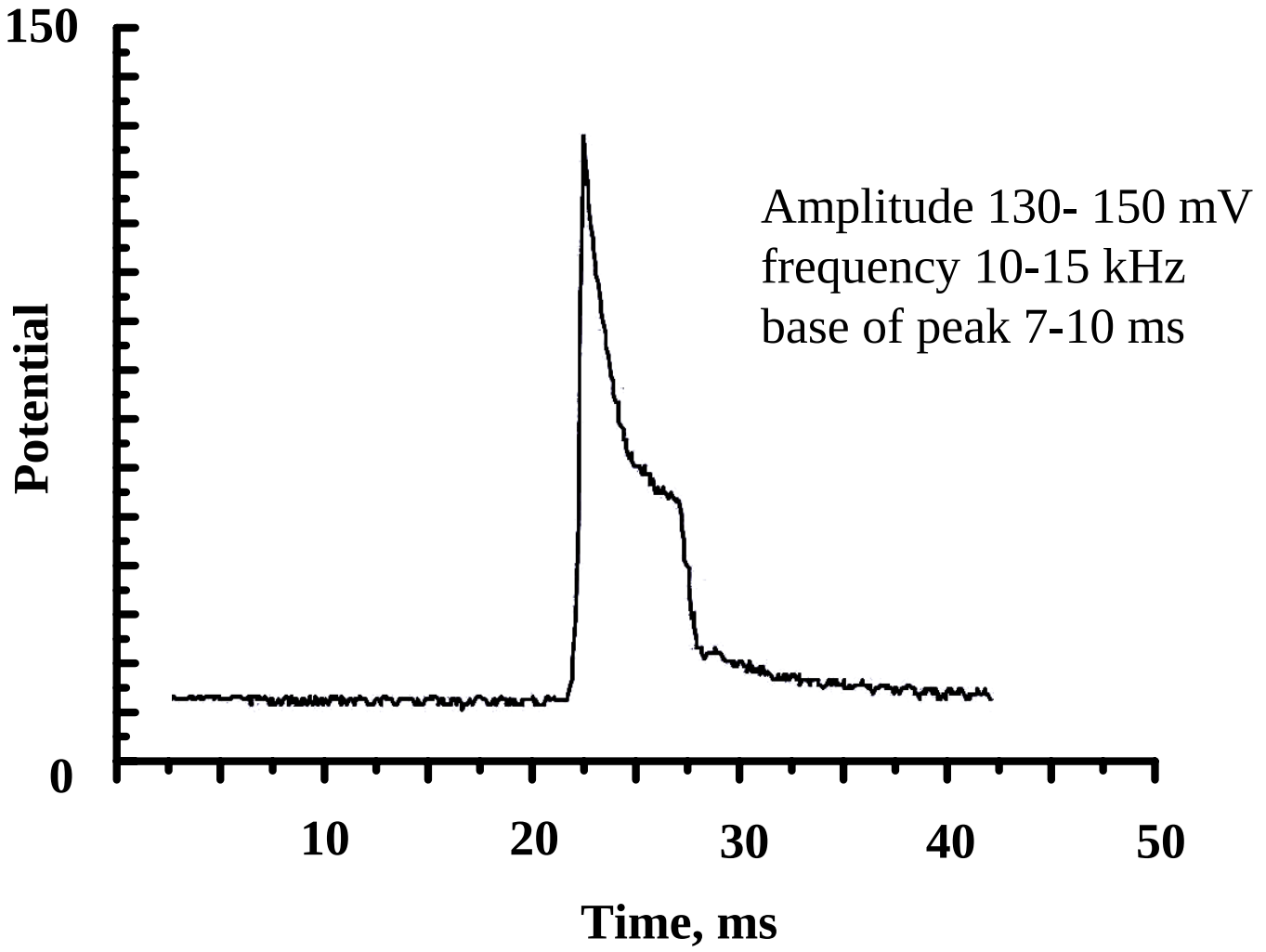
150
Potential
0
10
20
30
40
50
Time, ms
Amplitude 130- 150 mV
frequency 10-15 kHz
base of peak 7-10 ms

Figure 3

The pulses from Solargizer were superimposed on the potential which was used in the charging process of PbO_2 electrode. A typical tracing recorded galvanostatistically (at constant current i = 150 mA/cm^2) during charge/discharge of PbO_2 electrode is shown in Figure 4. At constant current i = 150 mA/cm^2 the electrode was completely charged during 20-22 minutes. During subsequent discharge process at constant current i = 150 mA/cm^2 the potential slightly dropped during the first 10 minutes and after that period a rapid decrease of potential was observed reaching zero after about 40-42 minutes.

The galvanostatic curves obtained for sequential continuous charging and discharging process of the PbO_2 electrode at a constant current density of 150 mA/cm^2 without pulsation during a time period of about seven hours is shown in Figure 5. The single 25th and 50th cycles in this continuous charging/discharging process are shown in Figures 6. The significant changes in the pattern of potential change during discharge process are observed. The potential decreased rapidly after 5 minutes and 1.5 minutes during discharge of 25th and 50th cycles. The first drop of the potential is due to significant decrease of the charge capacity of PbO_2 electrode. A distinctive difference in the change of the shape of the galvanostatic curve was also observed when pulses generated by the Solargizer were applied during the charging/discharging process (Figure 7-9). An initial capacity of the PbO_2 electrode (after electrochemical formation process) was 56±4 C/cm^2. This capacity decreased about 70% (17±4 C/cm^2) after 50 cycles of deep discharge/fast charge (galvanostatic,

150 mA/cm^2) of the electrode without pulses. However, when the electrode was charged/discharged with superimposed pulses from the Solargizer its capacity decreased only to 5±2 (5±2 C/cm^2) after 50 cycles. Figure 10 shows a plot of decrease of the charge capacity of the PbO_2 electrode as a function of the number of charge/discharge cycles. The charge capacity decreases for the PbO_2 electrode with the number of cycles. However, the rate of decrease of the charge capacity is much faster if the electrode is charged/discharged without pulses. The difference of the rate is substantial and statistically significant.

A decay of the charge of the PbO_2 electrode to zero capacity is observed approximately after 100 cycles. However, the PbO_2 electrode charged/discharged with pulses can survive about 300 pulses before reaching zero charge capacity. PbO_2 electrodes also show a different surface morphology after the charge/discharge process with or without pulses (Figure 11-14). A microstructure of the surface of electrodes after 35 and 55 cycles of charge/discharge correlates with charge capacity. The surface of the PbO_2 electrode charged/discharged without pulses showed high irregularity with sharp crystal spikes. Without pulse treatment, the surface of the PbO_2 electrode is rapidly developed showing large dendrites. The surface of

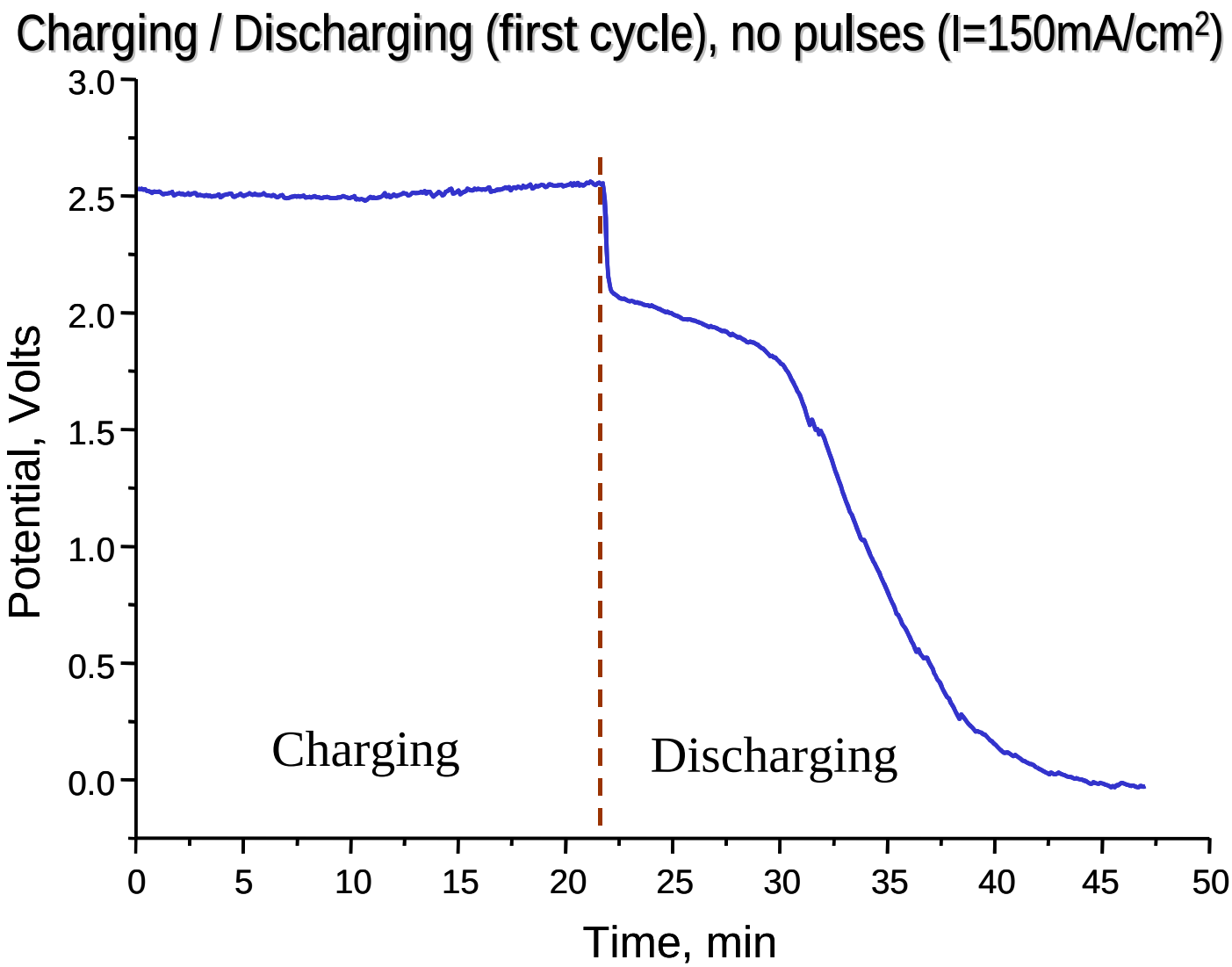
Charging / Discharging (first cycle), no pulses (I=150mA/cm2)
Potential, Volts
3.0
2.5
2.0
1.5
1.0
0.5
0.0
0
5
10
15
20
25
30
35
40
45
50
Time, min
Charging
Discharging

Figure 4

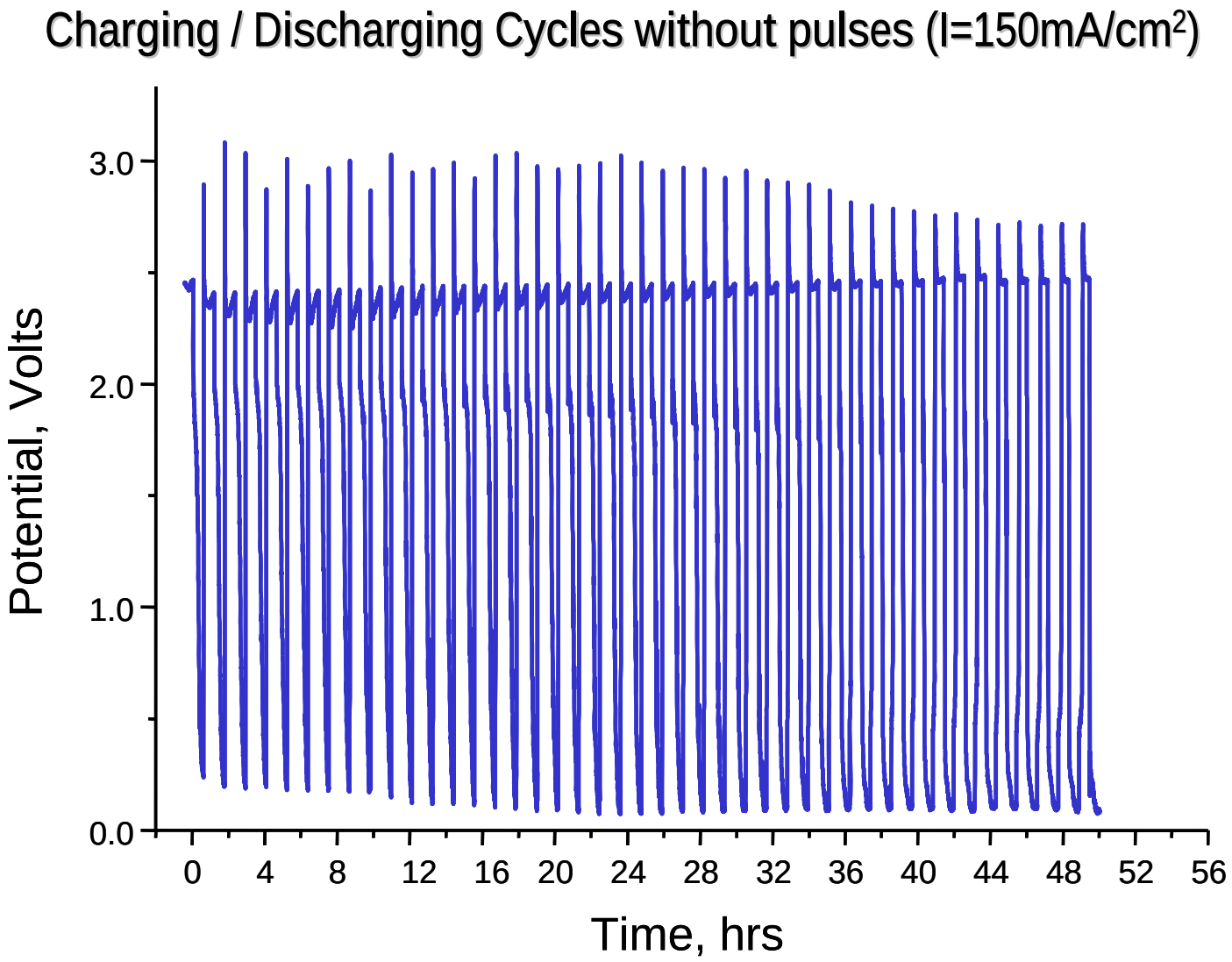
Charging / Discharging Cycles without pulses (I=150mA/cm2)
Potential, Volts
3.0
2.0
1.0
0.0
0
4
8
12
16
20
24
28
32
36
40
44
48
52
56
Time, hrs

Figure 5

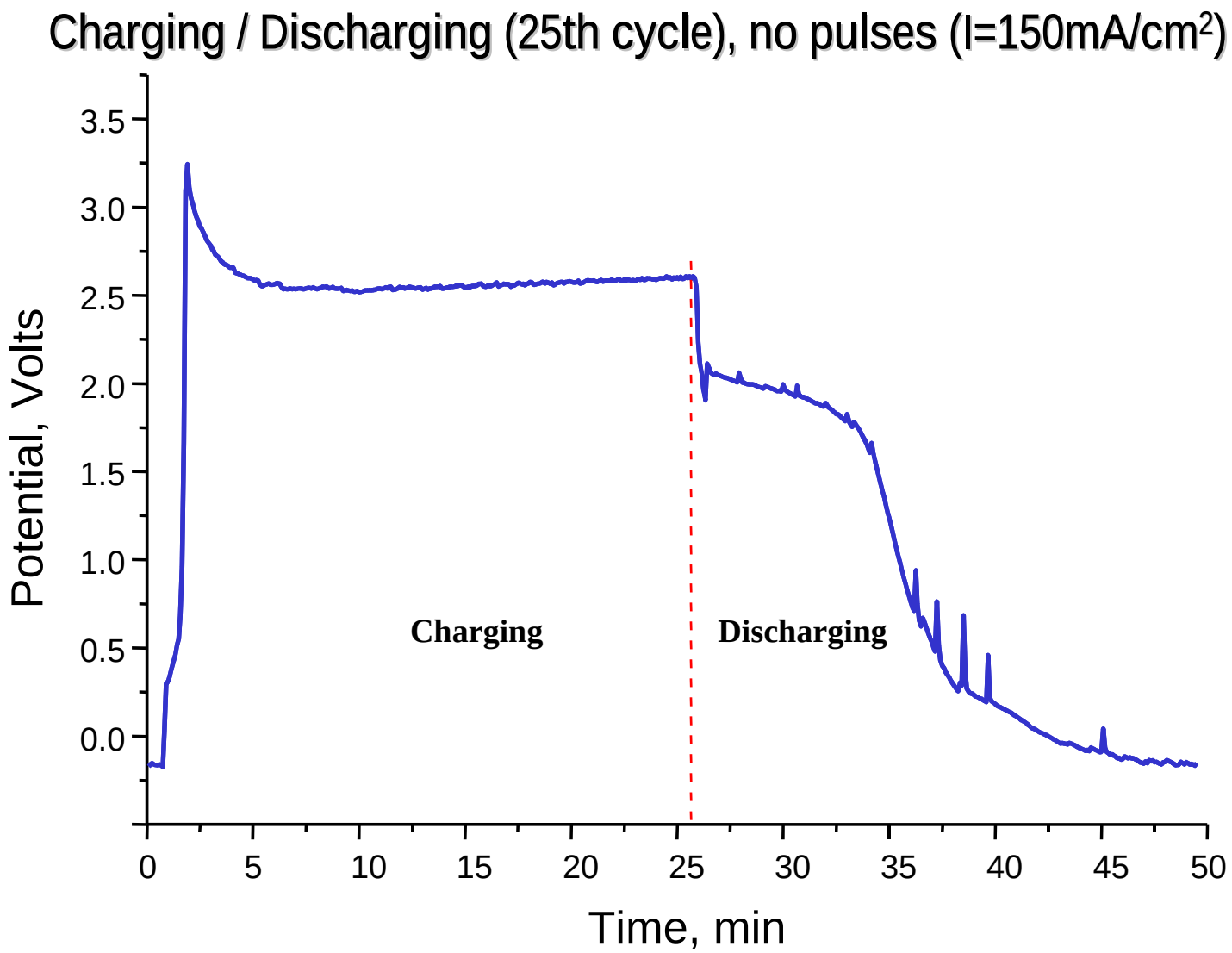
Charging / Discharging (25th cycle), no pulses (I=150mA/cm2)
Potential, Volts
Time, min
Charging
Discharging
3.5
3.0
2.5
2.0
1.5
1.0
0.5
0.0
0
5
10
15
20
25
30
35
40
45
50

Figure 6a

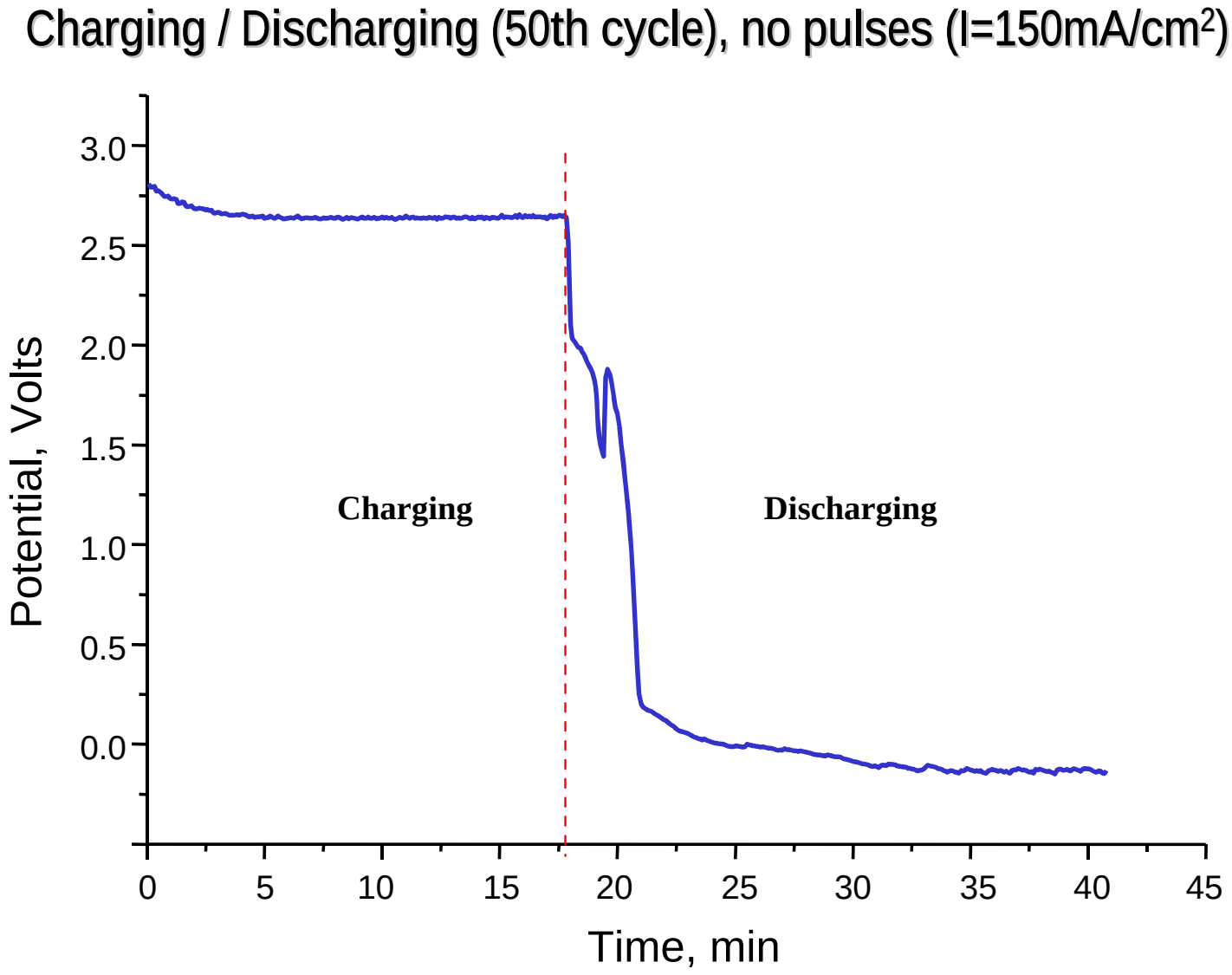
Charging / Discharging (50th cycle), no pulses (I=150mA/cm2)
Potential, Volts
3.0
2.5
2.0
1.5
1.0
0.5
0.0
Charging
Discharging
0
5
10
15
20
25
30
35
40
45
Time, min

Figure 6b

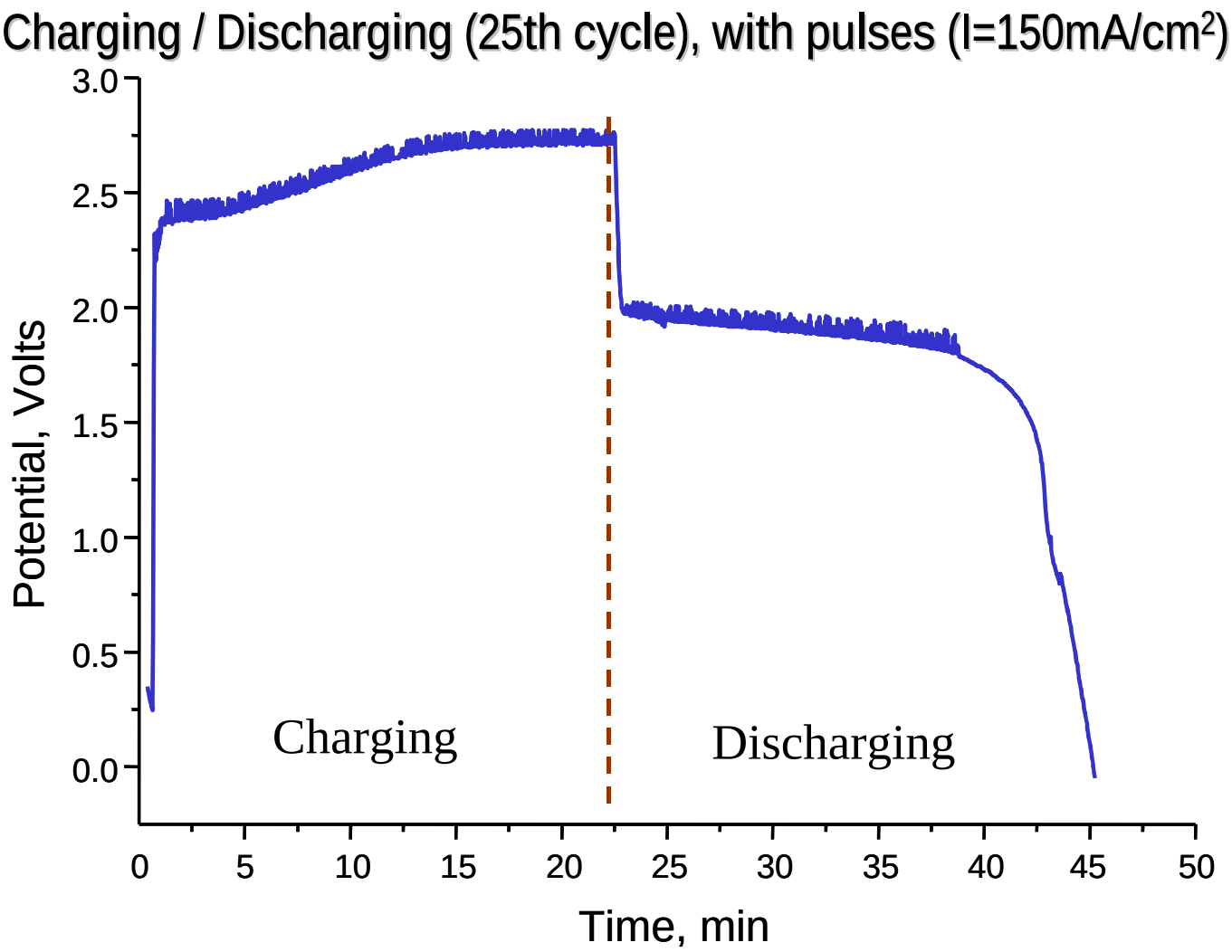
Charging / Discharging (25th cycle), with pulses (I=150mA/cm²)
Potential, Volts
3.0
2.5
2.0
1.5
1.0
0.5
0.0
Charging
Discharging
0
5
10
15
20
25
30
35
40
45
50
Time, min

Figure 7

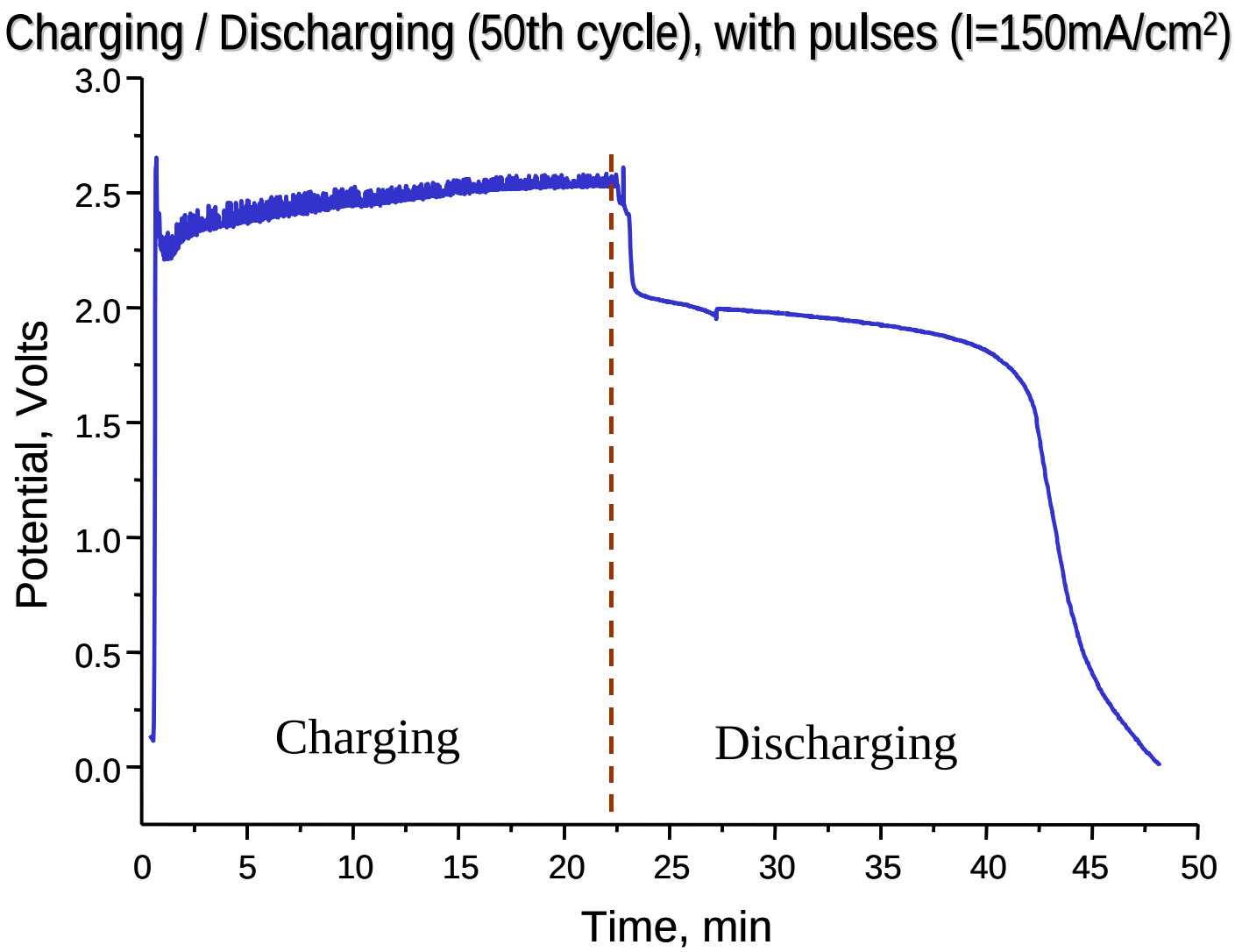
Charging / Discharging (50th cycle), with pulses (I=150mA/cm2)
Potential, Volts
3.0
2.5
2.0
1.5
1.0
0.5
0.0
Charging
Discharging
0
5
10
15
20
25
30
35
40
45
50
Time, min

Figure 8

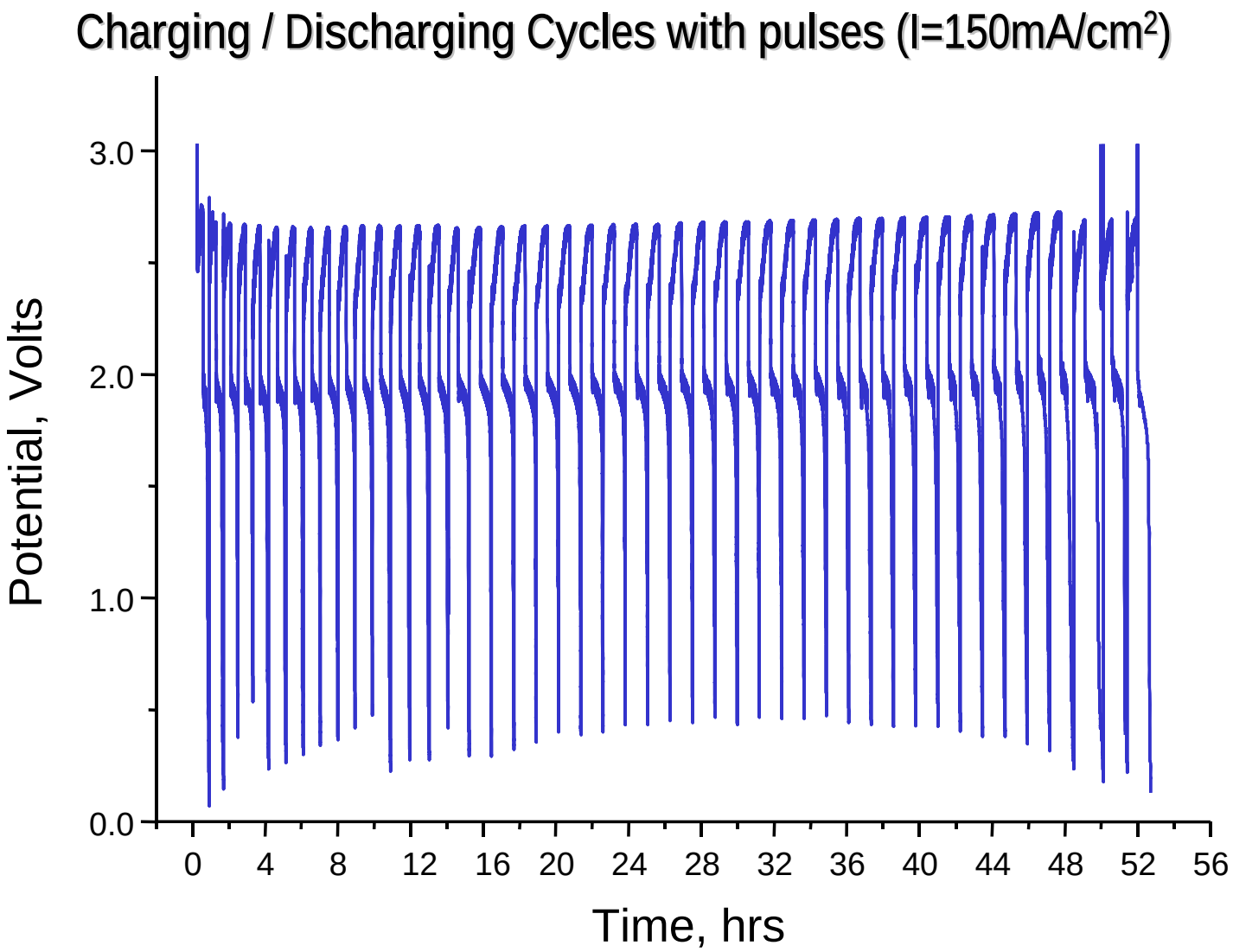
Charging / Discharging Cycles with pulses (I=150mA/cm2)
Potential, Volts
3.0
2.0
1.0
0.0
0
4
8
12
16
20
24
28
32
36
40
44
48
52
56
Time, hrs

Figure 9

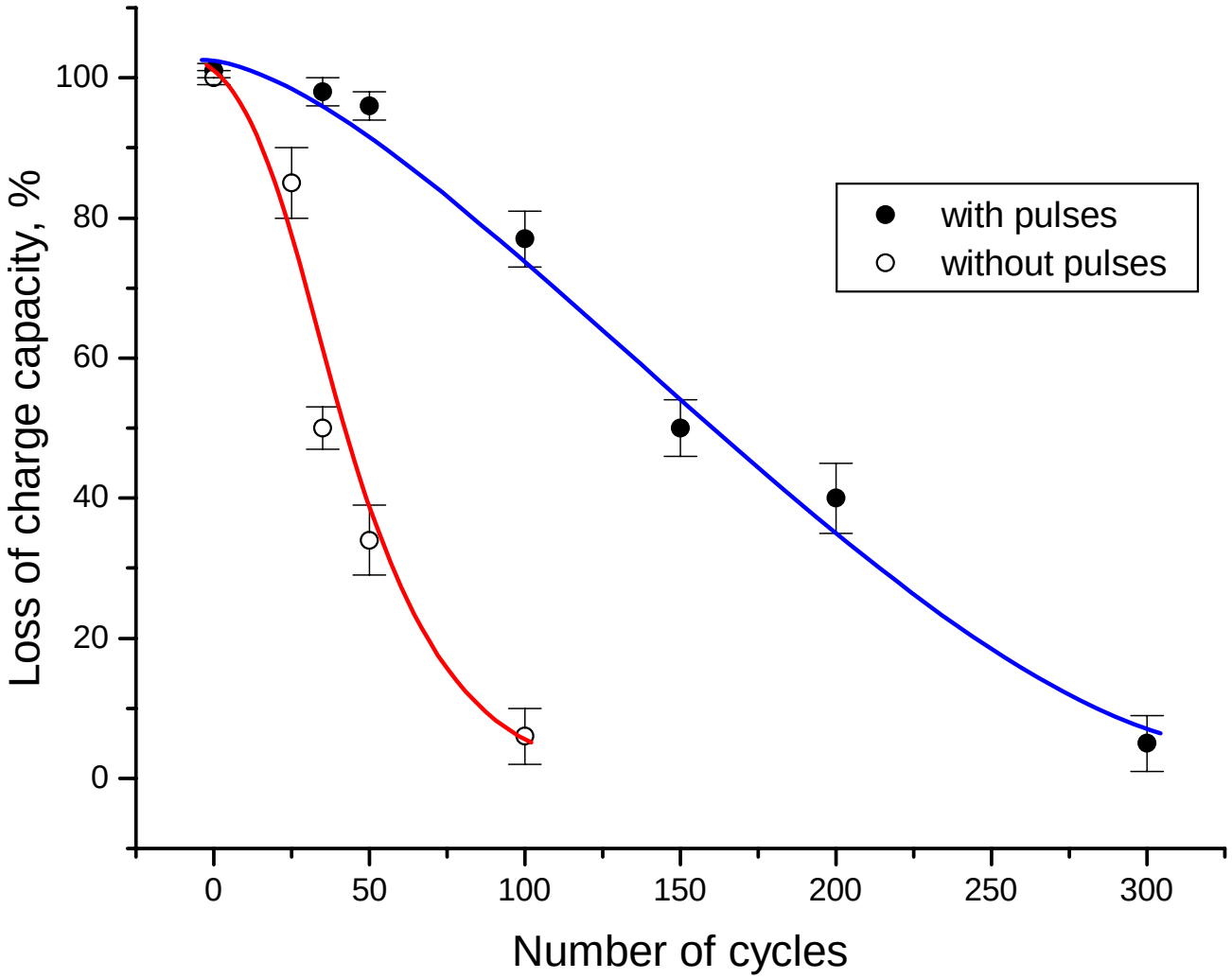
Loss of charge capacity, %
Number of cycles
with pulses
without pulses
0
20
40
60
80
100
0
50
100
150
200
250
300

Figure 10

electrodes treated with pulses during the charge/discharge process is better organized, homogenous and relatively smooth without major irregularities and craters.

The most uniform surface of the PbO_2 electrode was observed after the initial 5-10 cycles of charge/discharge with pulses. This is a strong indication that pulse improves the "formation" of the PbO_2 plates on the beginning of the charge/discharge process.

The surface reflectance microimaging spectra also correlate with data obtained from x-ray diffraction spectroscopy (Figure 15-18). X-ray spectra were recorded after the electrode was charged (last cycle). X-ray diffraction shows a formation of larger crystals during charge/discharge treatment without pulses. Also the number of crystallographic phases (the indicator of a formation of new crystallographic entities – mostly different forms of lead oxides and lead sulfates mixed in different preparations) increases after 50 discharge/charge cycles without pulsation compared to that observed with pulsation. It can be clearly seen that the amount of $PbSO_4$ in the positive electrode not treated with pulses is much higher than in the electrode treated with pulses (Figure 19). The amount of $PbSO_4$ (which cannot be converted to PbO_2) after 50 cycles of charge/discharge is about eight times higher in the electrodes not treated with pulses than in the electrodes treated with pulses. This effect is generally known as "sulfation effect" that contributes to the

PbO_2 electrodes after continuous charge/discharge cycles ($I=150mA/cm^2$)

35 cycles

55 cycles

NO PULSES

SURFACE 1 (macroscopic view)

SURFACE 2 (macroscopic view)

WITH PULSES

SURFACE 1 (macroscopic view)

SURFACE 2 (macroscopic view)

Figure 11

Micromorphology (I=150mA/cm^2)

NO PULSES Magnification 17x

EDGE (microscopic view)

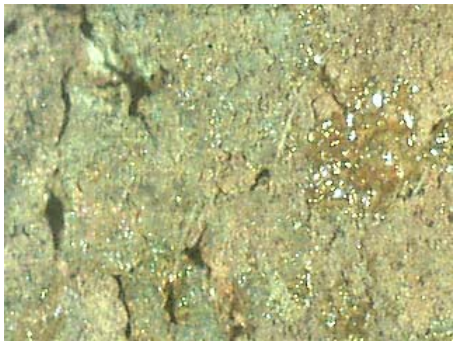

SURFACE 1 (microscopic view)

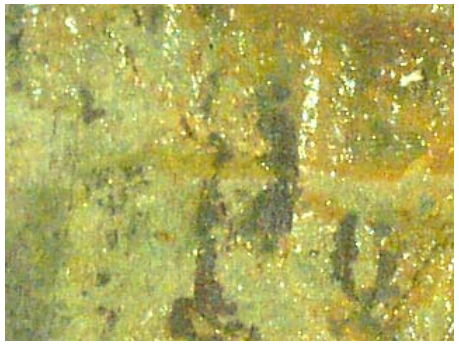

SURFACE 2 (microscopic view)

WITH PULSES Magnification 17x

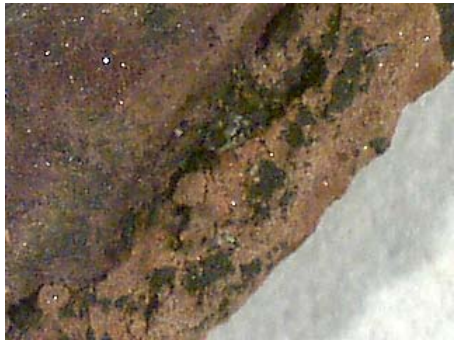

EDGE (microscopic view)

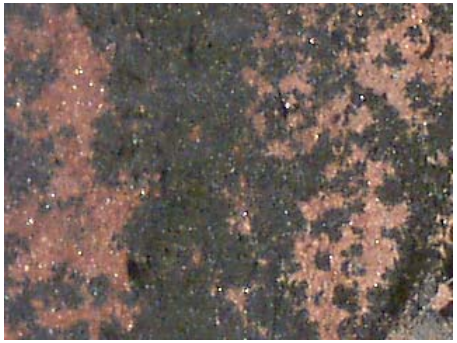

SURFACE 1 (microscopic view)

SURFACE 2 (microscopic view)

Figure 12

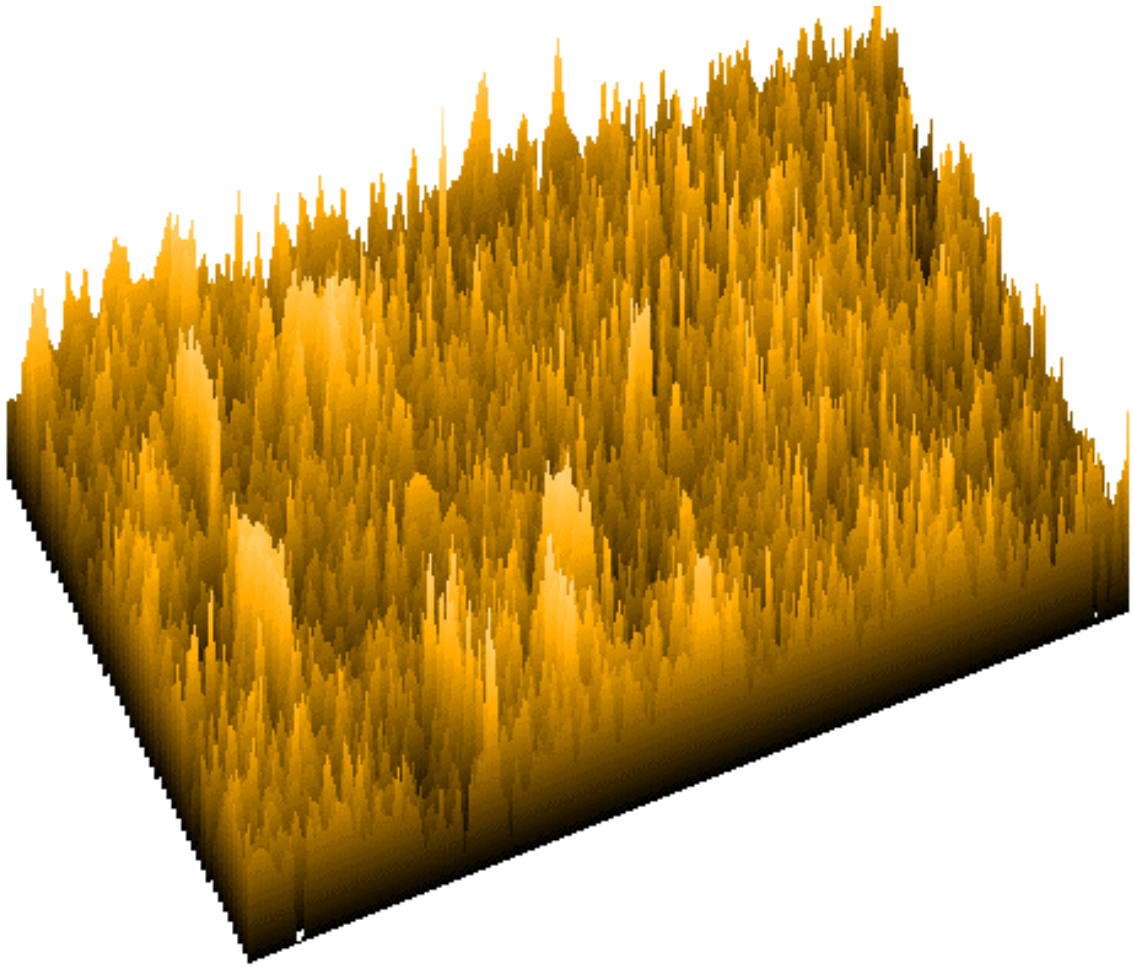

Figure 13

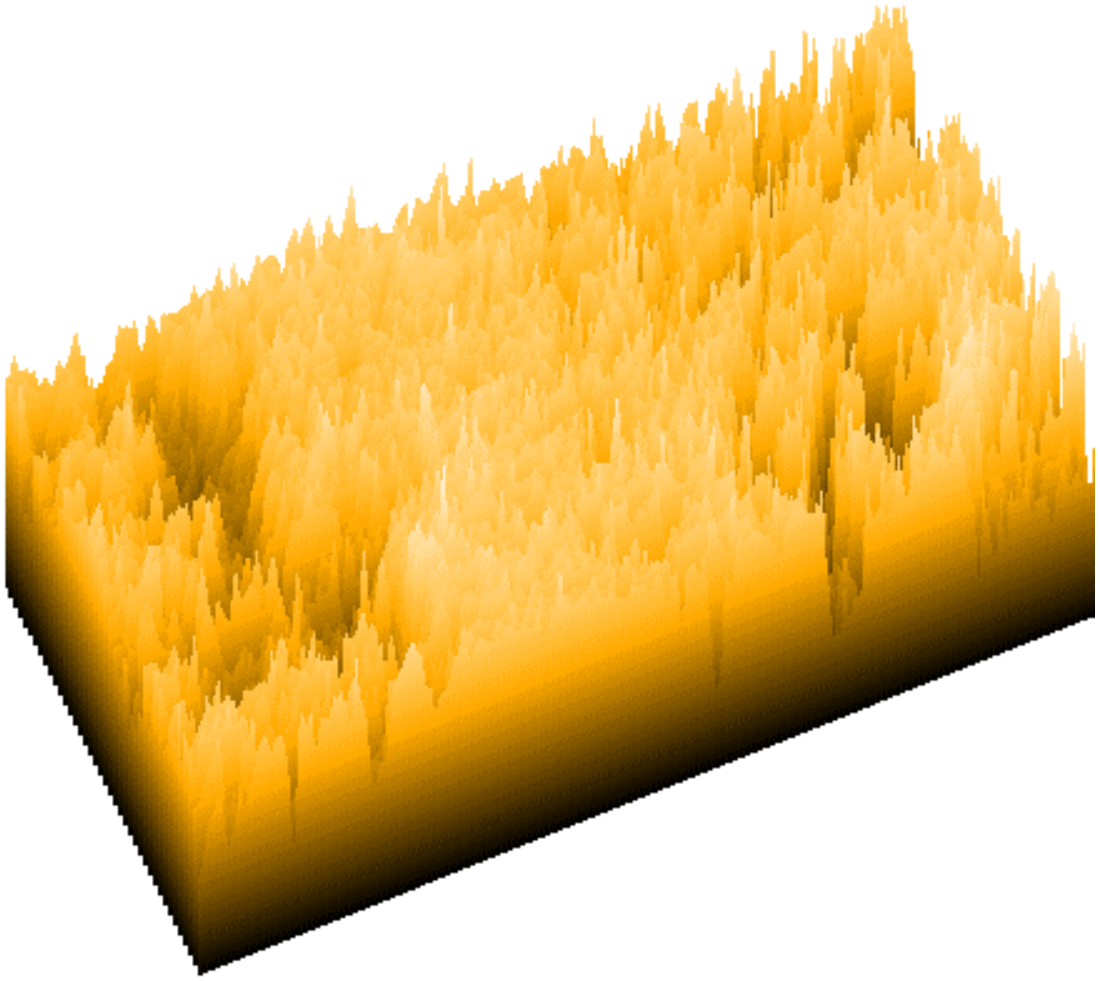

Figure 14

Positive electrode, 150mA, no solar, full spectrum

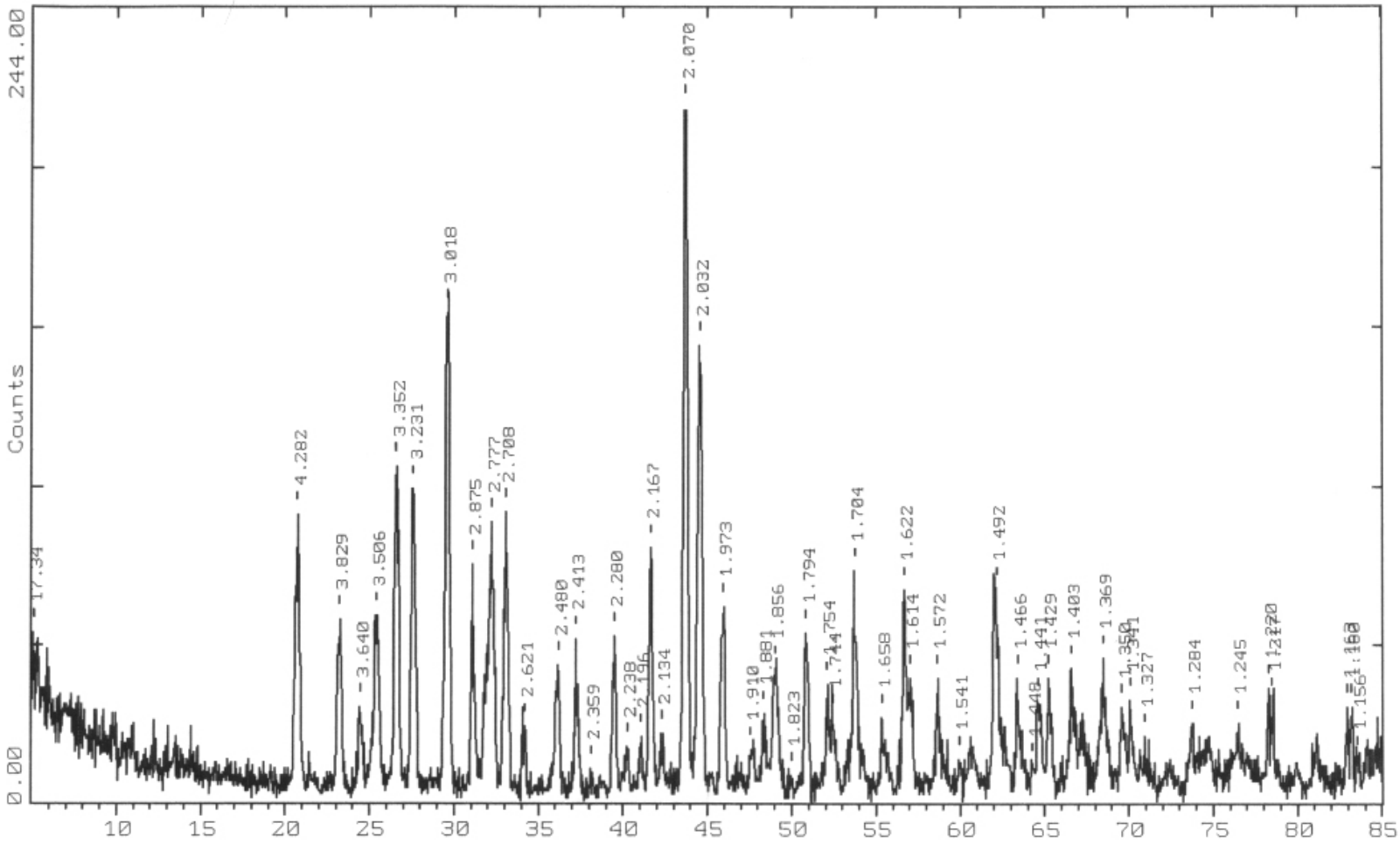

Figure 15

Positive electrode, 150mA, no solar, spectrum range: 15-45

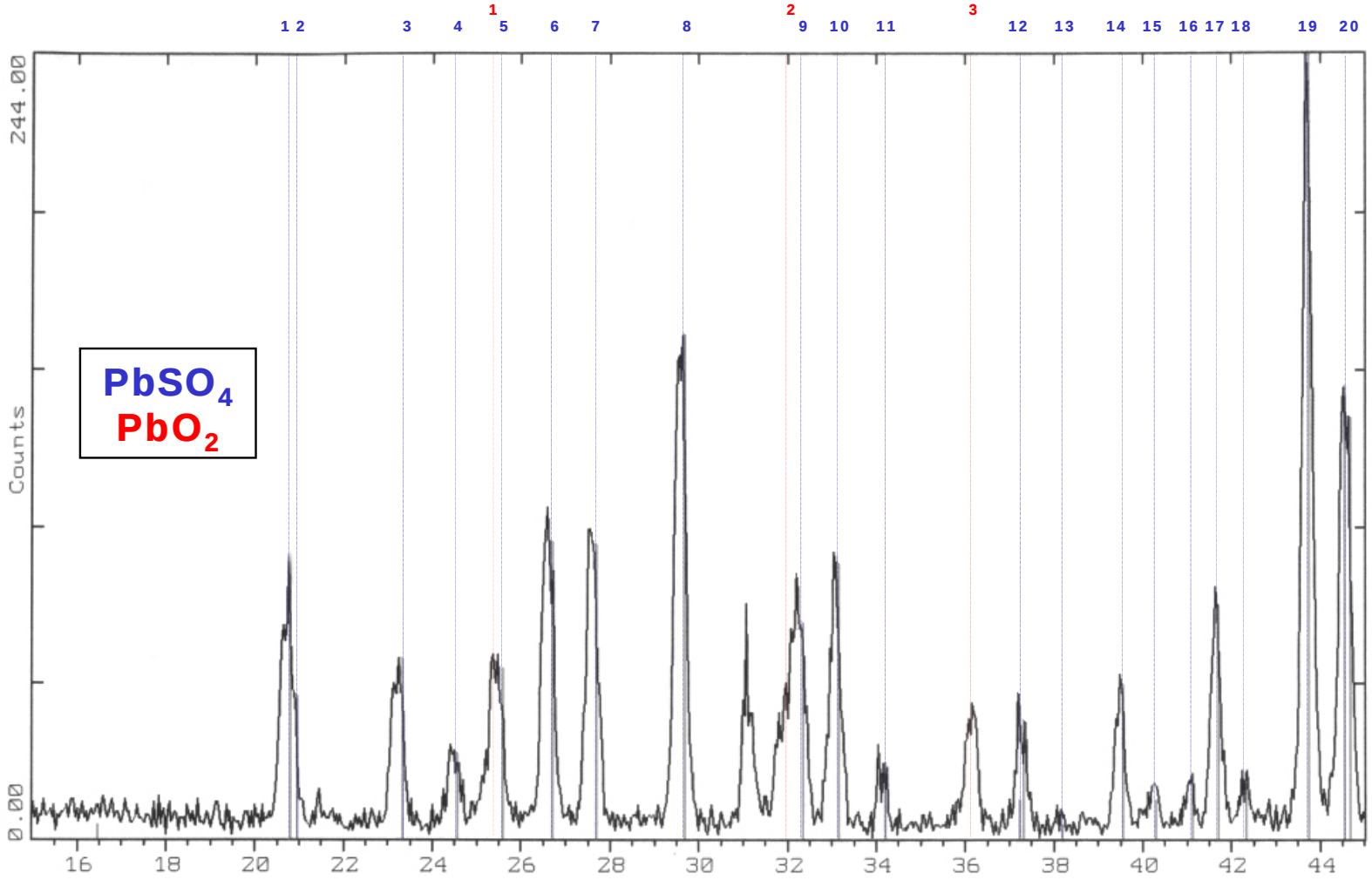

Figure 16a

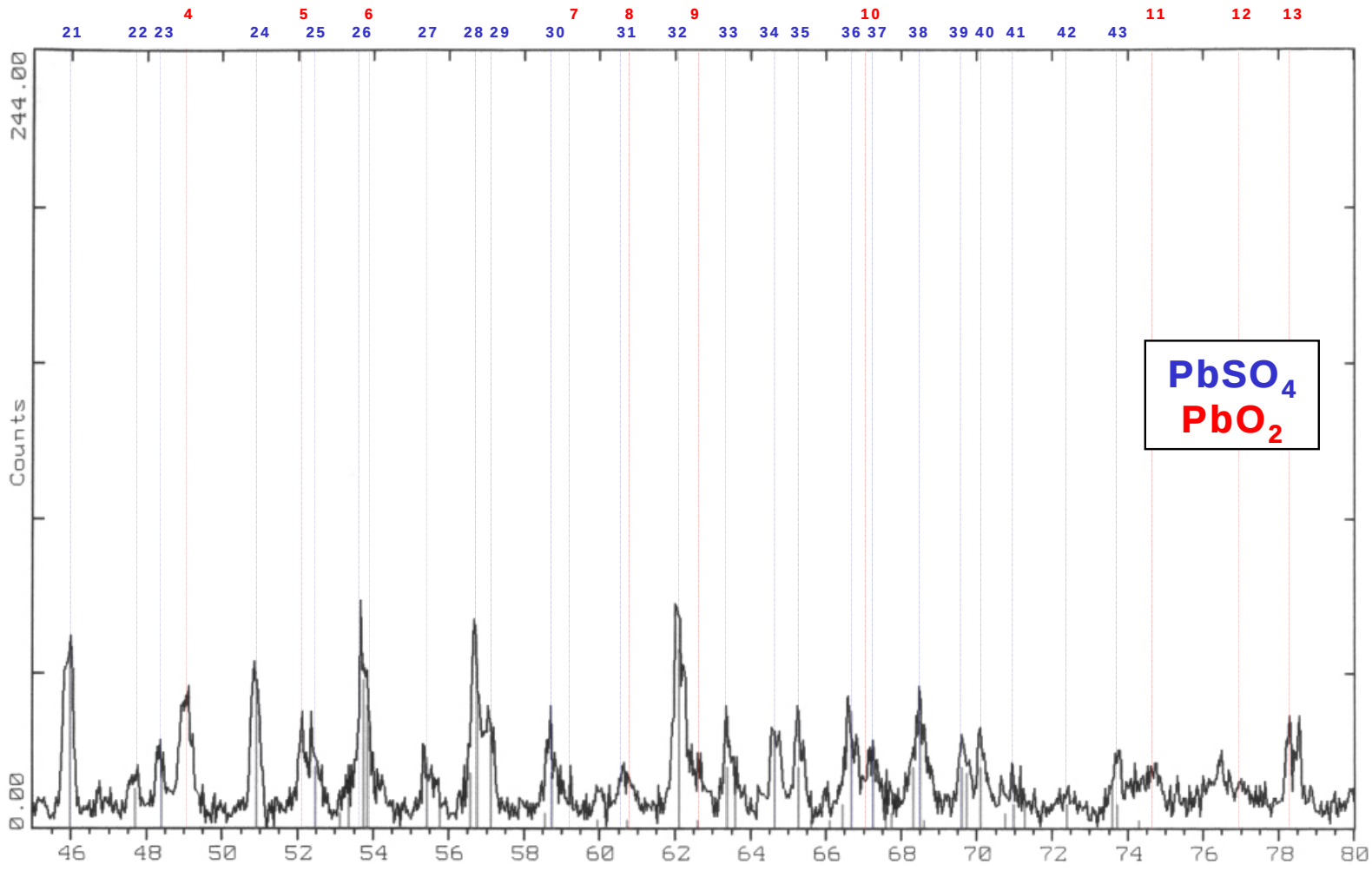
Positive electrode, 150mA, no solar, spectrum range: 45-80
PbSO4
PbO2
Counts
244.00
0.00
46 48 50 52 54 56 58 60 62 64 66 68 70 72 74 76 78 80

Figure 16b

Positive electrode, 150mA, with solar, full spectrum

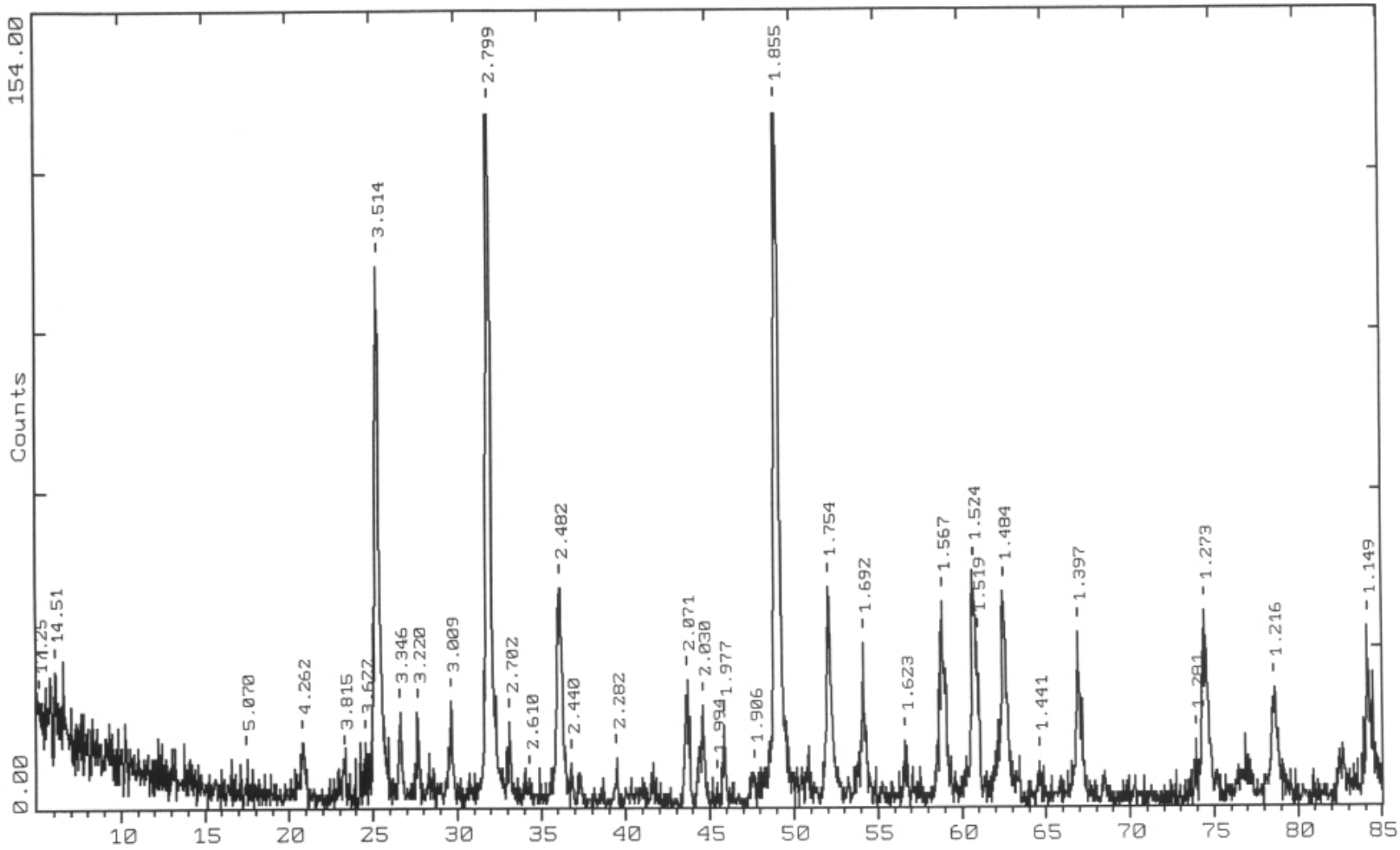

Figure 17

Positive electrode, 150mA, with solar, spectrum range: 15-45

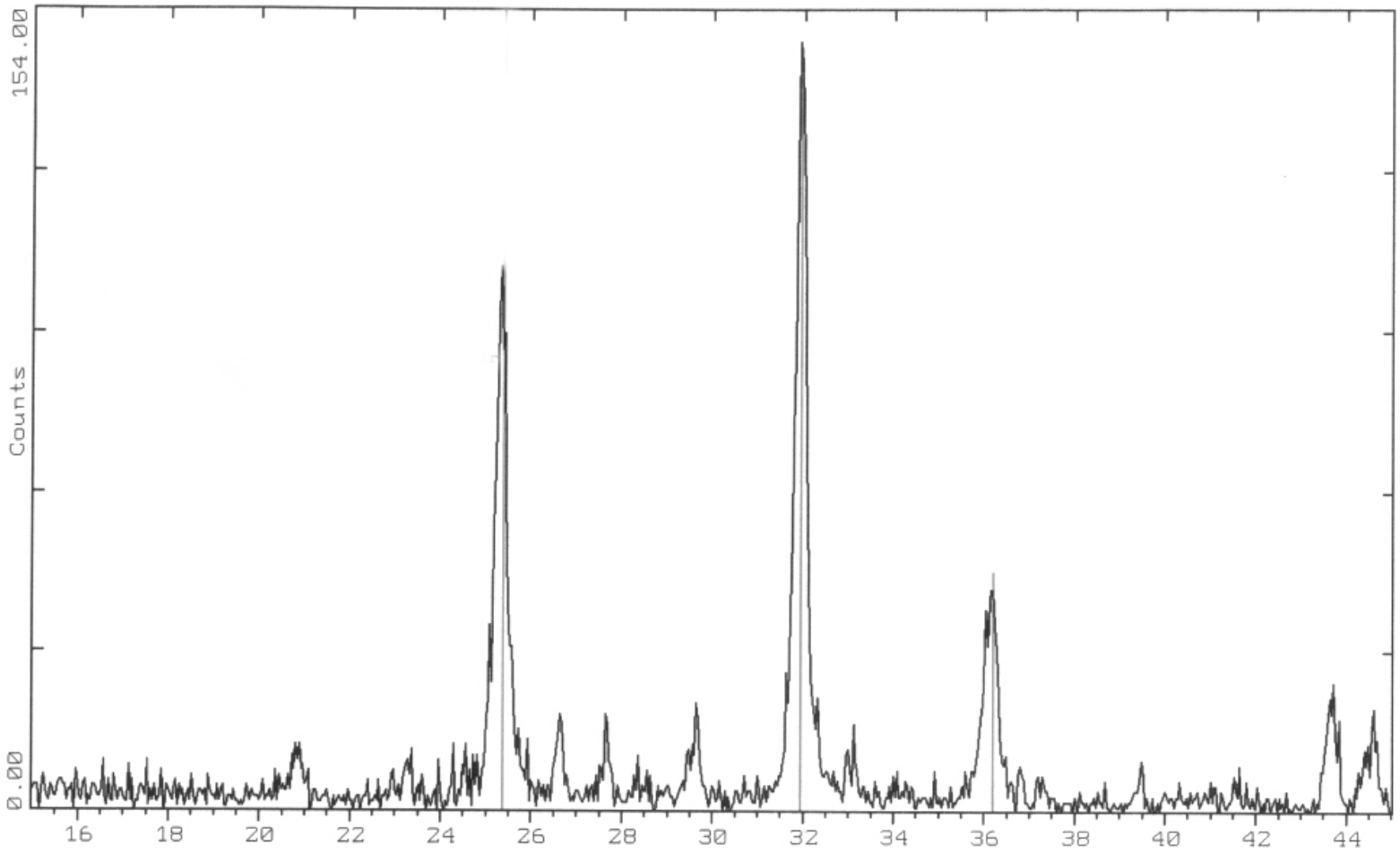

Figure 18a

Positive electrode, 150mA, with solar, spectrum range: 45-80

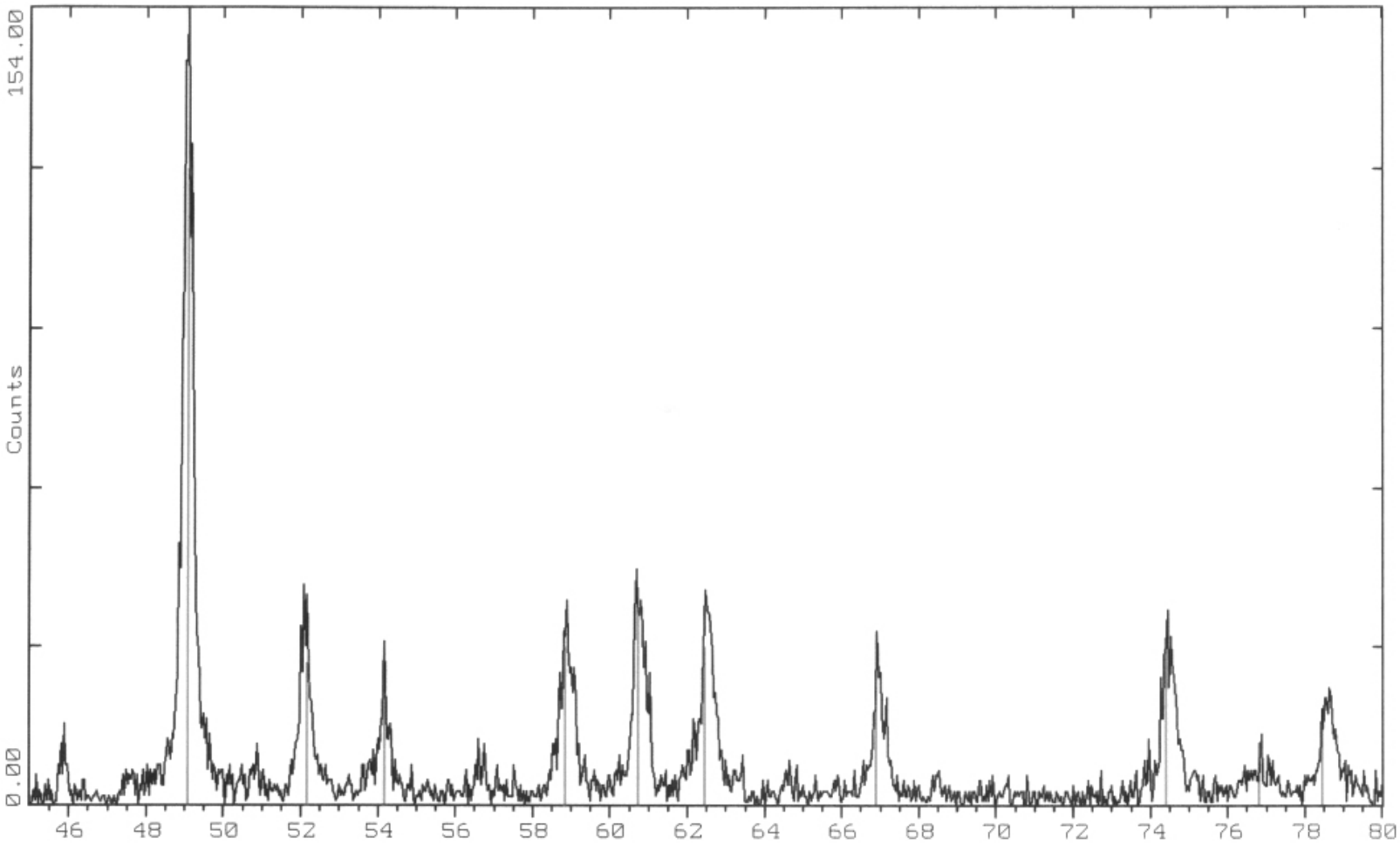

Figure 18b

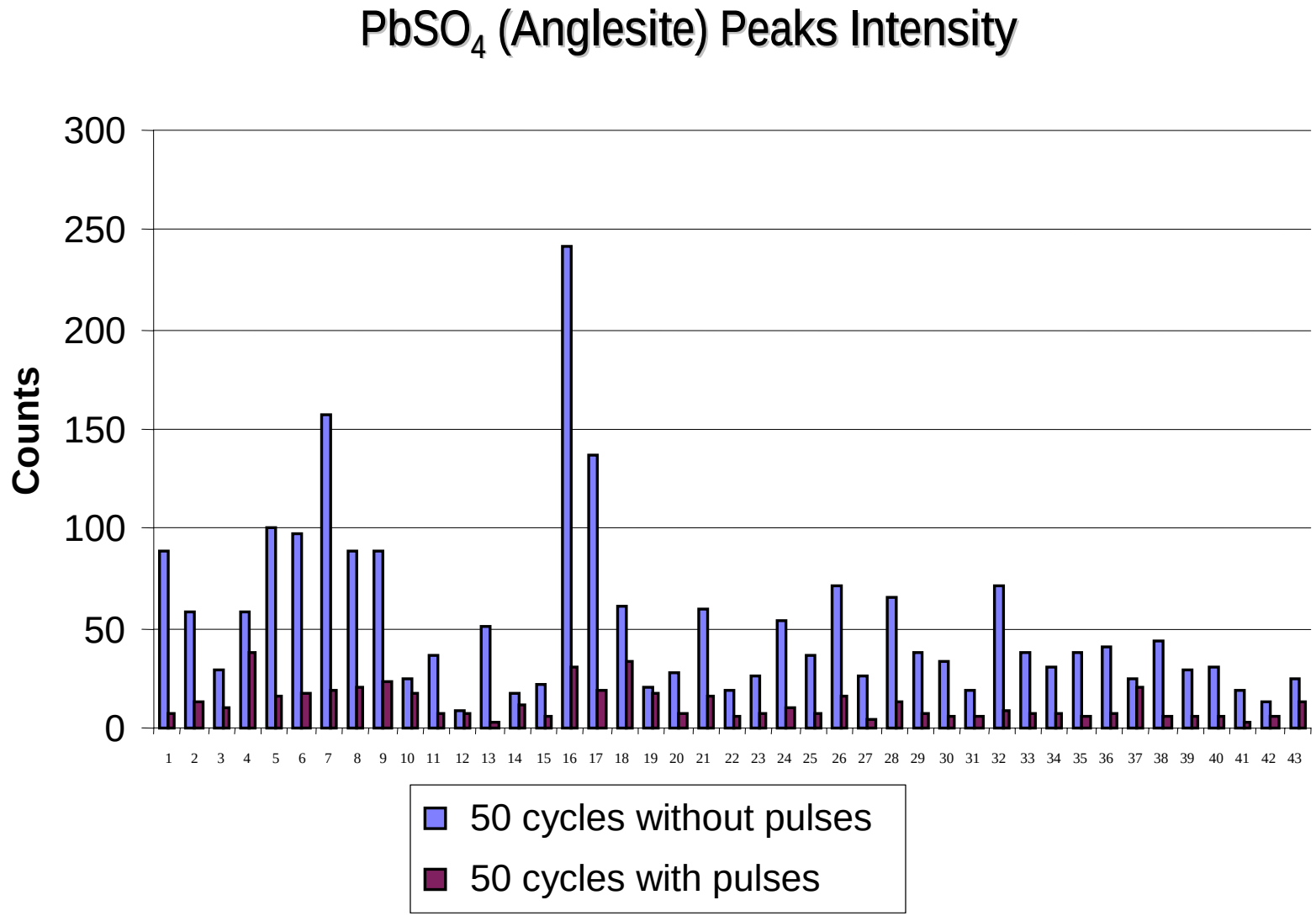
PbSO4 (Anglesite) Peaks Intensity
Counts
300
250
200
150
100
50
0
1 2 3 4 5 6 7 8 9 10 11 12 13 14 15 16 17 18 19 20 21 22 23 24 25 26 27 28 29 30 31 32 33 34 35 36 37 38 39 40 41 42 43
50 cycles without pulses
50 cycles with pulses

Figure 19

decrease of charge, which can be generated from lead-acid battery. The increase of nonconvertible" $PbSO_4$ is at the expense of the active PbO_2.

The decrease of the amount of active PbO_2 is very dramatic in the electrode charged/discharged without pulses (Figure 20). After 50 cycles of charge/discharge without pulses the amount of active PbO_2 in the positive electrode decreased by about 70±7% while the amount of $PbSO_4$ increased by about 65±6% (Figure 21).

When the positive electrodes were charged/discharged with pulses the decrease of PbO_2 and the increase of $PbSO_4$ is much slower. After 150 charge/discharge with pulses the amount of PbO_2 and $PbSO_4$ is about the same (about 50%) (Figure 22). It does indicate that the positive electrode when charged with pulses can sustain a much higher number of cycles than that charged without pulses. The amount of PbO_2 in the positive electrode continuously charged/discharged 150 times with pulses is almost two times higher than the electrode charged/discharged 50 times without pulses (Figure 22).

The charge/discharge current applied in the experiments with small, well-defined positive electrodes clearly indicates that the effect of pulsation (generated by the Solargizer) is substantial. The positive electrode when charged with pulses maintains a high charge capacity and durability, and sustains a much higher number of charge/discharge cycles under severe (high

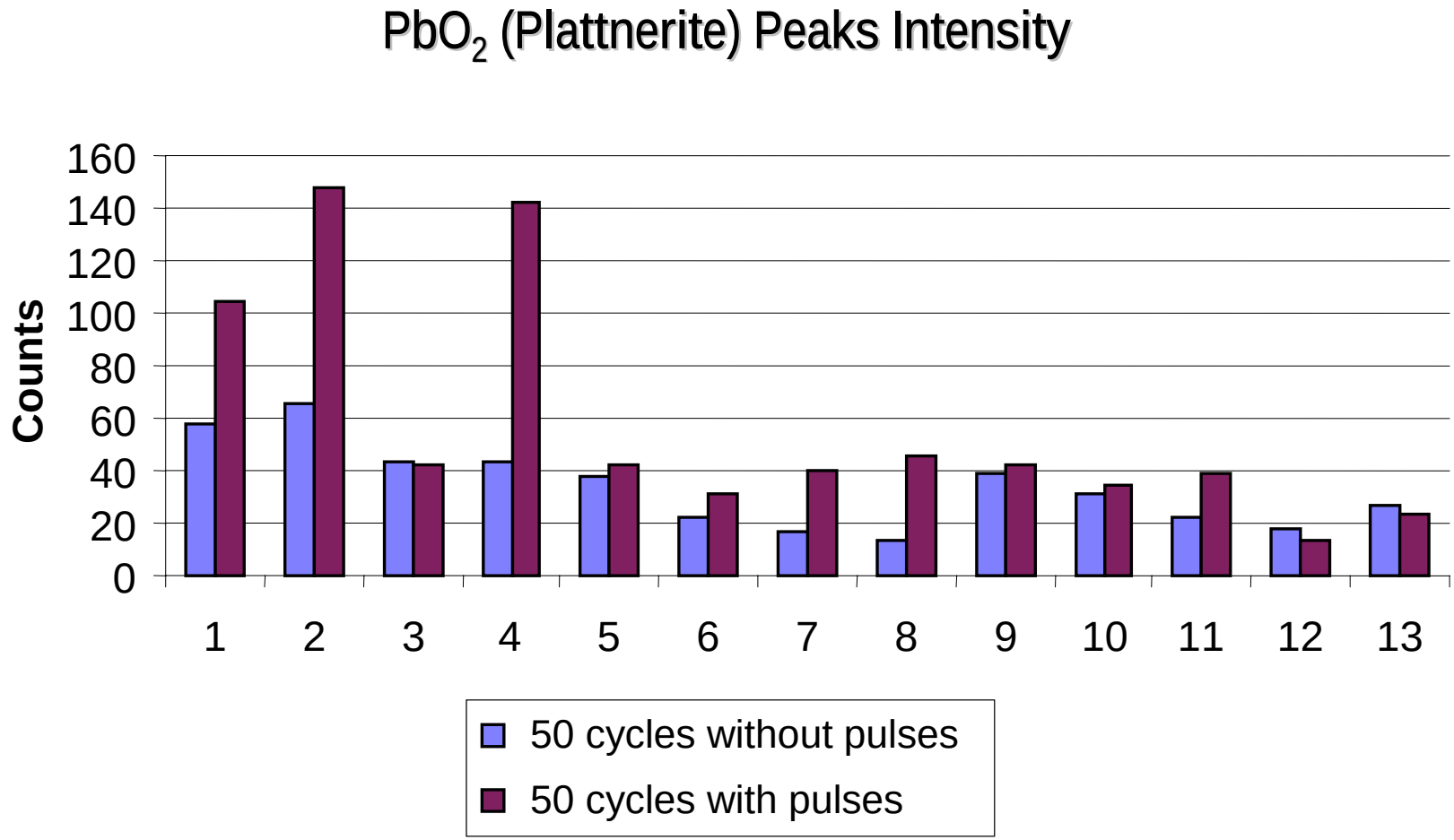
PbO2 (Plattnerite) Peaks Intensity
Counts
160
140
120
100
80
60
40
20
0
1
2
3
4
5
6
7
8
9
10
11
12
13
50 cycles without pulses
50 cycles with pulses

Figure 20

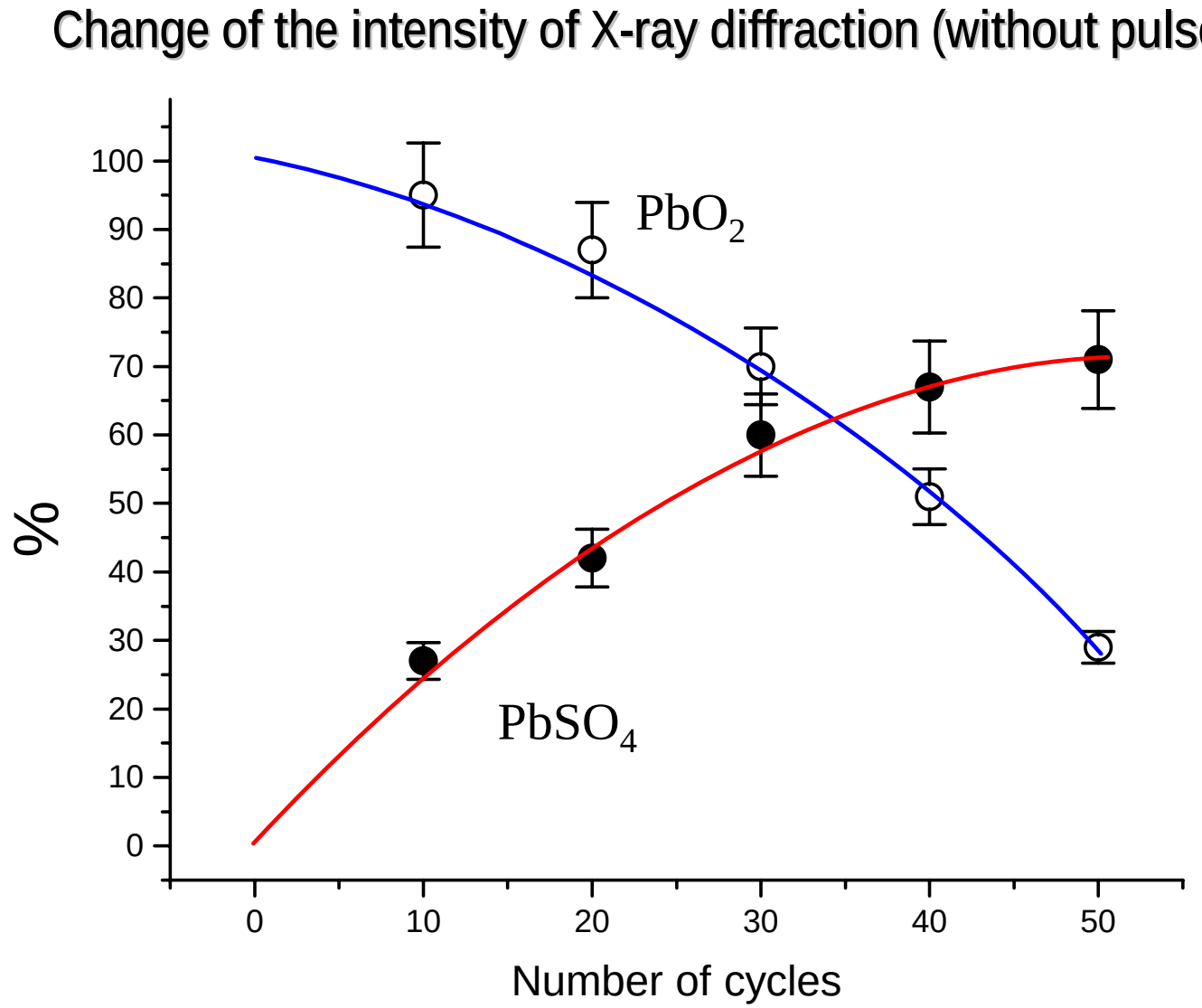
Change of the intensity of X-ray diffraction (without pulses)
PbO2
PbSO4
%
Number of cycles
0
10
20
30
40
50
60
70
80
90
100

Figure 21

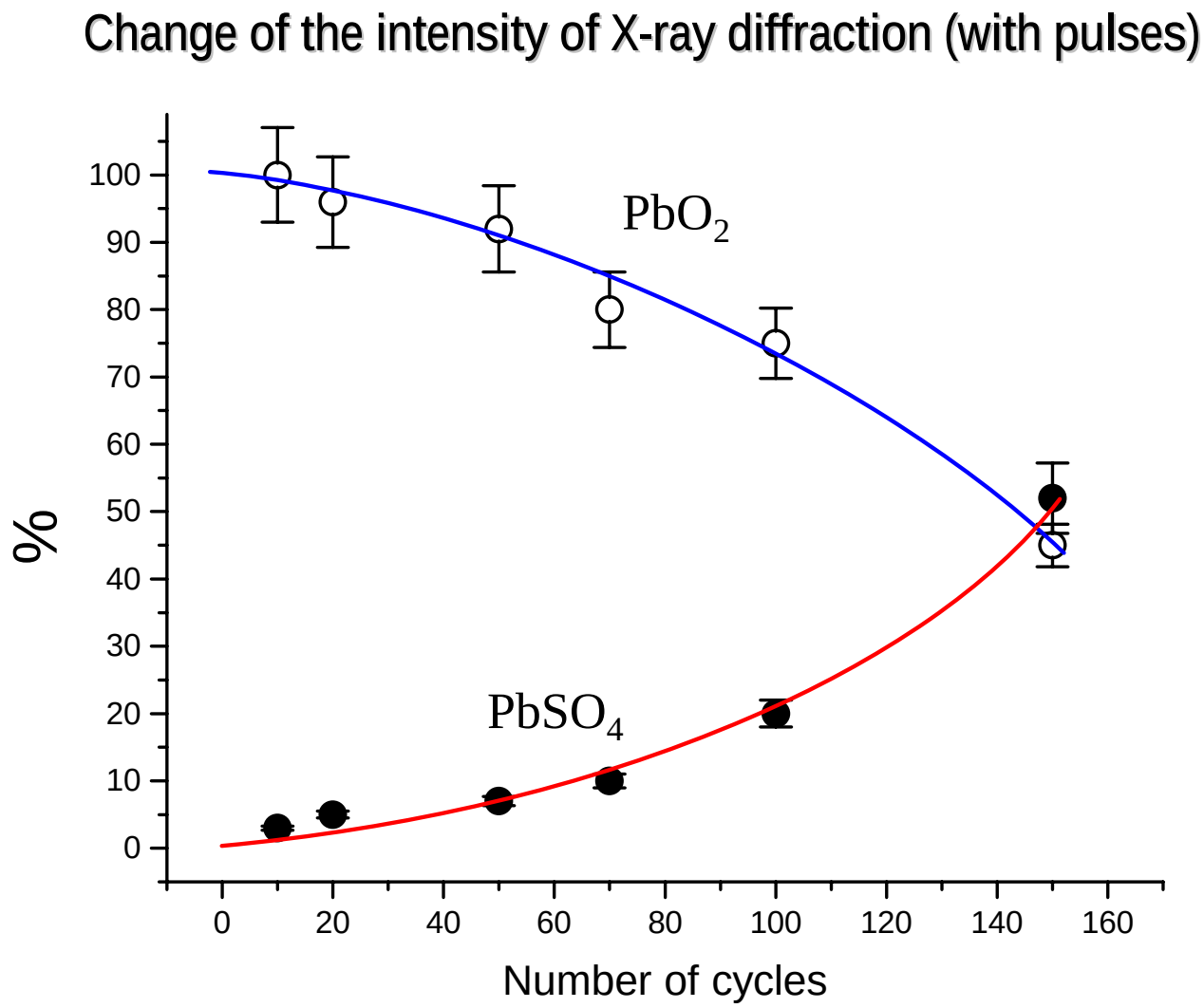
Change of the intensity of X-ray diffraction (with pulses)
PbO2
PbSO4
%
Number of cycles
0
10
20
30
40
50
60
70
80
90
100
0
20
40
60
80
100
120
140
160

Figure 22

current density) conditions. High current density was used in the charge/discharge cycles to accelerate a process of deterioration of the positive electrode with a small area. In order to extrapolate these findings to lower current density a separate set of experiments were performed using large capacity lead-acid batteries. A reproducibility of data obtained from a commercial battery is not as good as those obtained from well-defined small positive electrodes. Therefore, a large number of tests using a large number of batteries (usually 12) were performed to obtain statistical significance.

Pulsation effects on the charging/discharging process of lead-acid batteries

The studies of the influence of pulses generated by the Solargizer and applied during a charge/discharge of lead-acid batteries were performed using the instrumental set-up shown in Figure 23. The parallel experiments were done using a battery test system and constant current (10 A) for charge/discharge of lead-acid batteries in the presence or absence of pulses. The pulses were generated by the Solargizer and superimposed on charging current. Four different types of batteries were studied with a wide range of charge capacity from 15 Ah to 60 Ah. After the charge/discharge cycles the electrodes from each of the batteries were removed and analyzed using x-ray diffraction spectroscopy and specular reflectance spectroscopy. Figure 24 shows a galvanostatic curve recorded during discharge (first cycle) of a lead-acid battery (40 Ah). A typical plateau followed by the decrease of potential after about 3.5 hrs was observed. However, during the subsequent charge/discharge cycles, the duration time of the plateau becomes shorter (Figure 25). The shorter discharge time is an indicator of the decrease of electrical charge capacity of the battery. After the 50^{th} cycle the charge capacity decreased about 70% and a rapid and step-like decrease of the potential was observed after about 20 min of battery discharge (Figure 26).

A deterioration of the charge capacity was much less severe when the battery was charged/discharged in the presence of pulsation generated by the Solargizer.

Figure 26 shows the galvanostatic curves observed during the fifth and 50th charge/discharge cycle. After the 50th cycle the battery has about 60% of its original capacity. Under this same experimental condition, the charge capacity of the battery charged without pulses was only 30% of its original capacity. Figures 27-30 depict the changes of the charge capacity of batteries 15, 20, 40 and 60 Ah with number of charging/discharging cycles. All batteries were charged /discharged 50 times. As expected all batteries studied were loosing charge capacity with the increasing number of charge/discharge cycles. However, the batteries not treated with pulses were loosing charge at a much faster rate than those treated with pulses (Figure 31). The decrease of battery charge capacity depends on its original value. It is well known that batteries with a high charge capacity deteriorate faster than small batteries.

High charge capacity is associated with a large surface of the electrodes and maintenance of desirable properties of electrodes is more difficult for high capacity and large surface area batteries. For low capacity batteries (15-20 Ah) and a small number of cycles the decrease of charge capacity is small (but statistically significant) as well as the difference between batteries charged with or without pulses. However, for a high power battery and/or high

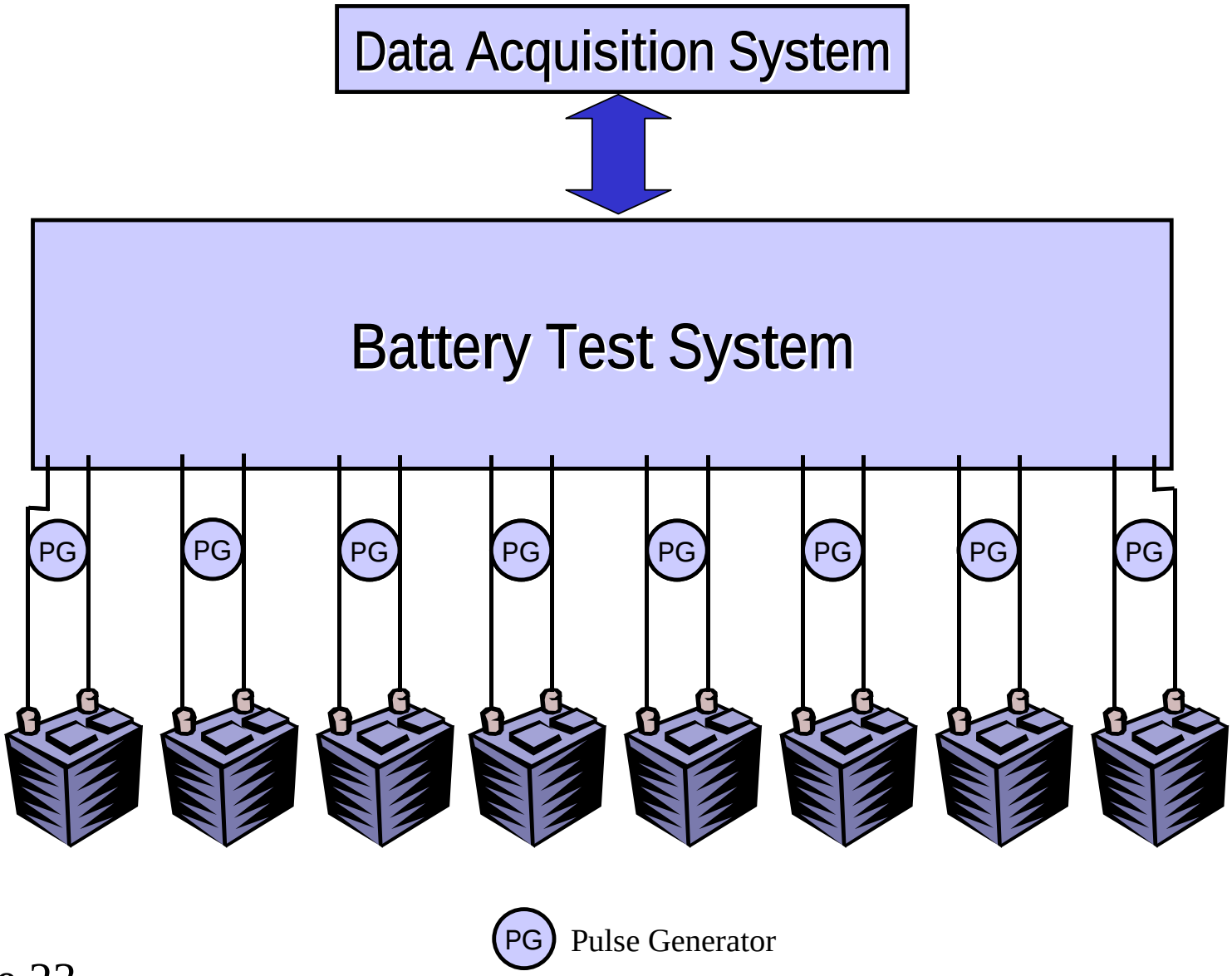
Data Acquisition System
Battery Test System
PG
PG
PG
PG
PG
PG
PG
PG
PG
Pulse Generator

Figure 23

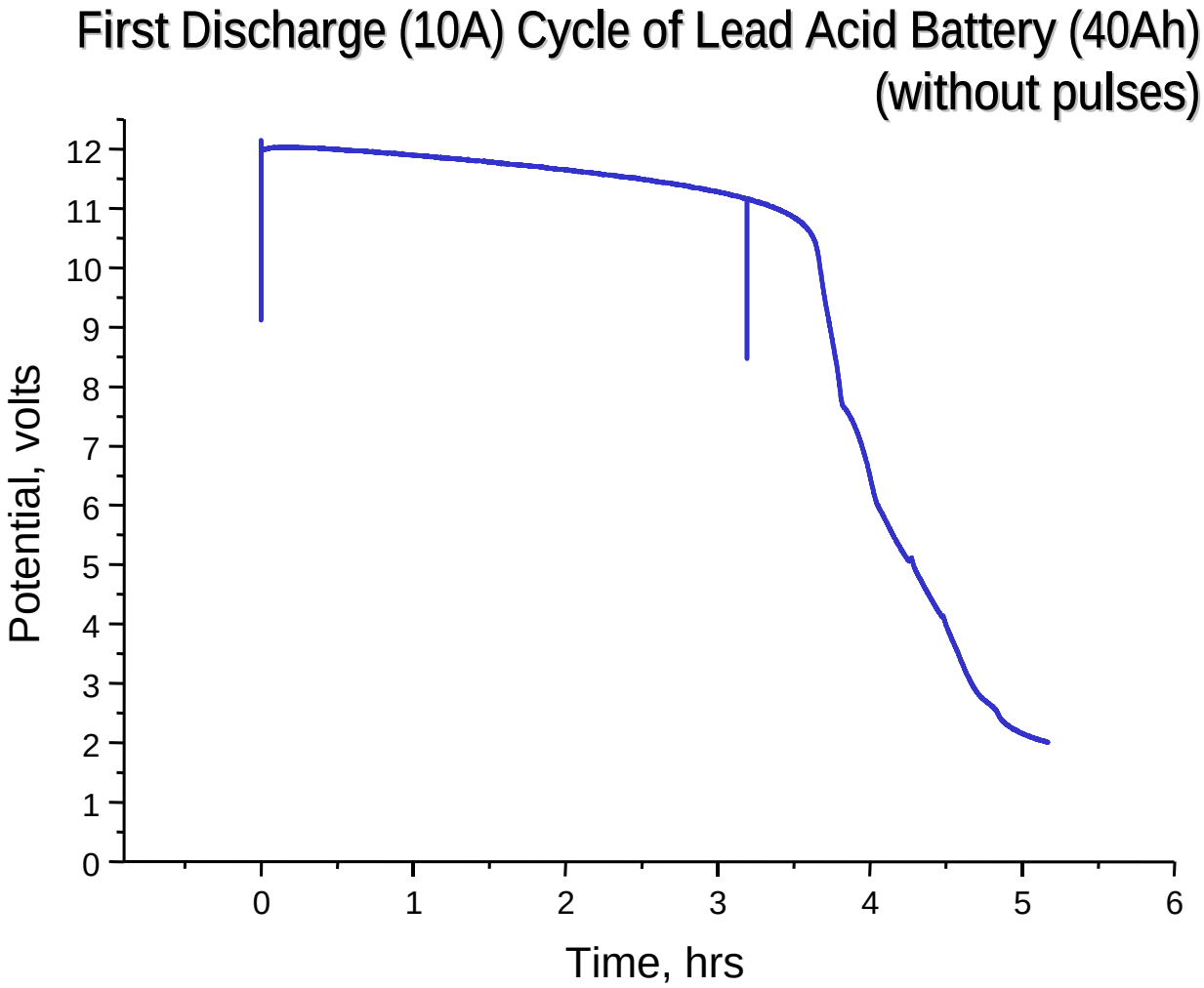
First Discharge (10A) Cycle of Lead Acid Battery (40Ah)
(without pulses)
Potential, volts
Time, hrs
0
1
2
3
4
5
6
7
8
9
10
11
12

Figure 24

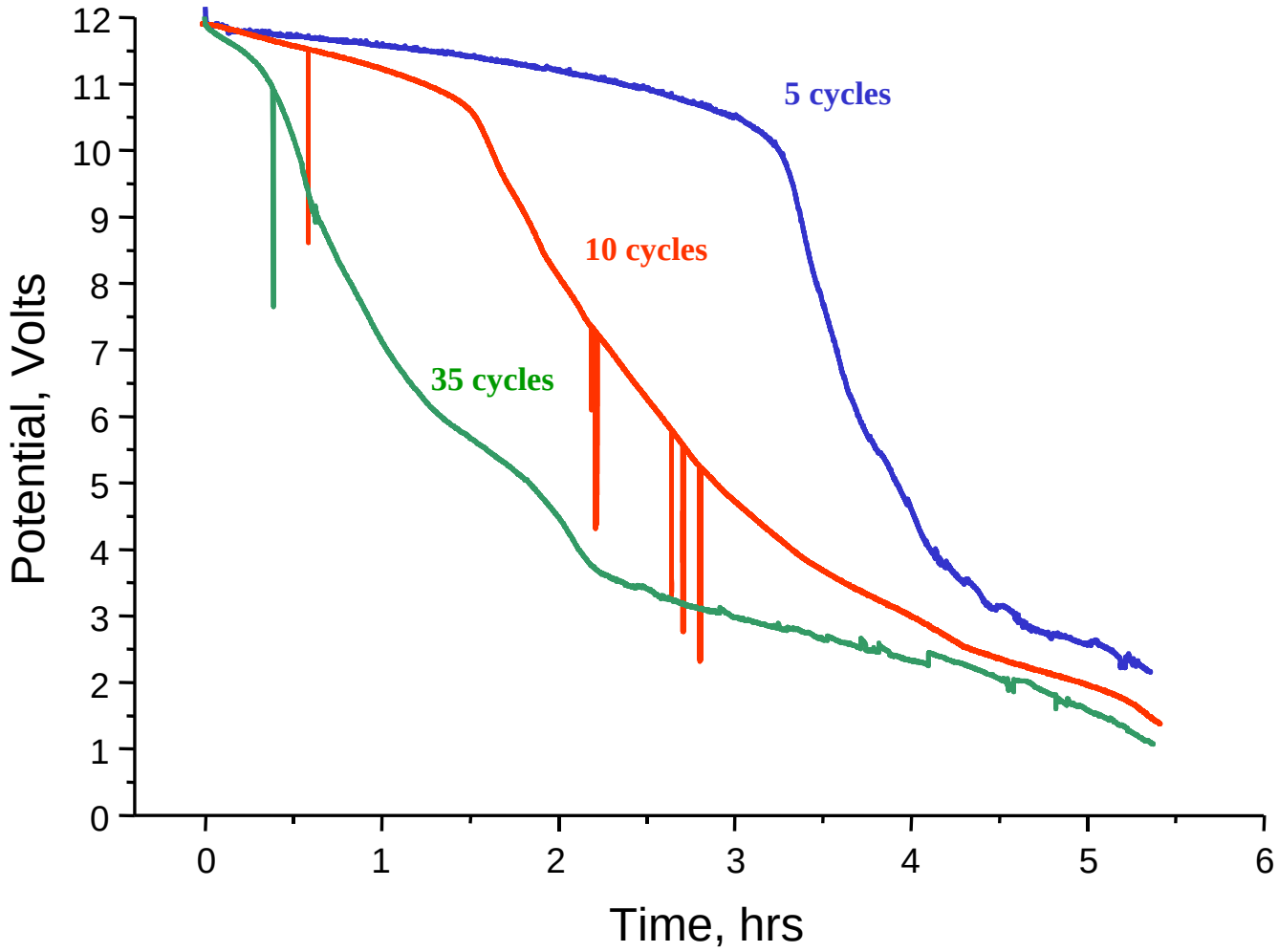
Discharge (10A) cycle of lead-acid battery (40Ah, without pulses)
Potential, Volts
Time, hrs
5 cycles
10 cycles
35 cycles
0
1
2
3
4
5
6
7
8
9
10
11
12

Figure 25a

A discharge of 50th cycle of lead-acid battery (40Ah, without pulses)

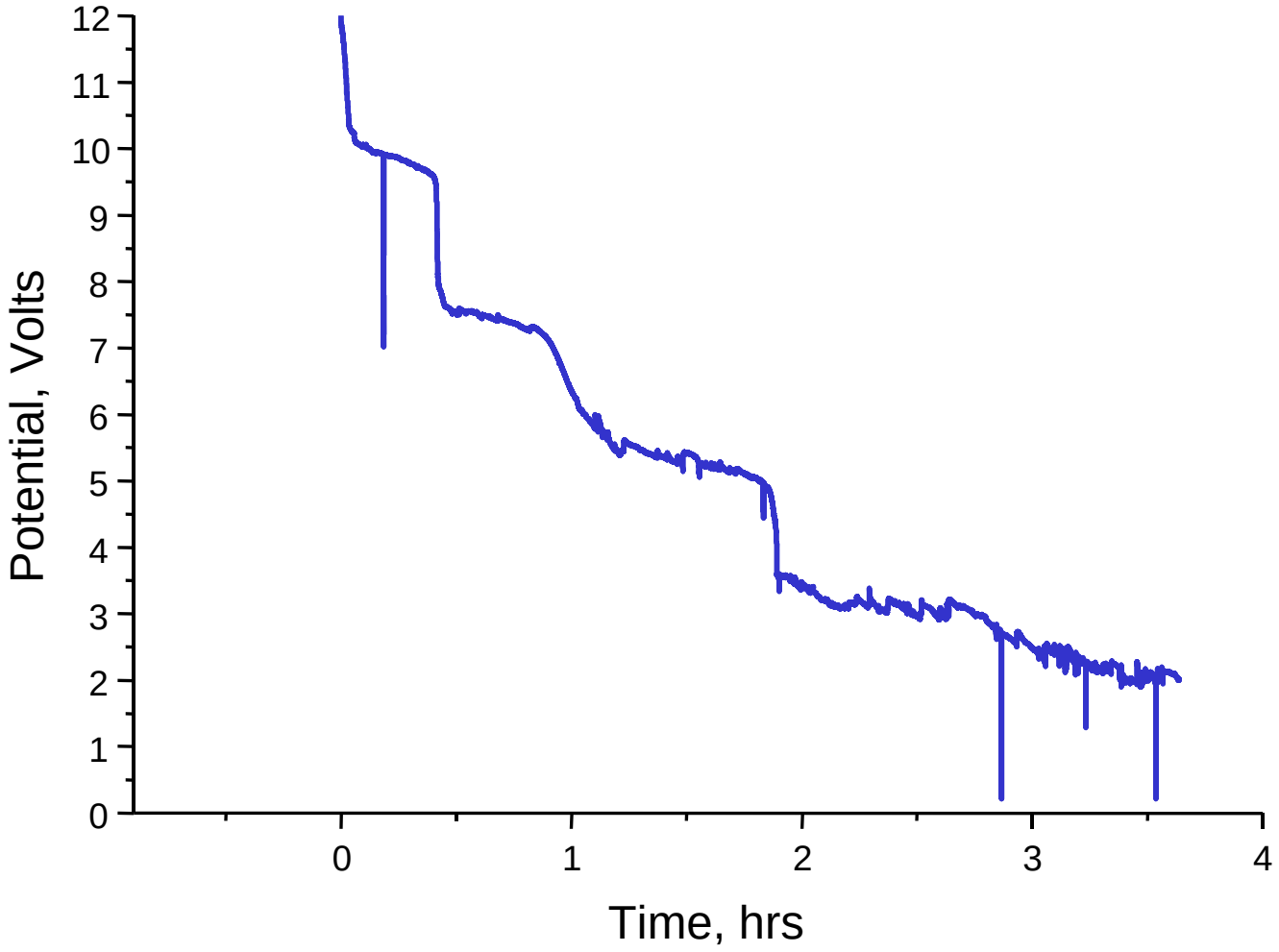

Figure 25b

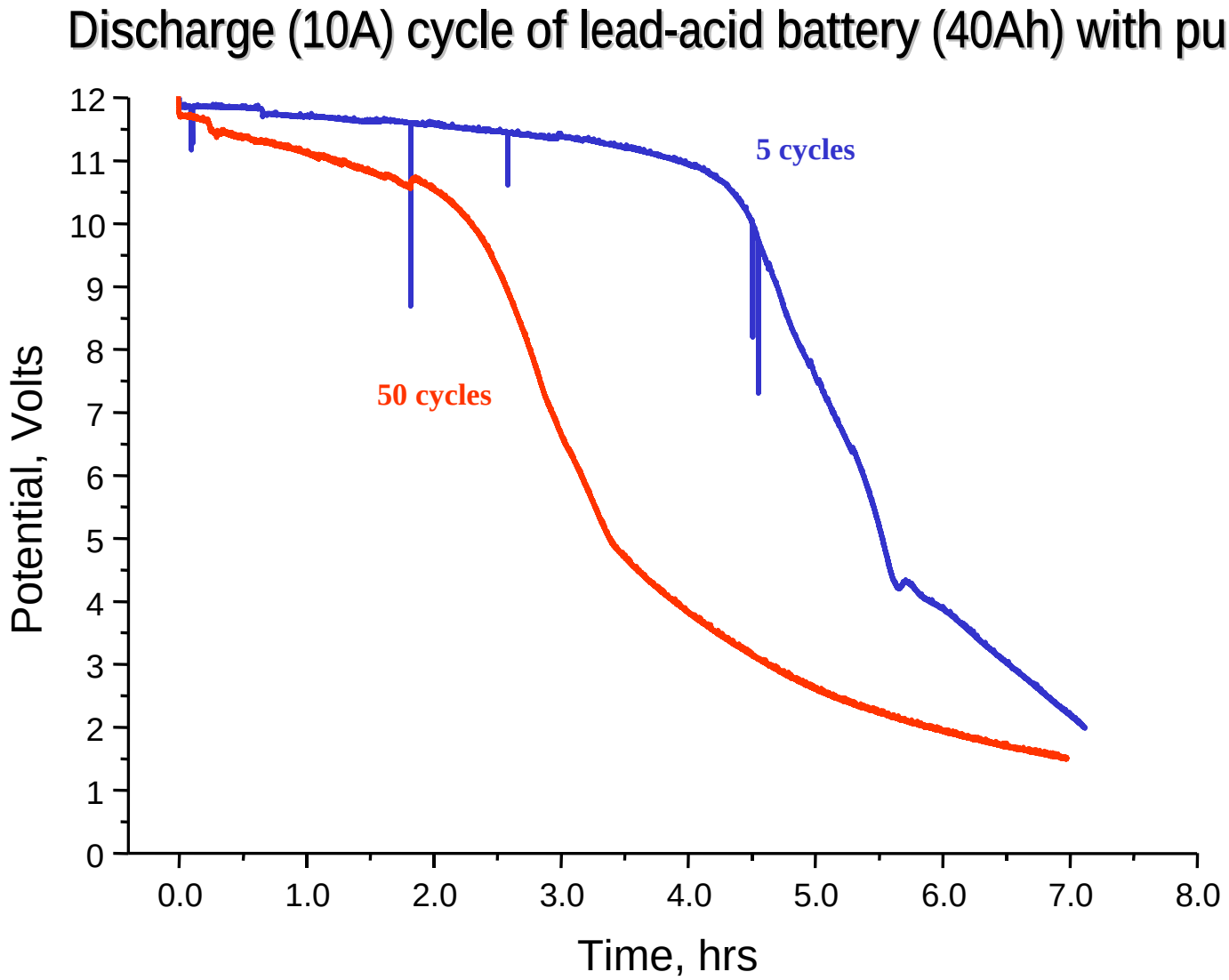
Discharge (10A) cycle of lead-acid battery (40Ah) with pulses
Potential, Volts
Time, hrs
5 cycles
50 cycles
0
1
2
3
4
5
6
7
8
9
10
11
12
0.0
1.0
2.0
3.0
4.0
5.0
6.0
7.0
8.0

Figure 26

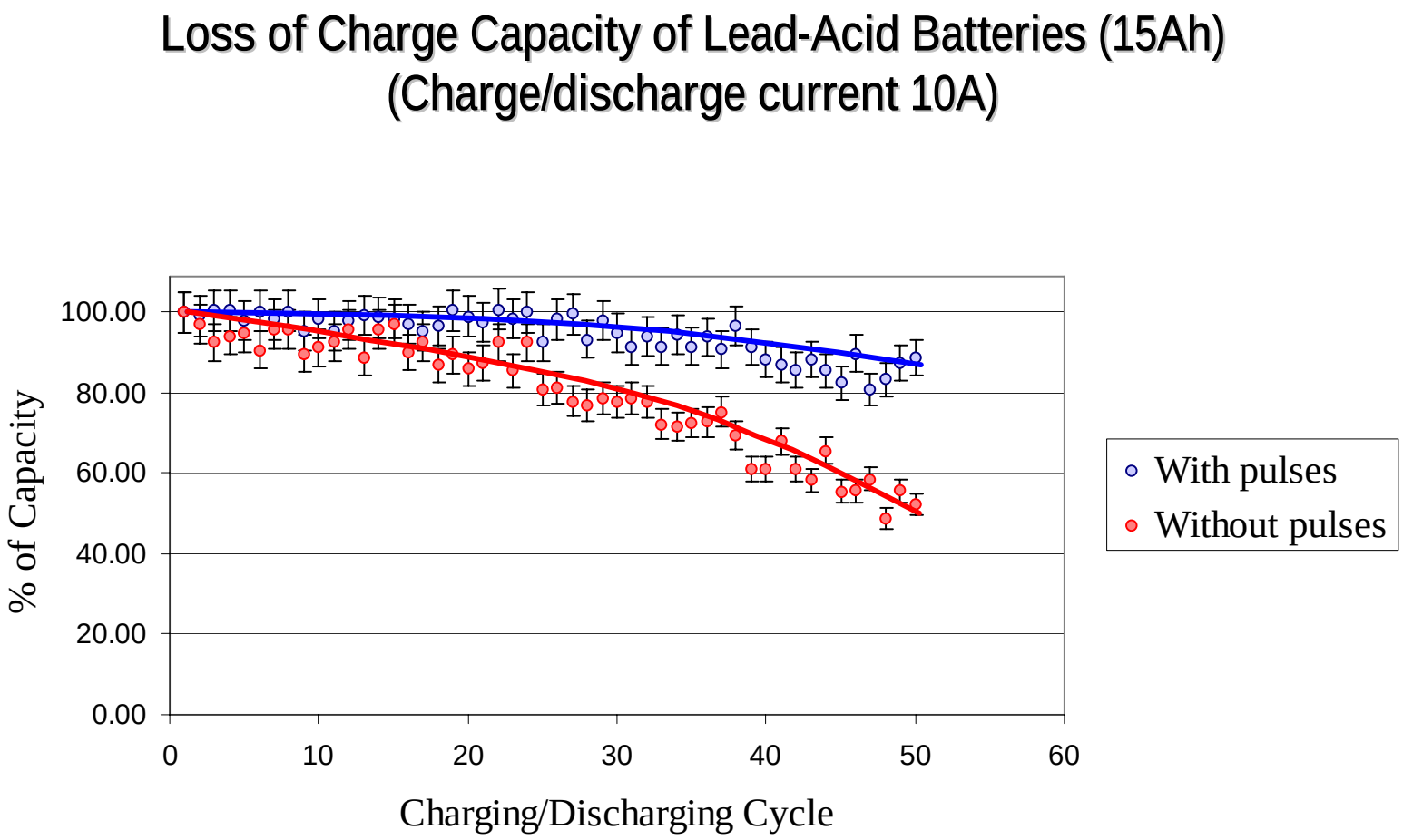
Loss of Charge Capacity of Lead-Acid Batteries (15Ah)
(Charge/discharge current 10A)
% of Capacity
100.00
80.00
60.00
40.00
20.00
0.00
0
10
20
30
40
50
60
Charging/Discharging Cycle
With pulses
Without pulses

Figure 27

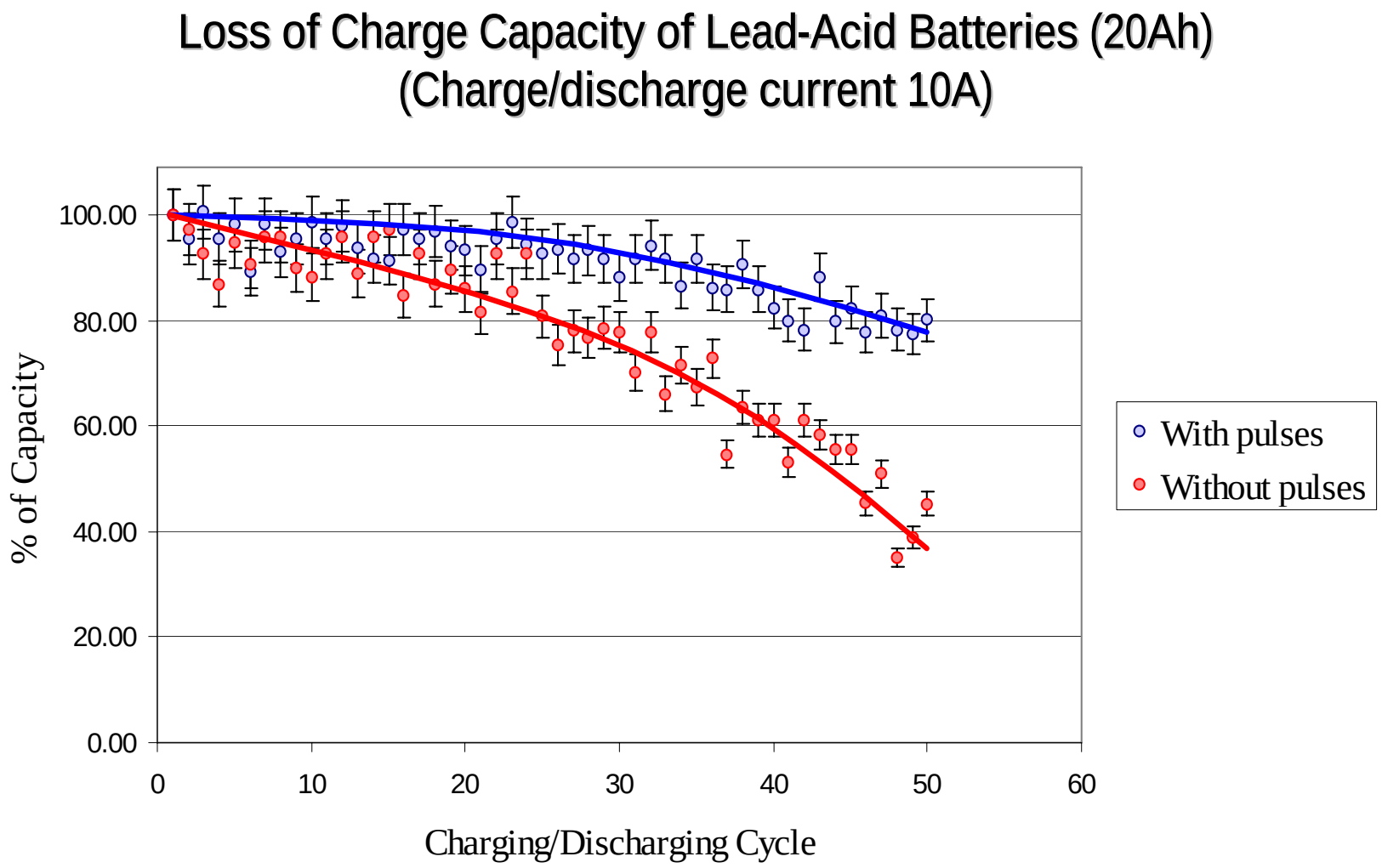
Loss of Charge Capacity of Lead-Acid Batteries (20Ah)
(Charge/discharge current 10A)
% of Capacity
100.00
80.00
60.00
40.00
20.00
0.00
0
10
20
30
40
50
60
Charging/Discharging Cycle
With pulses
Without pulses

Figure 28

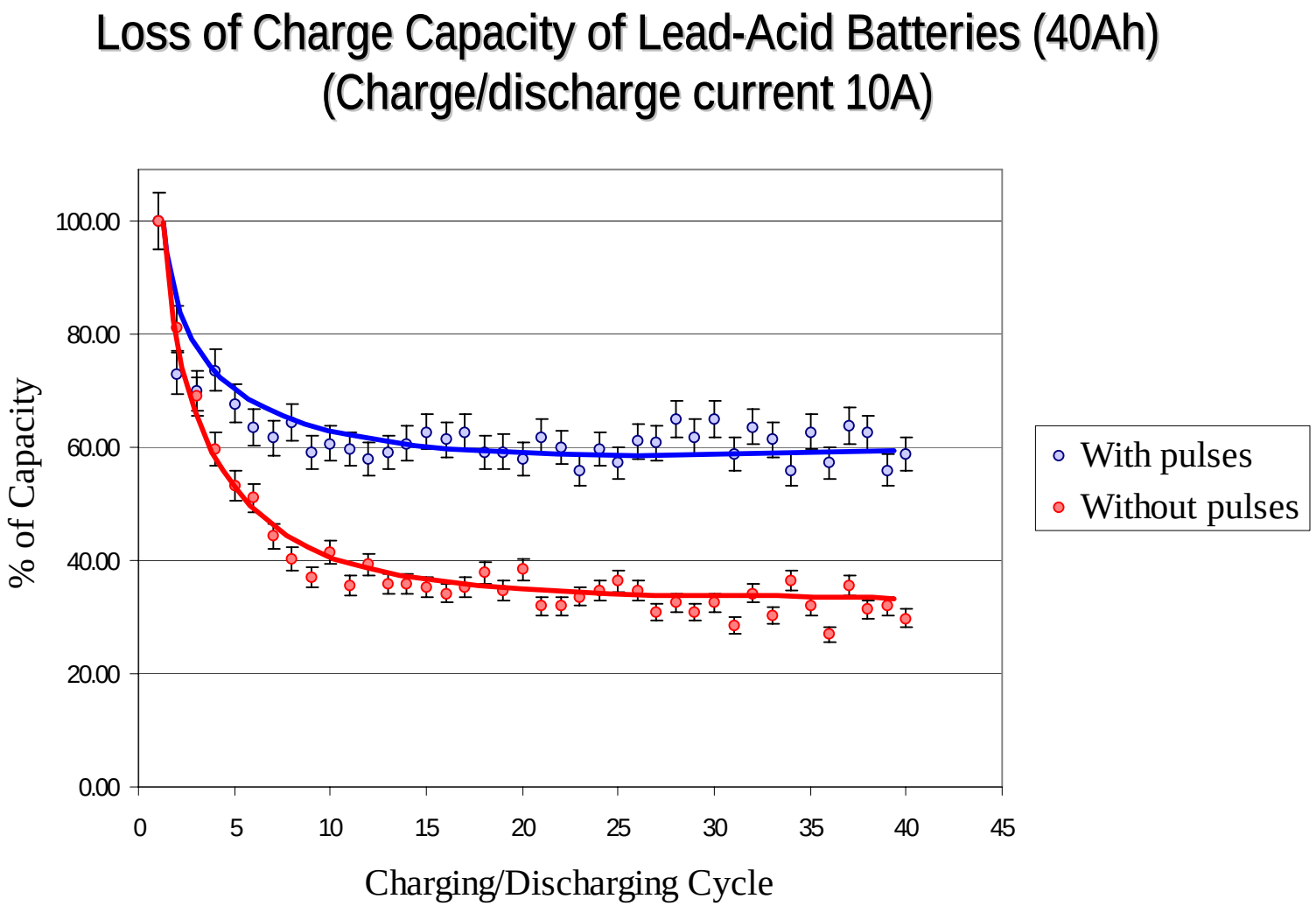
Loss of Charge Capacity of Lead-Acid Batteries (40Ah)
(Charge/discharge current 10A)
% of Capacity
100.00
80.00
60.00
40.00
20.00
0.00
0
5
10
15
20
25
30
35
40
45
Charging/Discharging Cycle
With pulses
Without pulses

Figure 29

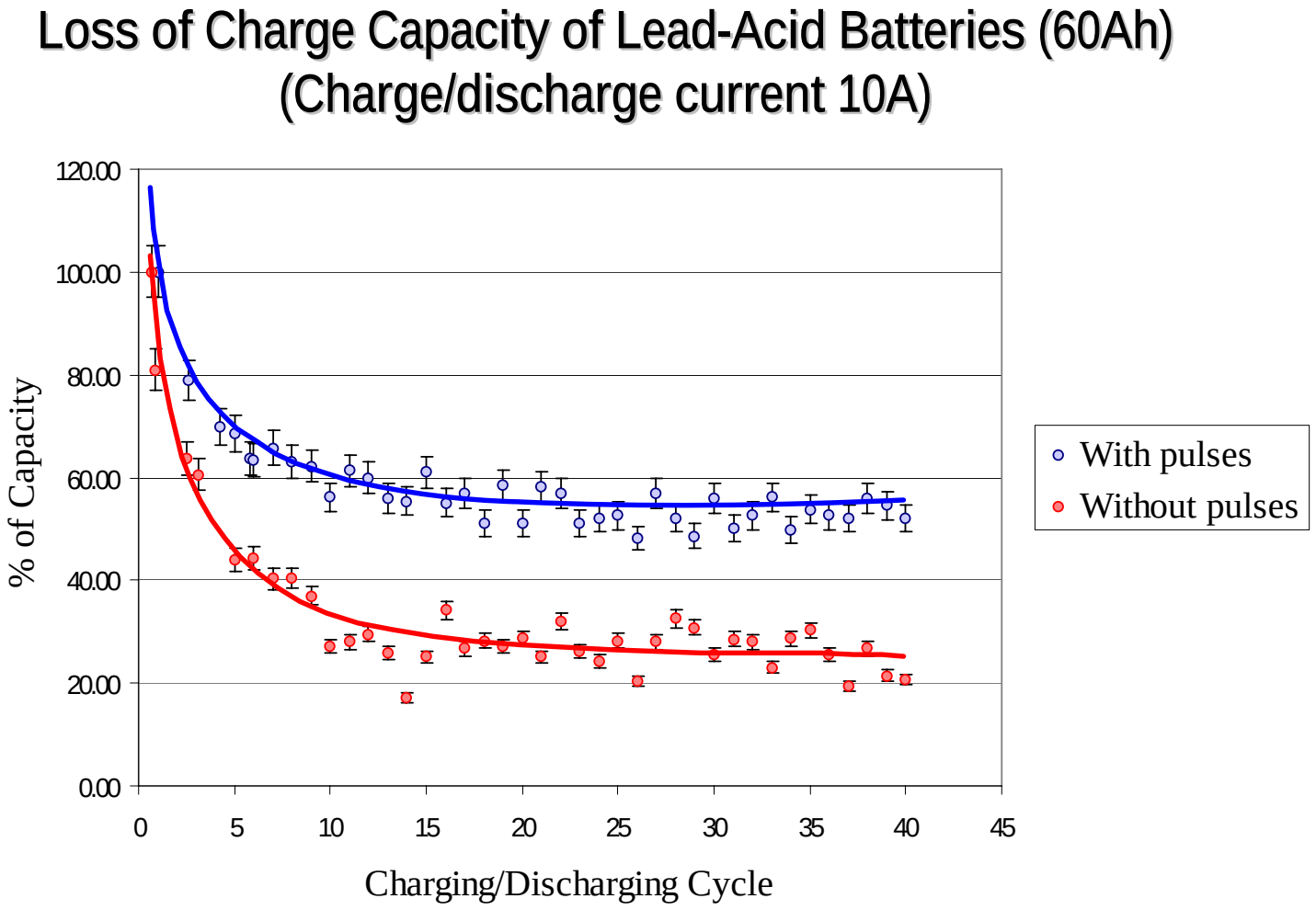
Loss of Charge Capacity of Lead-Acid Batteries (60Ah)
(Charge/discharge current 10A)
% of Capacity
120.00
100.00
80.00
60.00
40.00
20.00
0.00
0
5
10
15
20
25
30
35
40
45
Charging/Discharging Cycle
With pulses
Without pulses

Figure 30

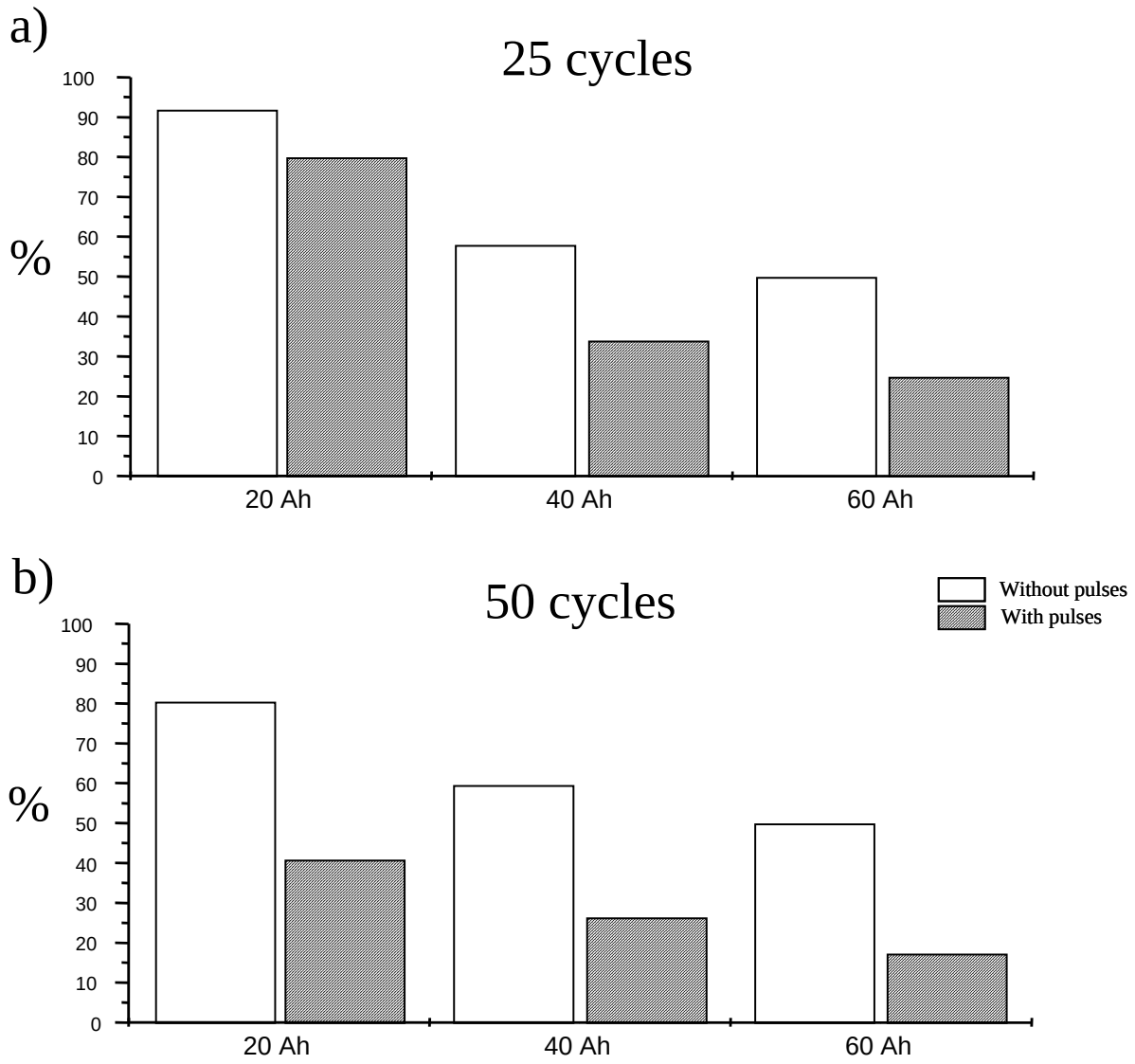
a)
25 cycles
%
100
90
80
70
60
50
40
30
20
10
0
20 Ah
40 Ah
60 Ah
b)
50 cycles
Without pulses
With pulses
%
100
90
80
70
60
50
40
30
20
10
0
20 Ah
40 Ah
60 Ah

Figure 31

Negative (Pb) electrodes (15Ah, without pulses)

a) 10 cycles

b) 50 cycles

Figure 32

Positive (PbO_2) electrodes (15Ah, without pulses)

a) 10 cycles

b) 50 cycles

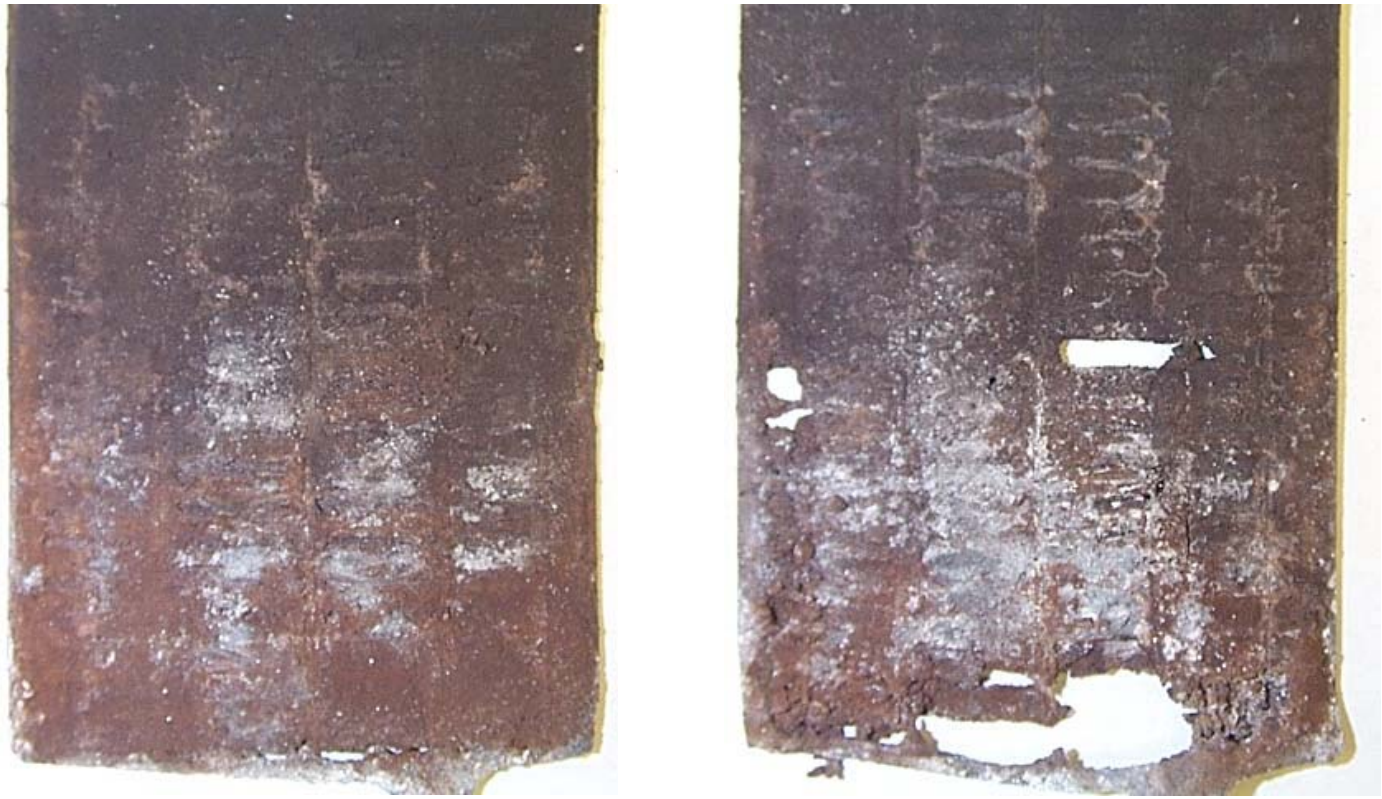

Figure 33

Micromorphology: negative plate (Pb, 15Ah) after 10 cycles (without pulses)

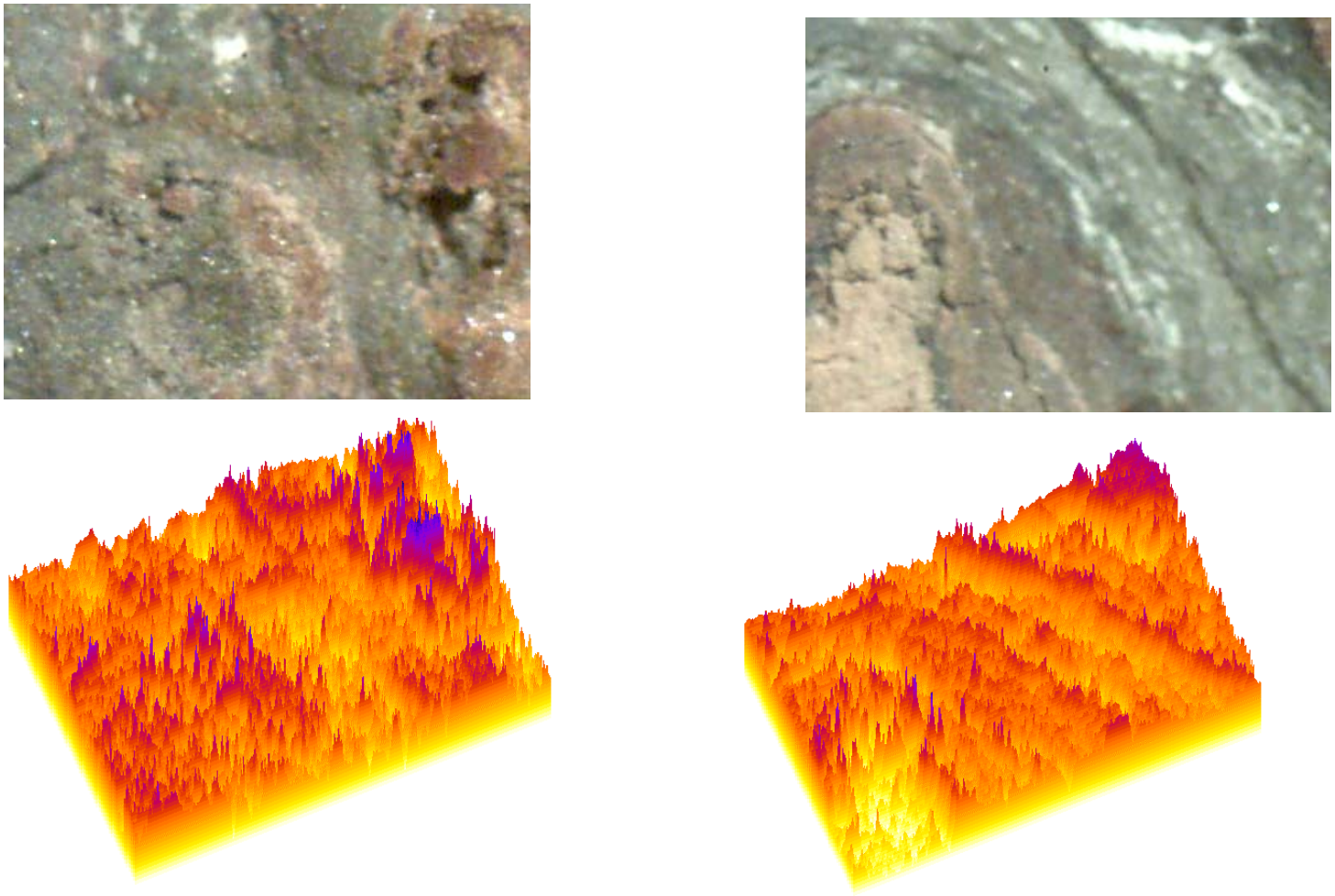

Figure 34a

Micromorphology: negative plate (Pb, 15Ah) after 25 cycles (without pulses)

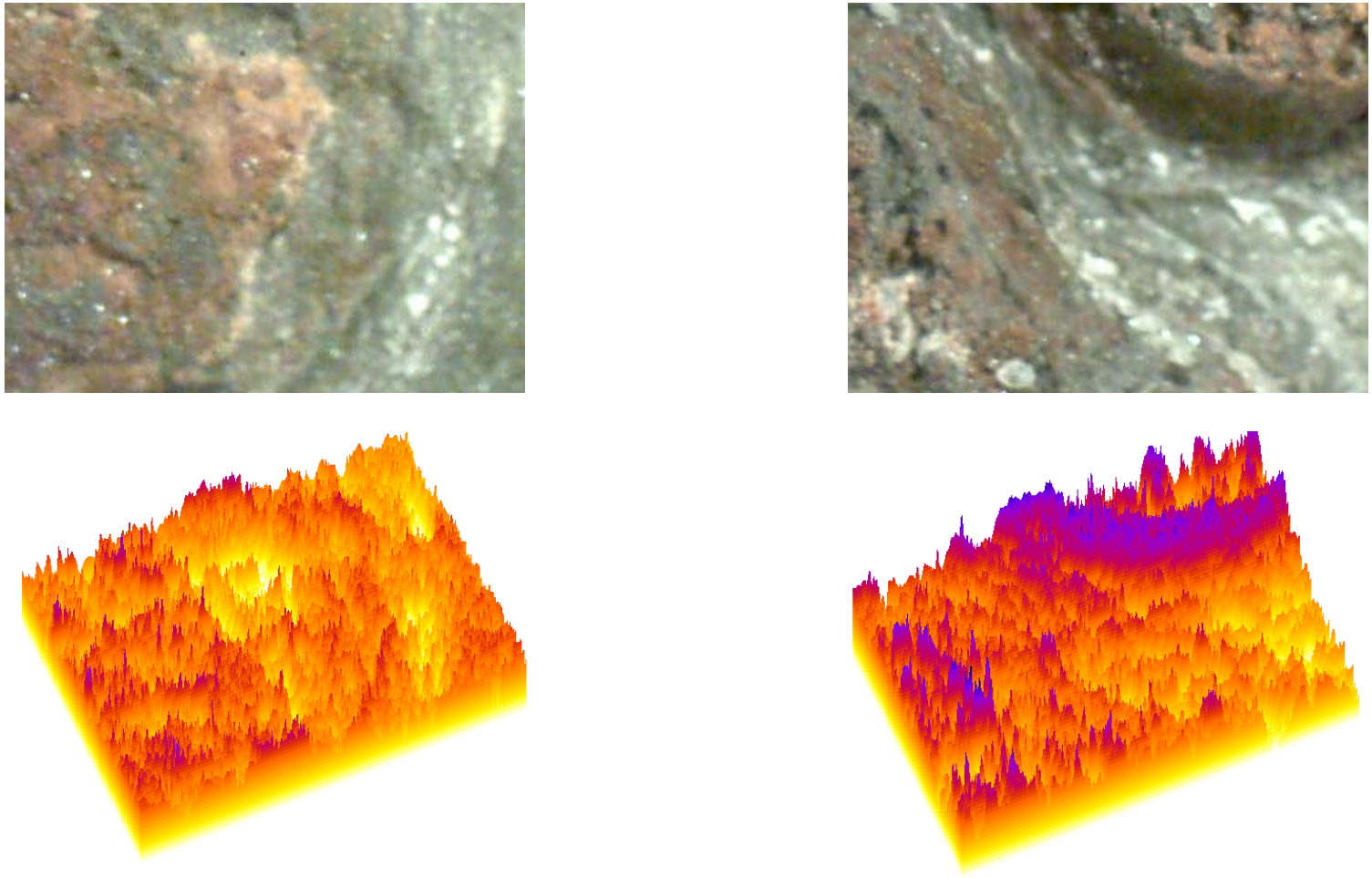

Figure 34b

Micromorphology: negative plate (Pb, 15Ah) after 50 cycles (without pulses)

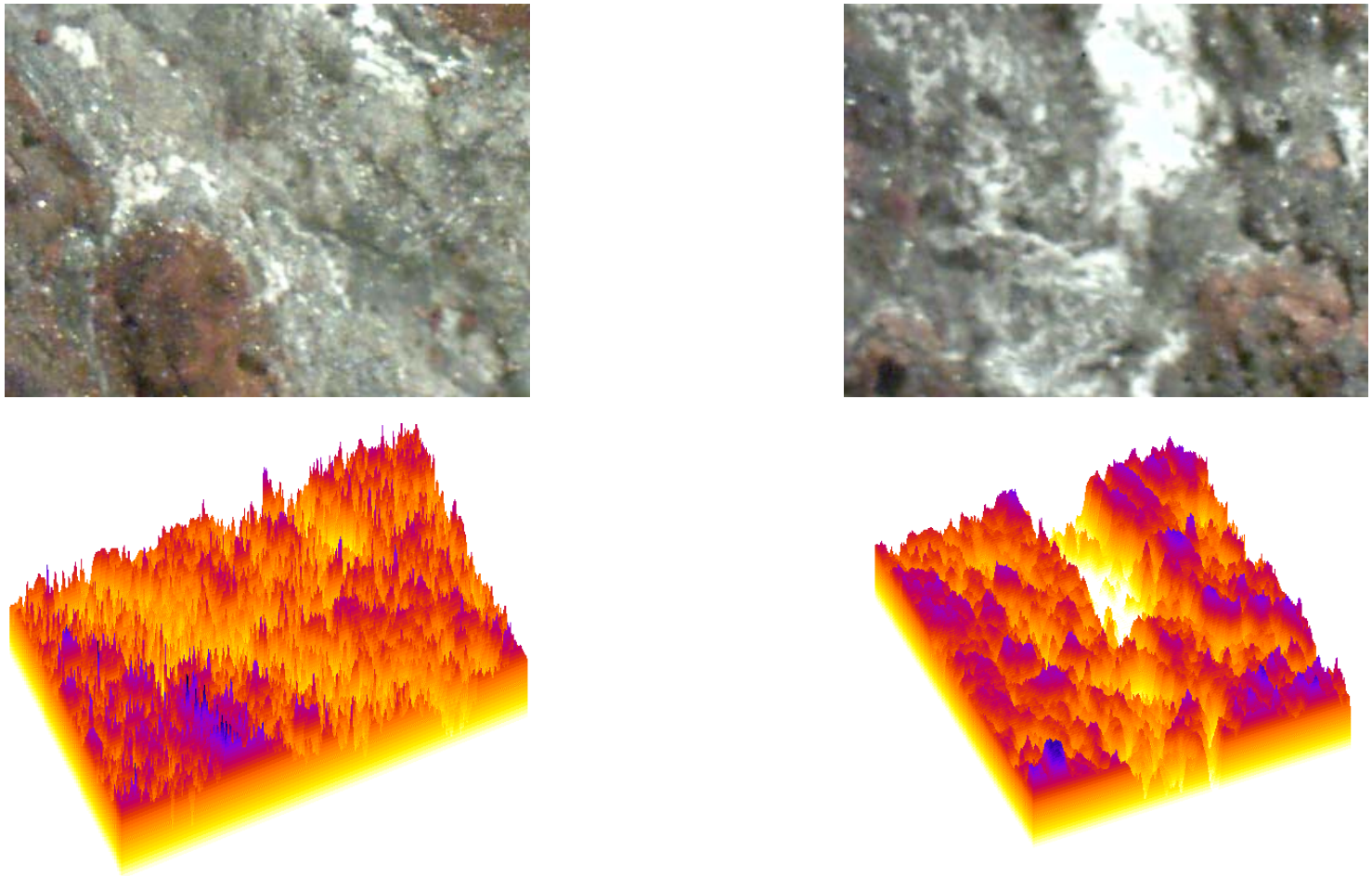

Figure 34c

Micromorphology: positive plate (PbO_2, 15Ah) after 10 cycles (without pulses)

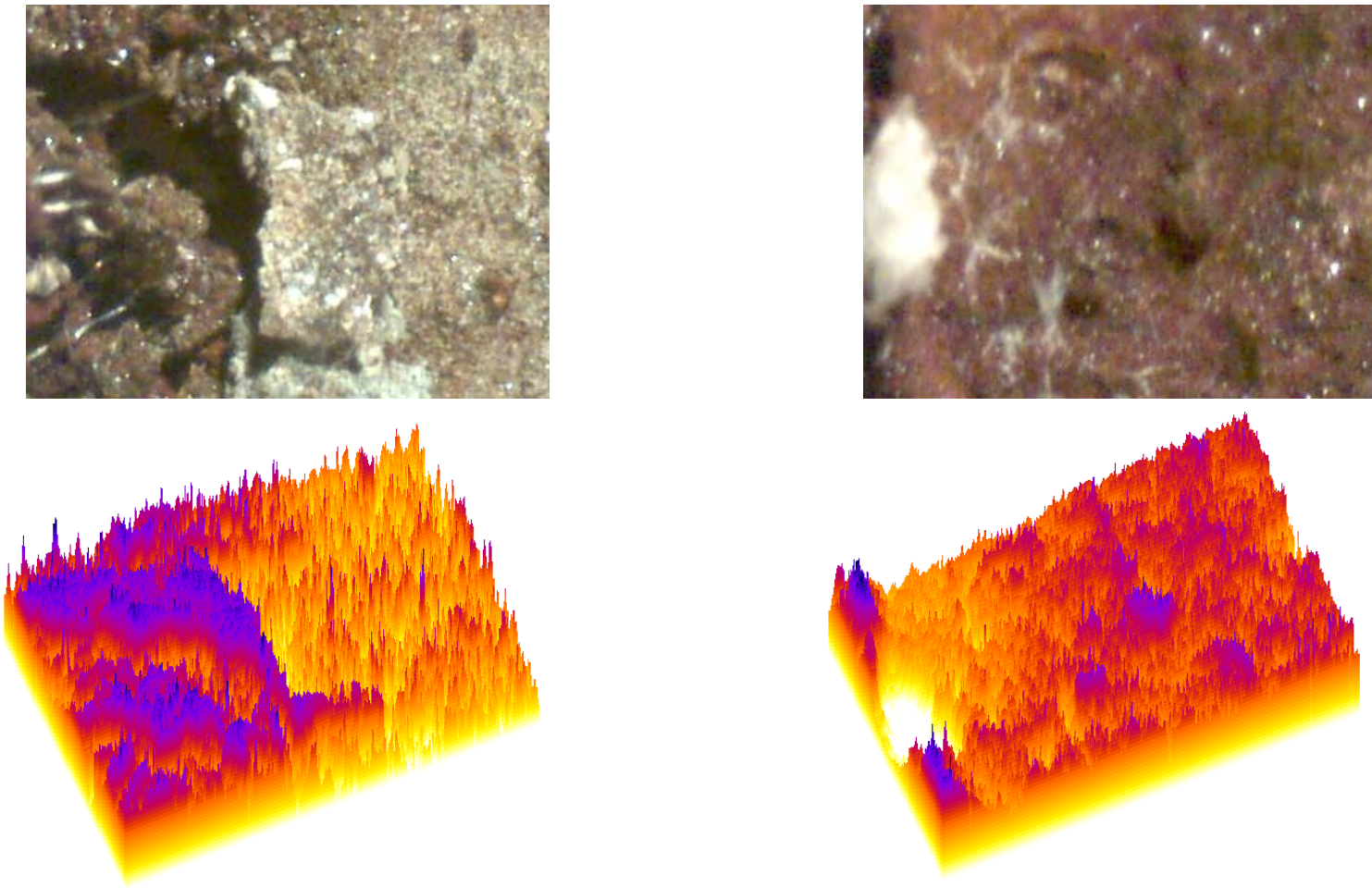

Figure 35a

Micromorphology: positive plate (PbO_2, 15Ah) after 25 cycles (without pulses)

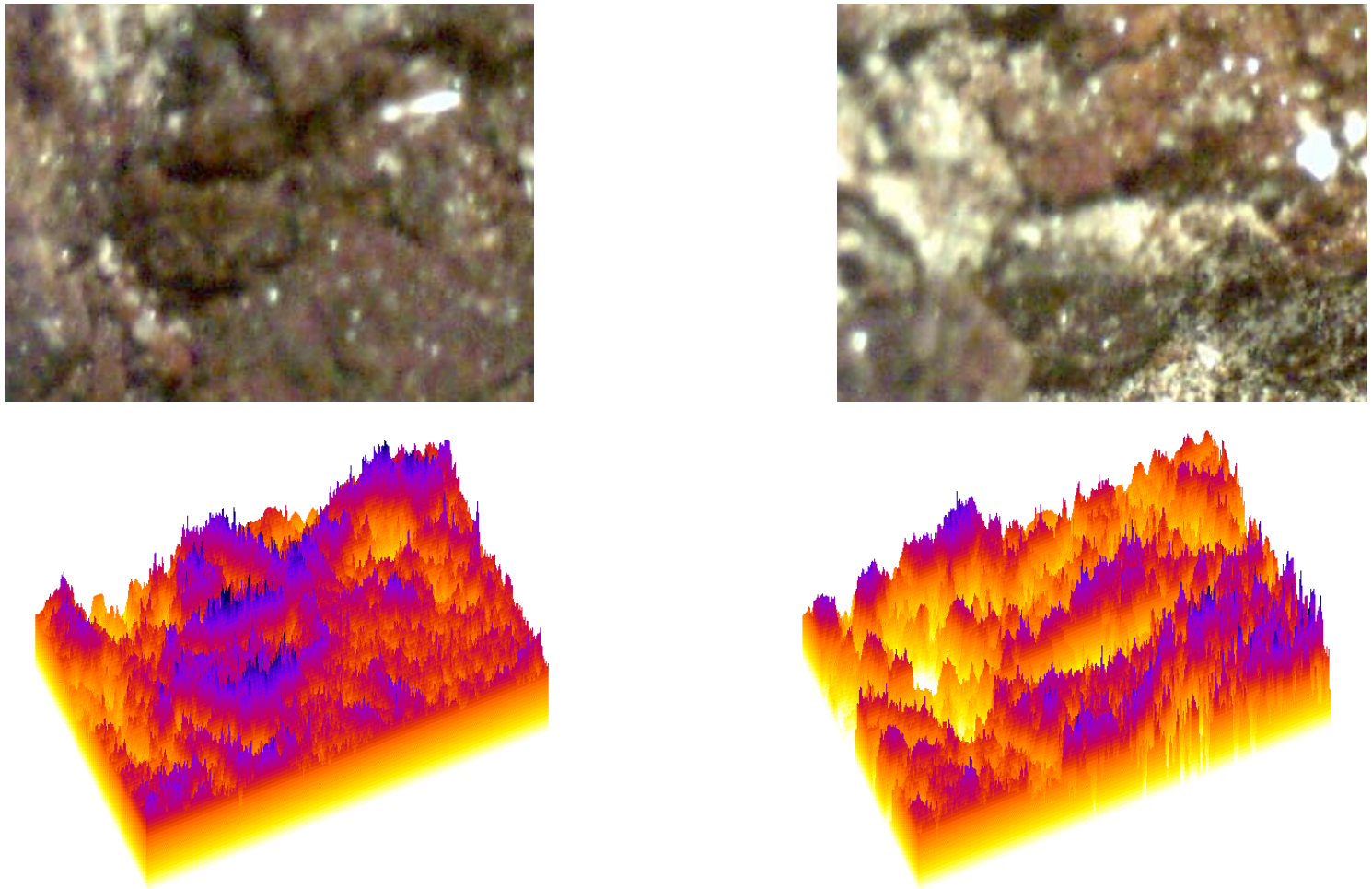

Figure 35b

Micromorphology: positive plate (PbO_2, 15Ah) after 50 cycles (without pulses)

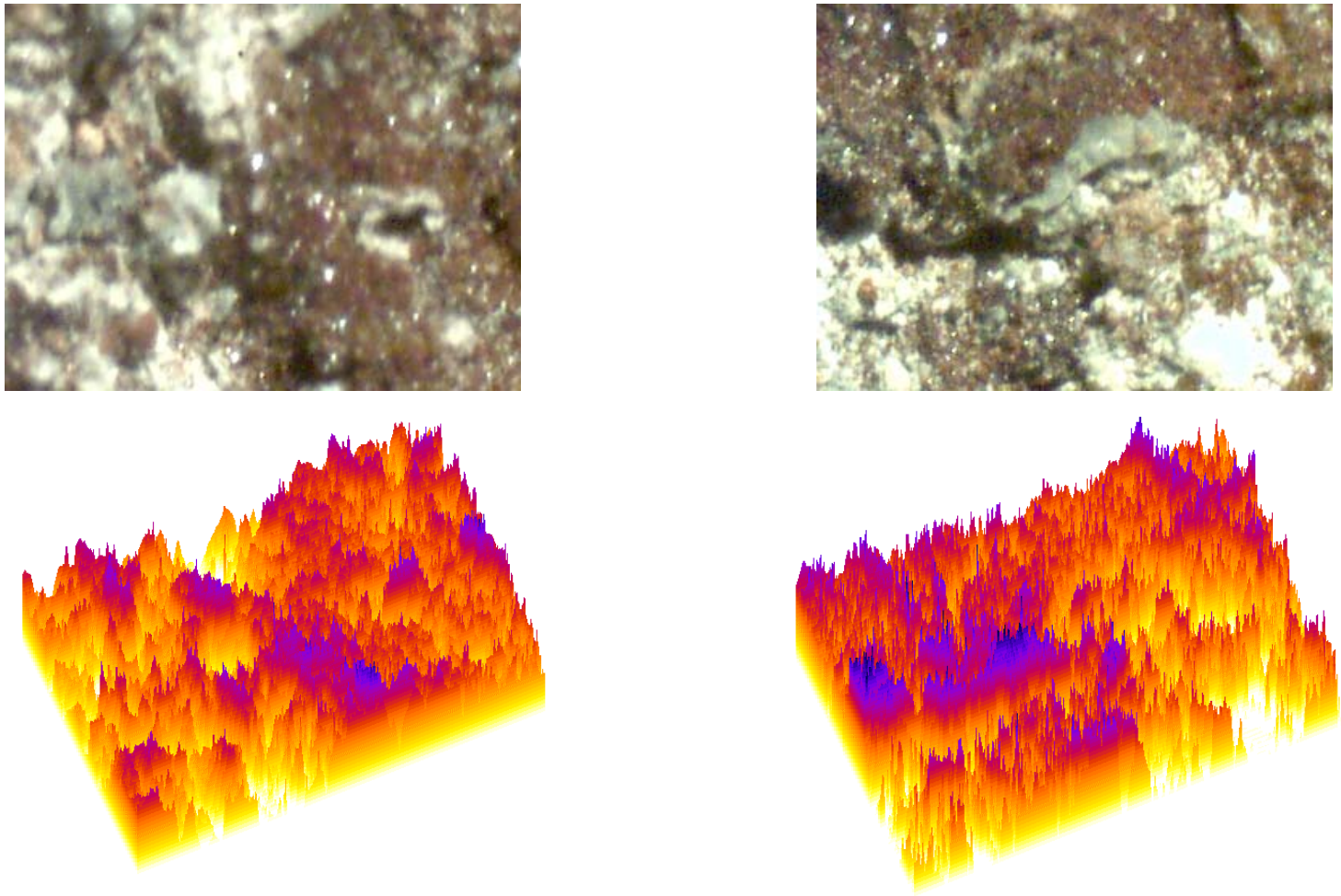

Figure 35c

number of cycles the difference between pulse and nonpulse charging is substantial. Generally, in this case the charge capacity is almost two times higher for the batteries charged (50 cycles) with pulses, than for that charged without pulses.

Surface Morphology of Electrodes

Photographic images of negative (Pb) and positive electrodes removed from lead-acid batteries (15Ah) are shown in Figure 32 and 33 respectively. There is a significant difference in the shape of the electrodes. Some defects in the negative mass is observed. However, a most severe corrosion is observed for the positive electrode after 50 cycles of charge/discharge without pulses. About 20-25% of positive mass is lost apparently due to the sludging and shedding process.

Microscopic images recorded in the specular reflectance mode show the microscopic changes of surface morphology with the increase of number of scans during charge/discharge process (Figures 34-35). The destruction of the positive electrode increases with the size and charge capacity of the battery. Figure 36 shows a photograph of positive and negative electrodes after 50 charge/discharge cycles without pulses of 20 Ah battery.

Macromorphology: 20Ah after 50 cycles (without pulses)

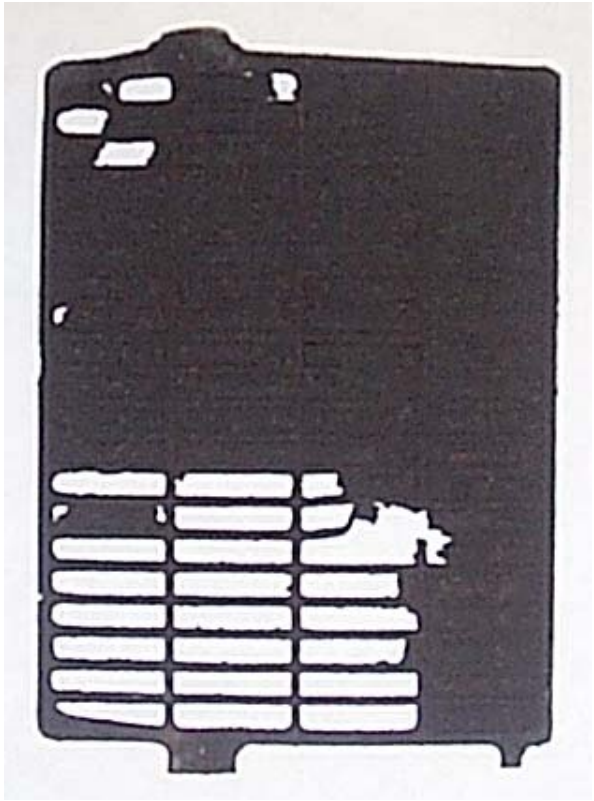

Positive, PbO_2

Negative, Pb

Figure 36

Micromorphology: negative plates, 20Ah (without pulses)

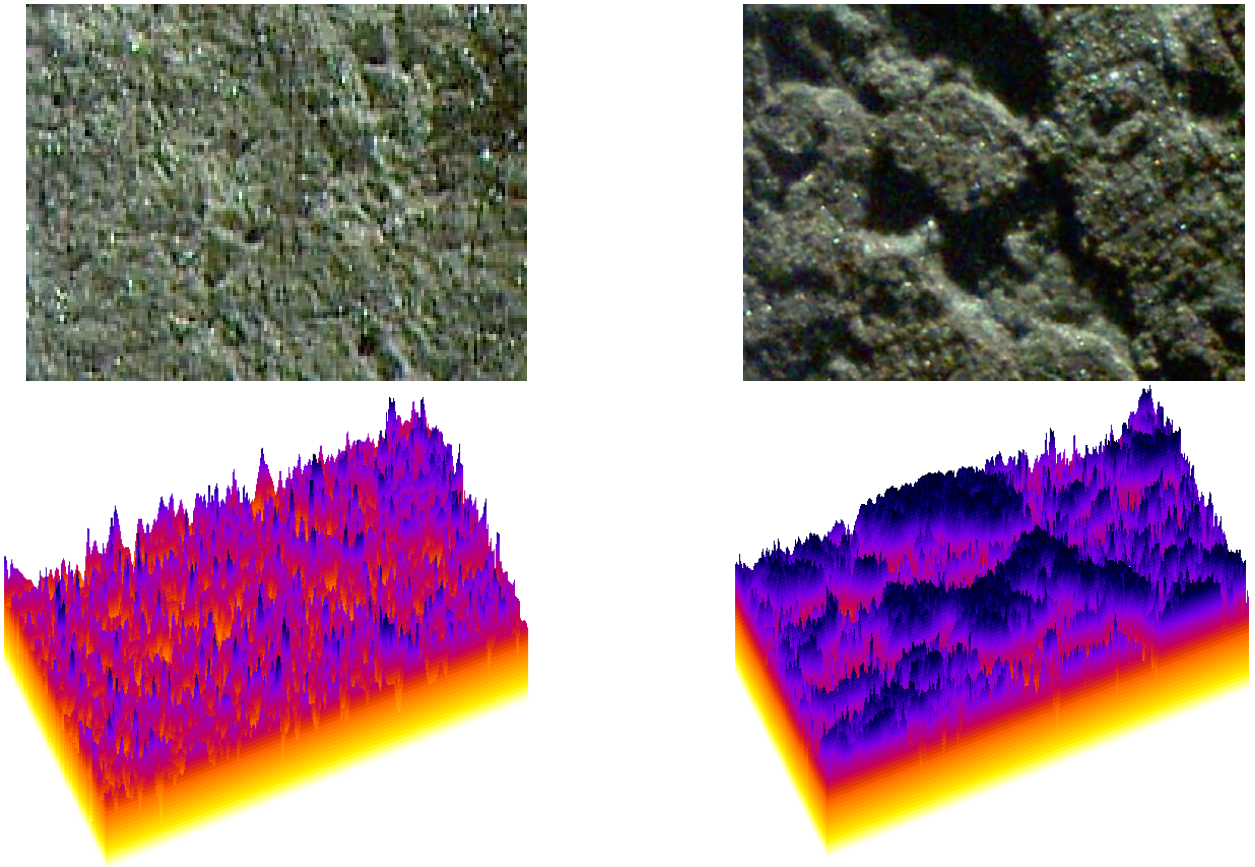

10 cycles

50 cycles

Figure 37

Micromorphology: positive plates, 20Ah, 10 cycles (without pulses)

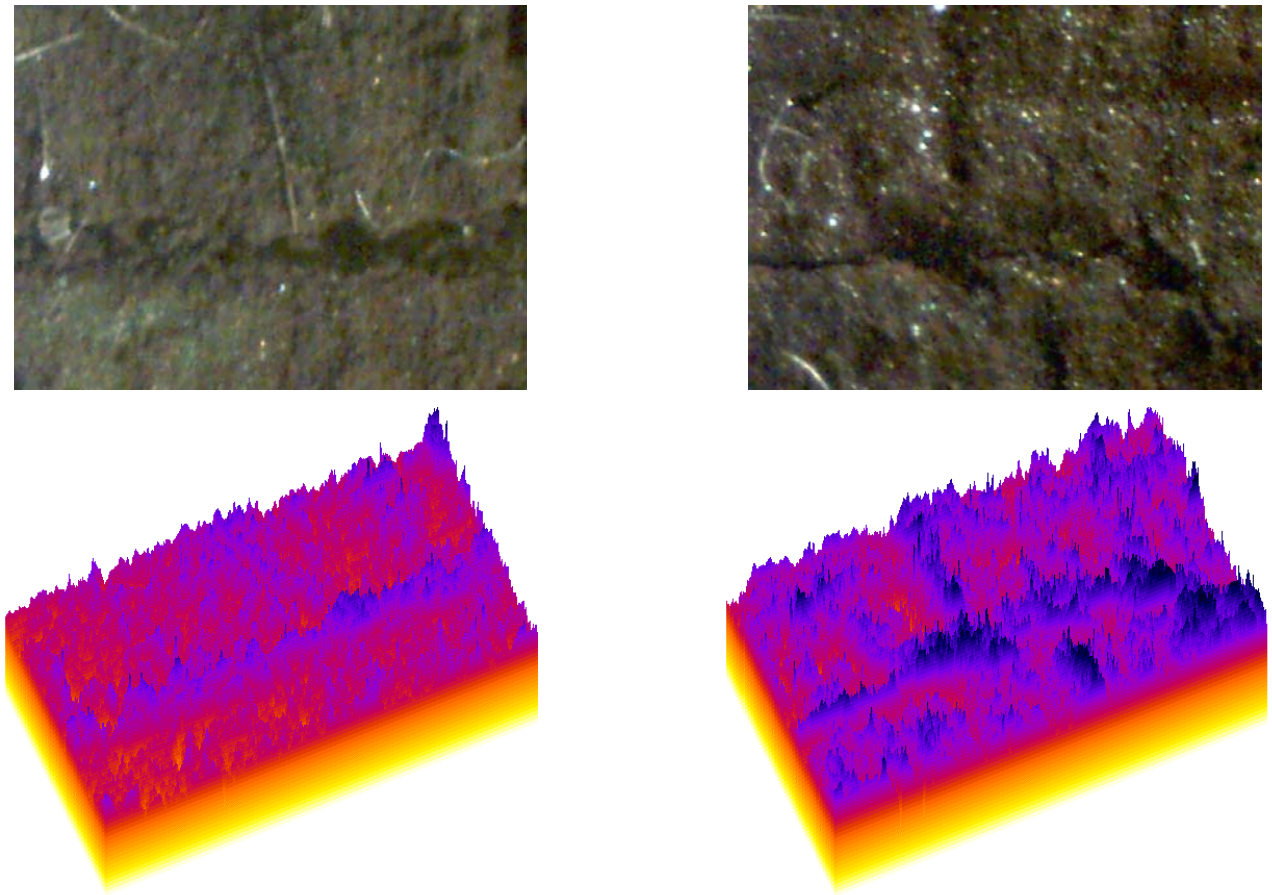

Figure 38a

Micromorphology: positive plates, 20Ah, 50 cycles (without pulses)

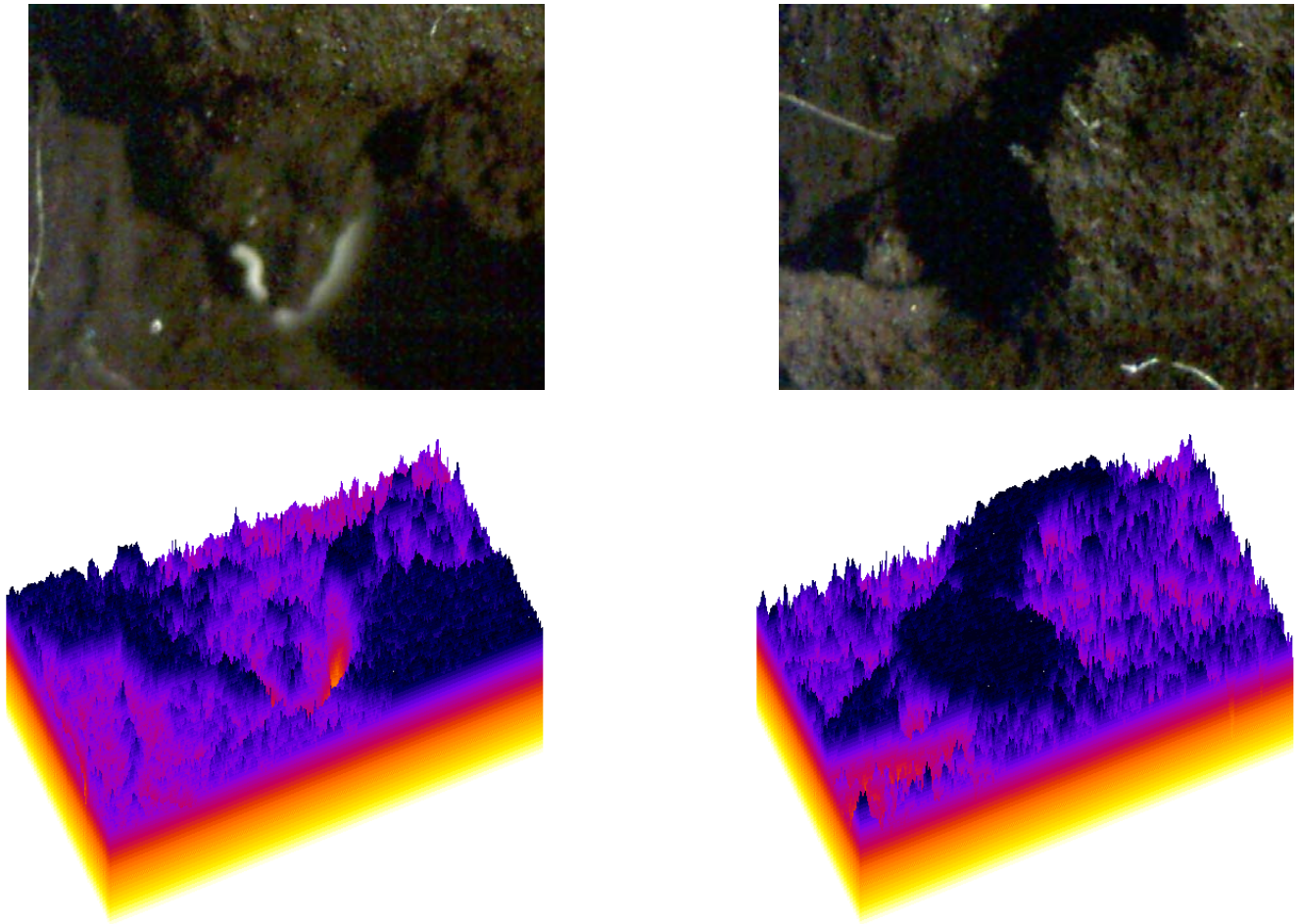

Figure 38b

An average of 35-45% of active mass of positive electrodes is lost after 50 cycles. This is significantly higher than the loss observed for 15 Ah battery. Significant changes in the morphology were also observed with the increasing number of cycles (Figures 37 and 38). Severe corrosion of negative electrode and the damage due to sludging of the positive plate can be noticed after 10 cycles of charge/discharge for 40 Ah battery without pulses (Figures 39 and 40). After 20 cycles about 10% of the active mass is already missed and after 50 cycles not only about 40% of PbO_2 mass but also a portion of Pb grid is missed. The microstructure of the electrodes also changed rapidly with the number of cycles and showed a lot of irregularities and craters (Figures 41 and 42).

The pulsation during the charge/discharge process makes a diametrical change of electrode morphology (Figures 43a and 44). This is especially true for the positive plate. After 50 cycles the positive as well as negative electrode maintain their integrity. The positive electrode after 50 cycles of charge/discharge with pulses shows no apparent damage due to sludging or shedding. The morphology of this electrode is better than the morphology of electrode charged/discharged without pulses. The reflectance microscopic images show well organized smooth surface of the positive and negative electrodes without major craters and defects (Figures 45 and 46).

Electron scan microscopy

Electron scan microscopy images provide additional insiight to the morphology of electrodes of lead-acid battery charged/discharged with or without pulses. Positive electrodes charged/discharged 50 times without pulses show a formation of large crystals on the surface (Figure 47). Electron scan micrographs of positive electrodes charged/discharged with this same number (50) of cycles with pulses show no formation of large crystals. The surface of this electrode is composed with fine crystals (Figure 48) and shows some amorphous characteristics. The effect of formation of large crystals (presumably $PbSO_4$ crystals) on the surface of positive electrodes is more pronounced in the positive electrodes of large batteries charged/discharged without pulses (Figure 49). Positive electrodes of large batteries (40-60 Ah) show very uniform microcrystalline structure after charge/discharge cycles with pulses (Figure 50).

Negative plate (Pb), 40Ah, 50 cycles (without pulses)

Figure 39

Positive plate (PbO_2), 40Ah, 10 cycles (without pulses)

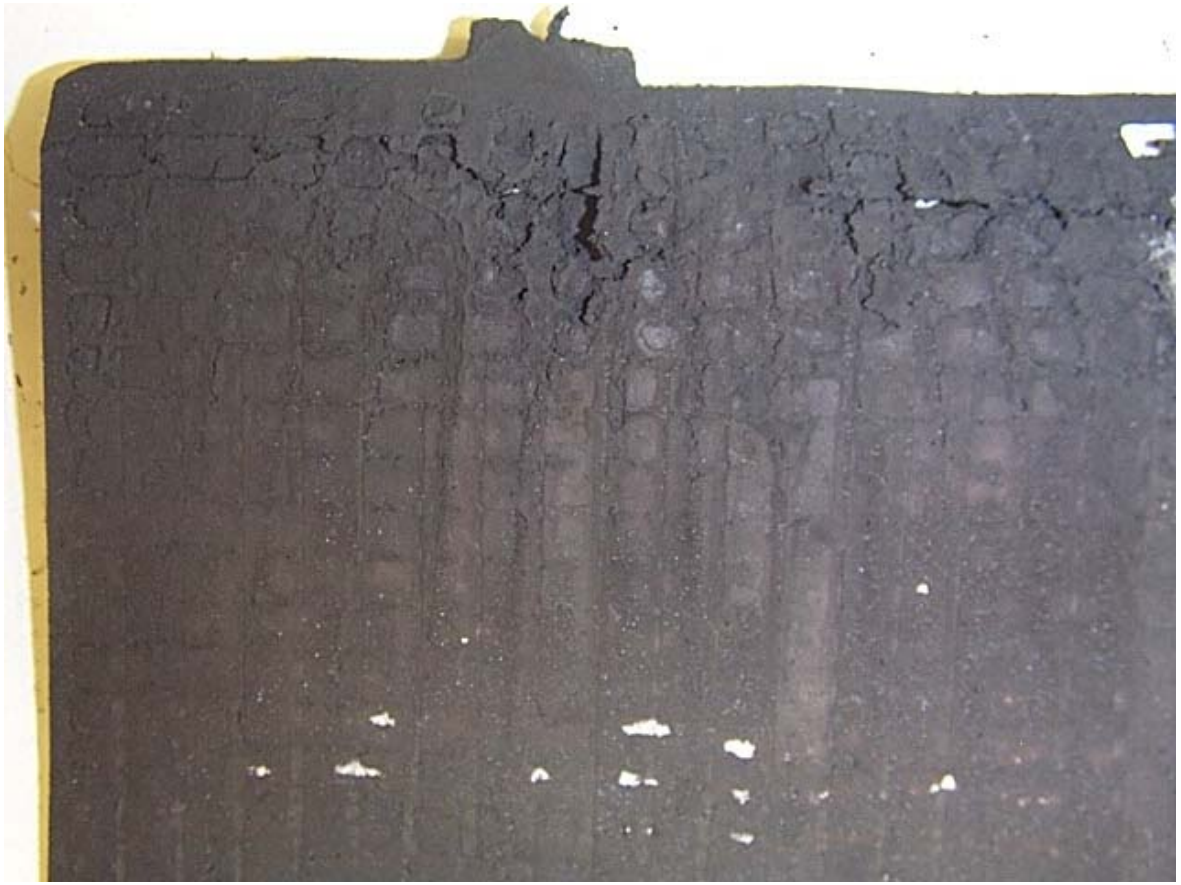

Figure 40a

Positive plate (PbO_2), 40Ah, 20 cycles (without pulses)

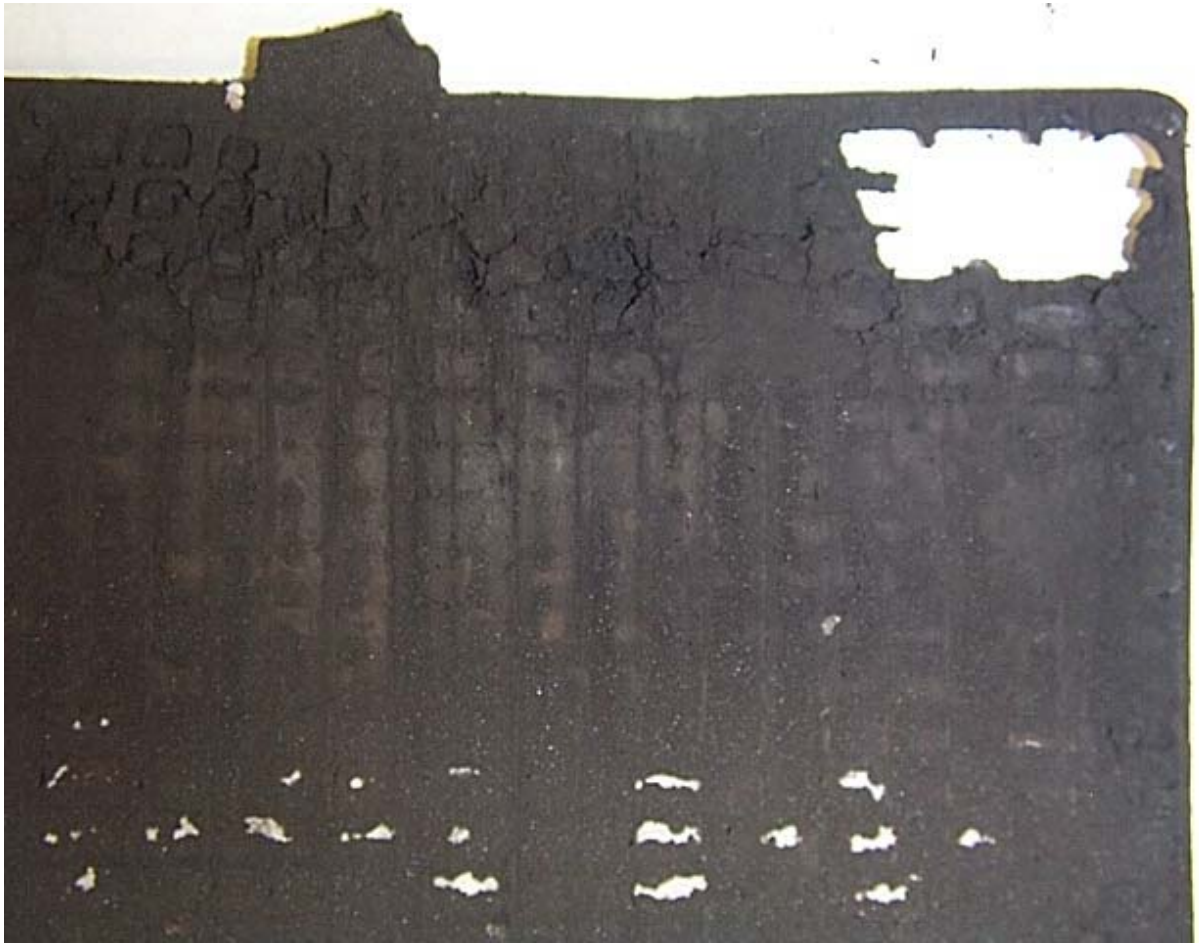

Figure 40b

Positive plate (PbO_2), 40Ah, 50 cycles (without pulses)

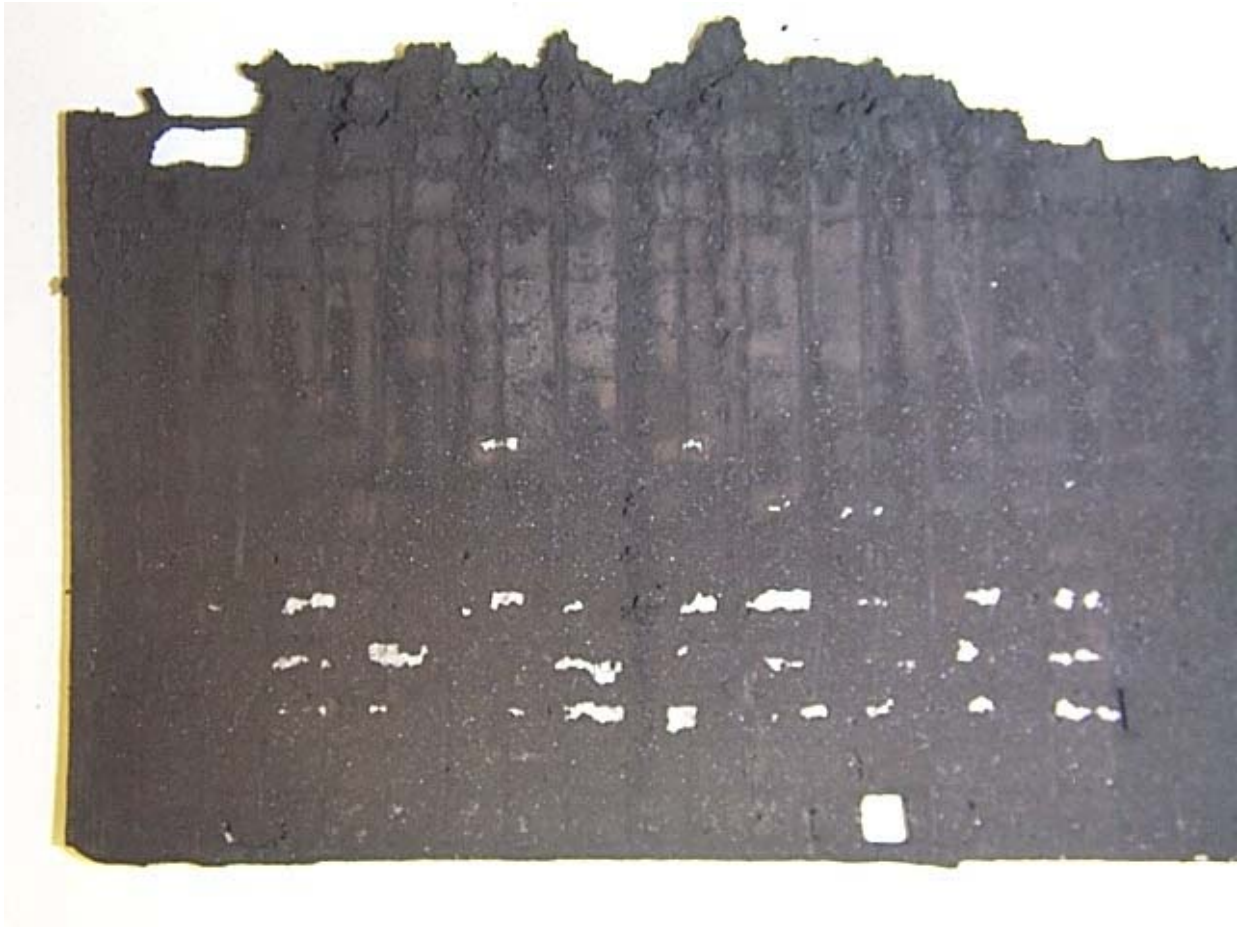

Figure 40c

Negative plate (Pb), 40Ah, 10 cycles (without pulses)

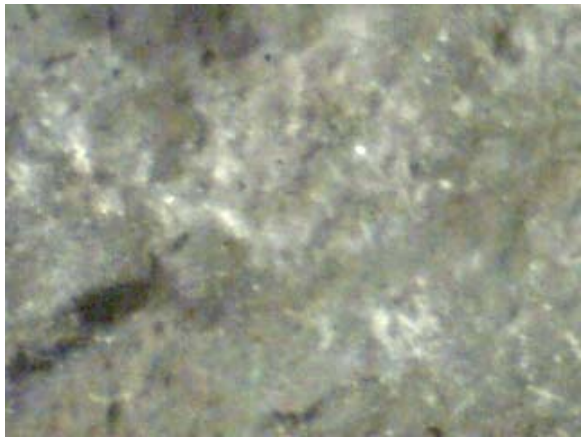

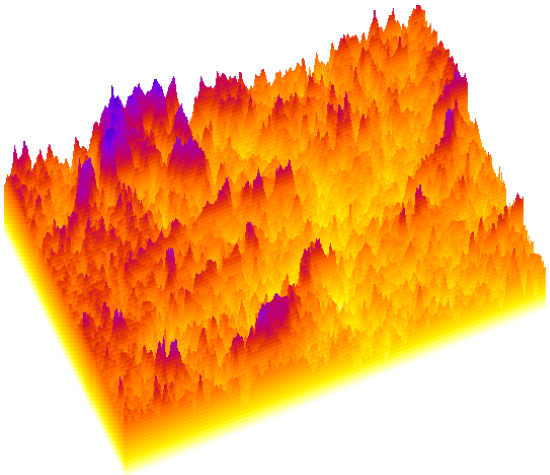

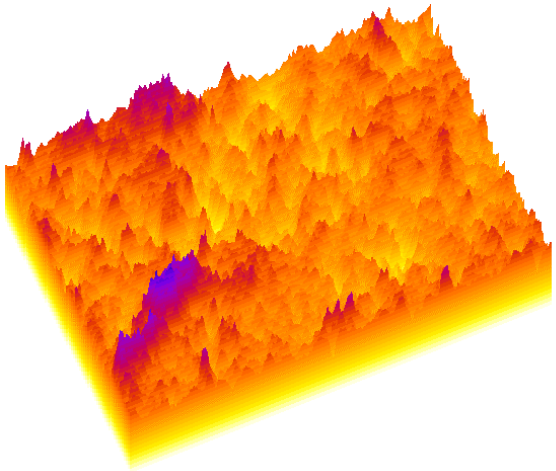

Figure 41a

Negative plate (Pb), 40Ah, 50 cycles (without pulses)

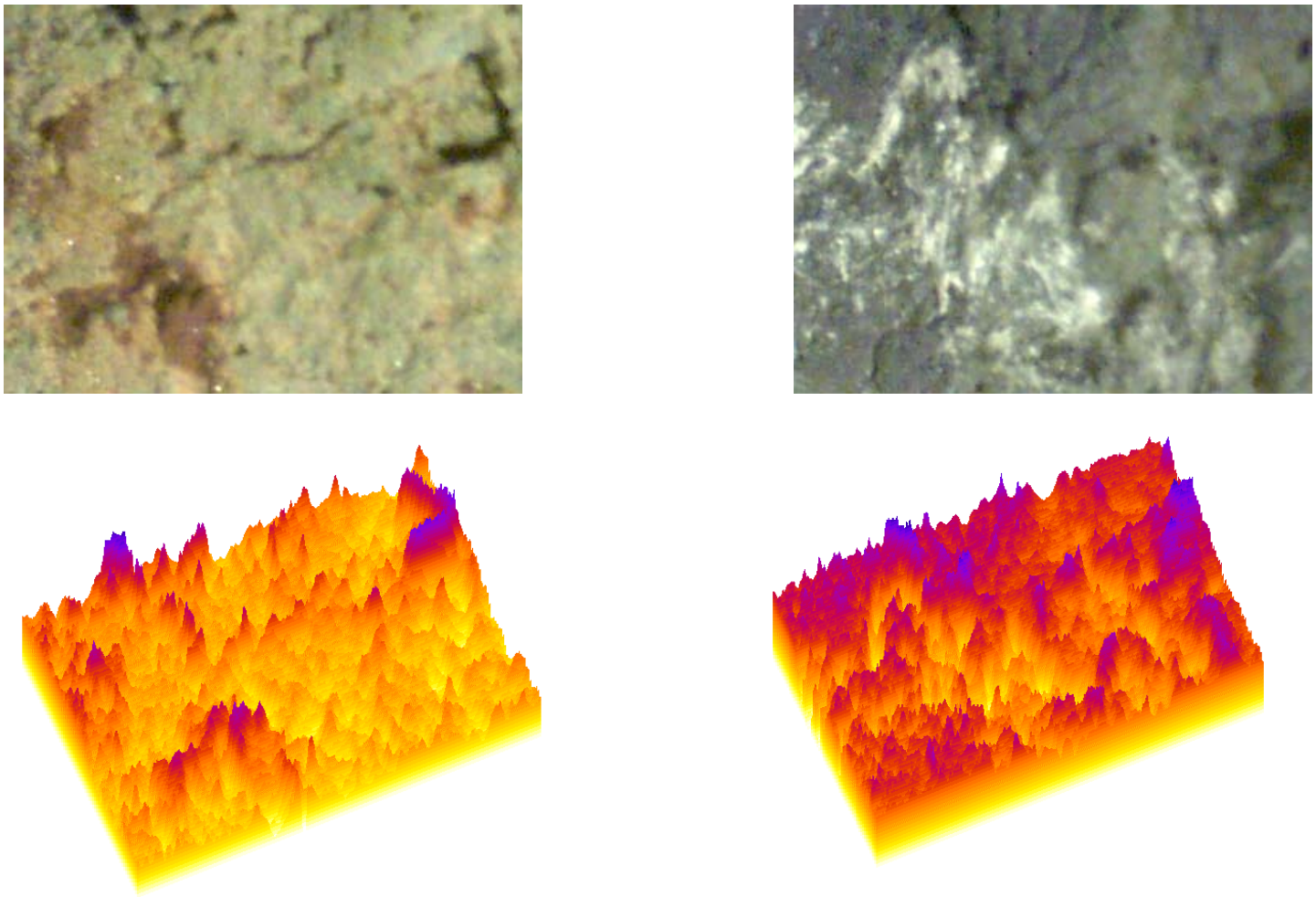

Figure 41b

Positive plate (PbO_2), 40Ah, 10 cycles (without pulses)

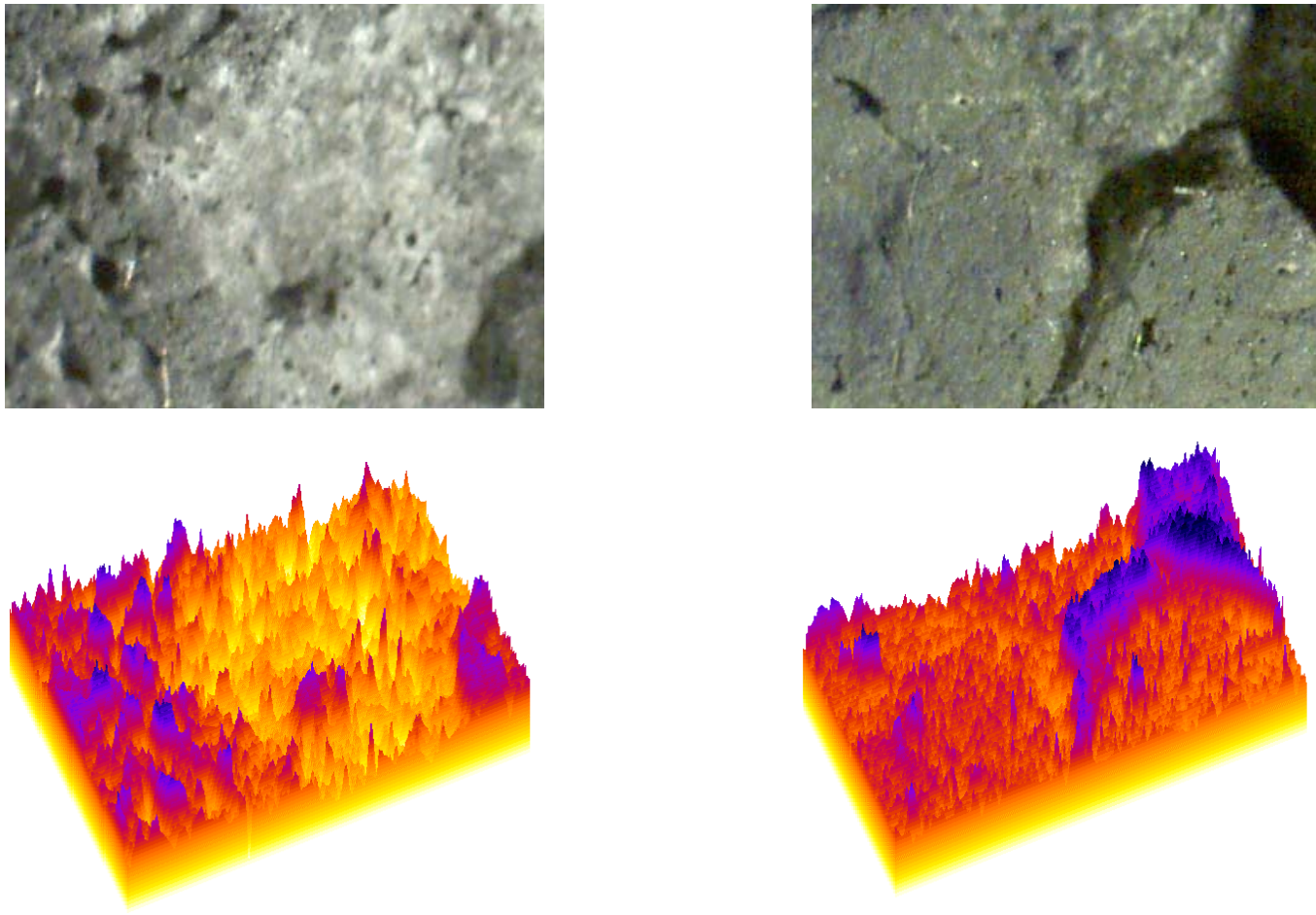

Figure 42a

Positive plate (PbO_2), 40Ah, 25 cycles (without pulses)

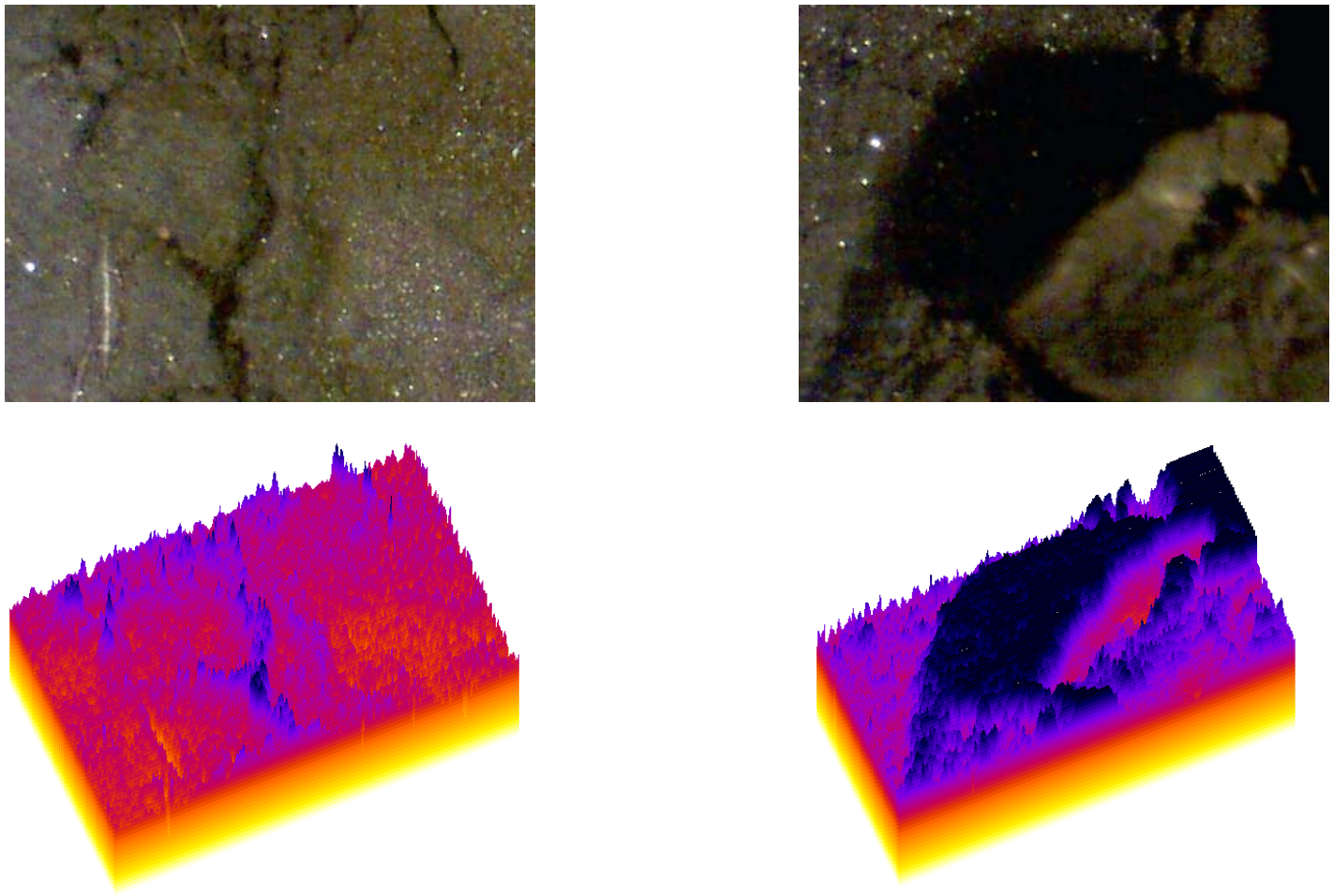

Figure 42b

Positive plate (PbO_2), 40Ah, 50 cycles (without pulses)

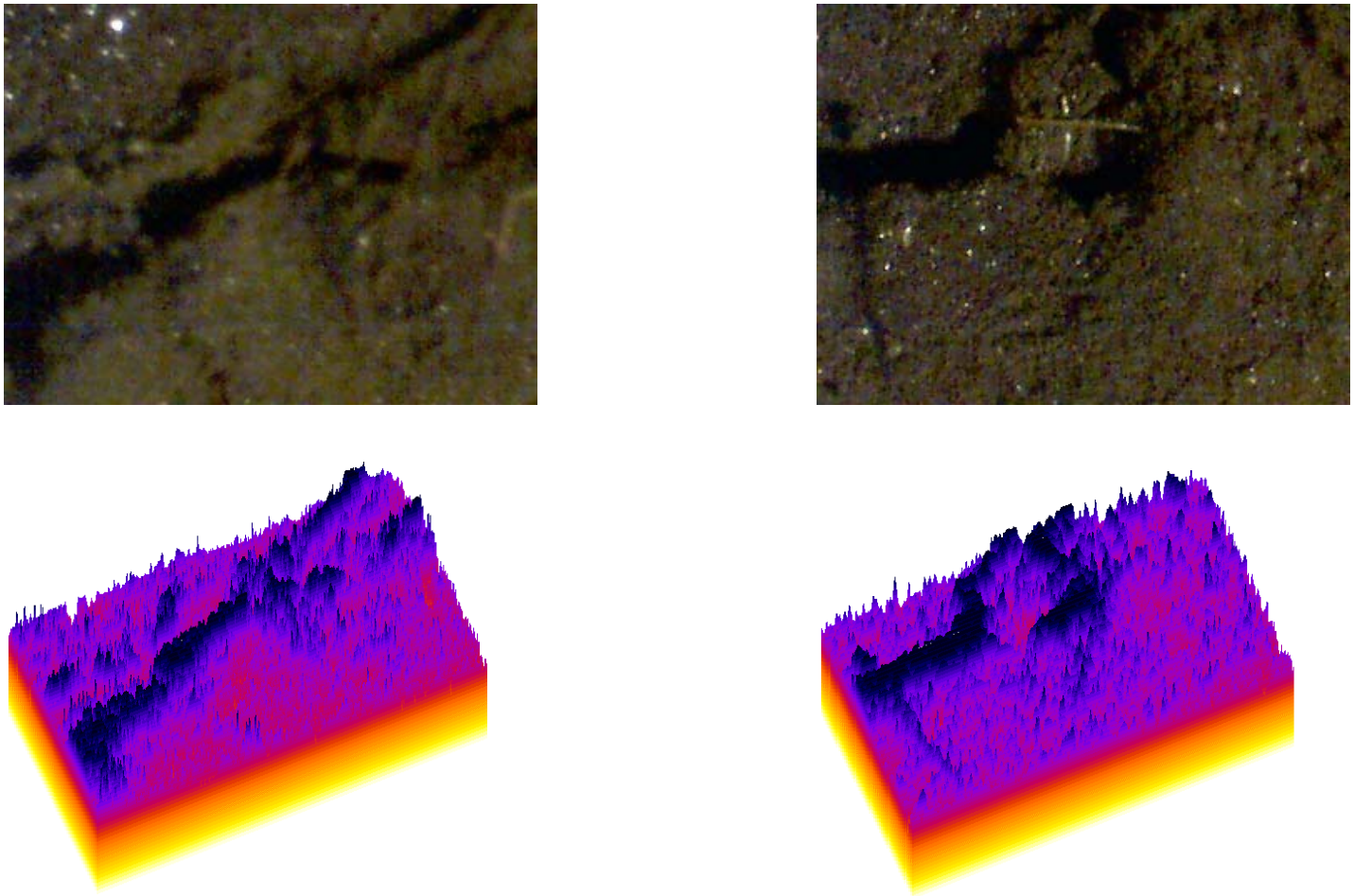

Figure 42c

Negative plate (Pb), 40Ah, 50 cycles (with pulses)

Figure 43

Positive plate (PbO_2), 40Ah, 10 cycles (with pulses)

Figure 44a

Positive plate (PbO_2), 40Ah, 25 cycles (with pulses)

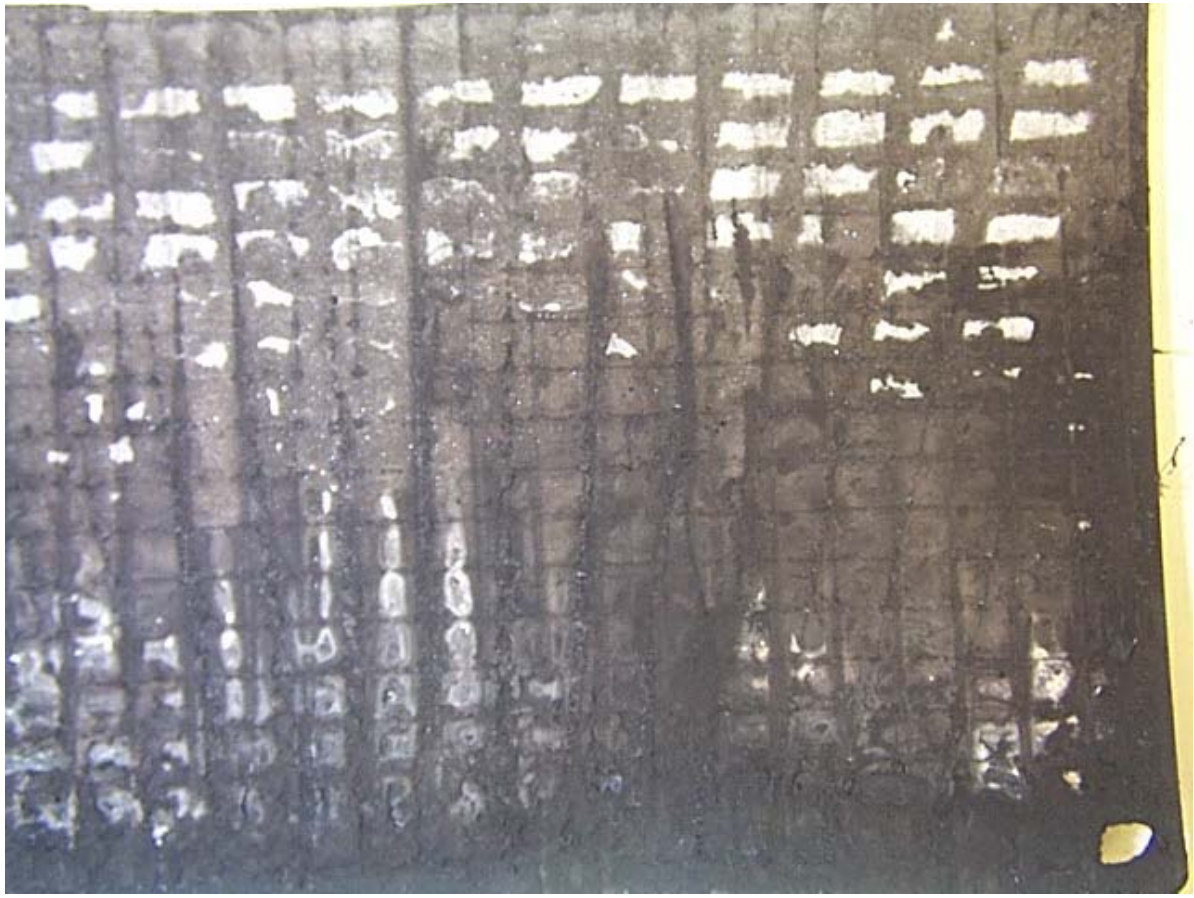

Figure 44b

Positive plate (PbO_2), 40Ah, 50 cycles (with pulses)

Figure 44c

Negative plate (Pb), 40Ah, 10 cycles (with pulses)

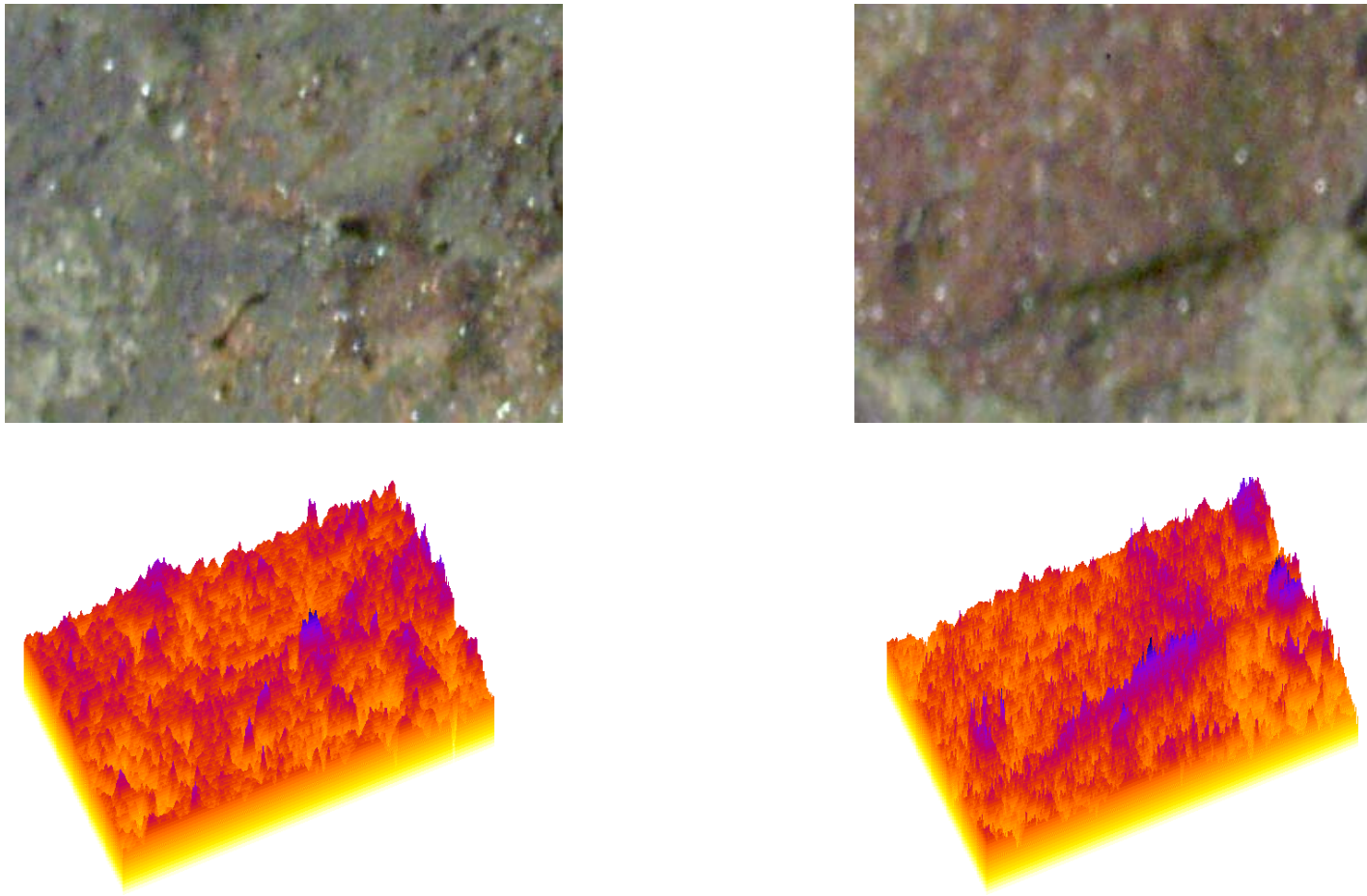

Figure 45a

Negative plate (Pb), 40Ah, 50 cycles (with pulses)

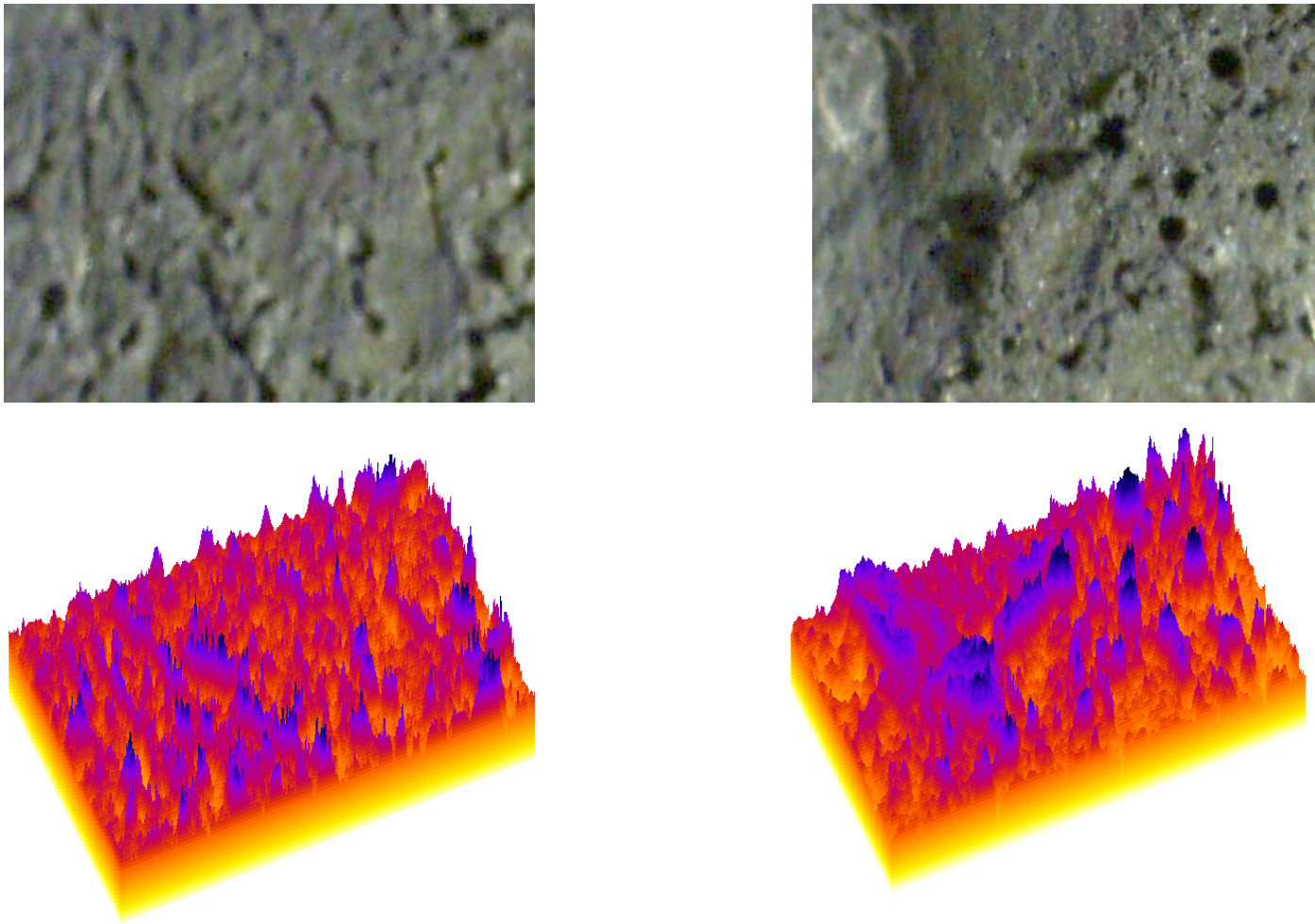

Figure 45b

Positive plate (PbO_2), 40Ah, 10 cycles (with pulses)

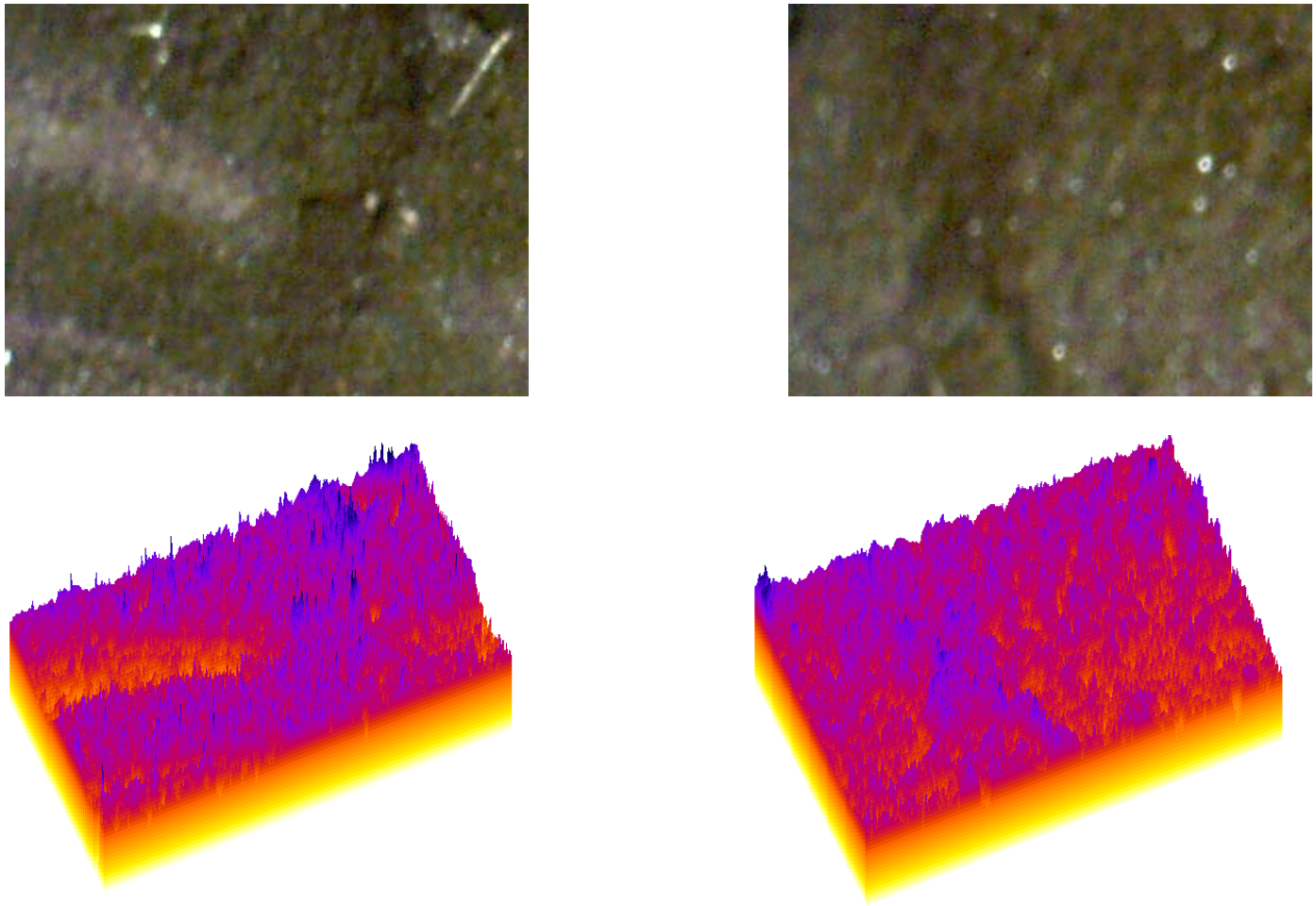

Figure 46a

Positive plate (PbO_2), 40Ah, 25 cycles (with pulses)

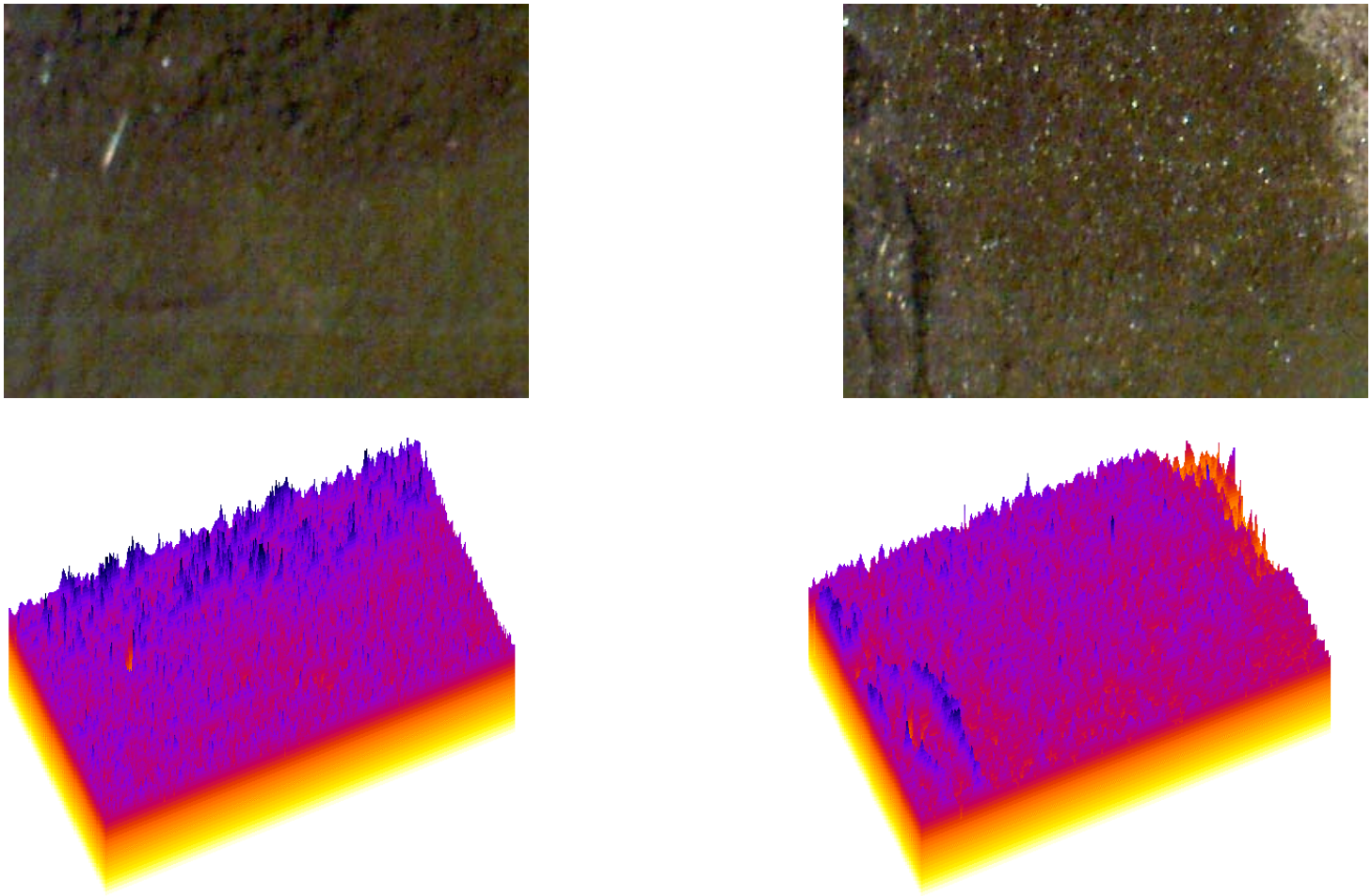

Figure 46b

Positive plate (PbO_2), 40Ah, 40 cycles (with pulses)

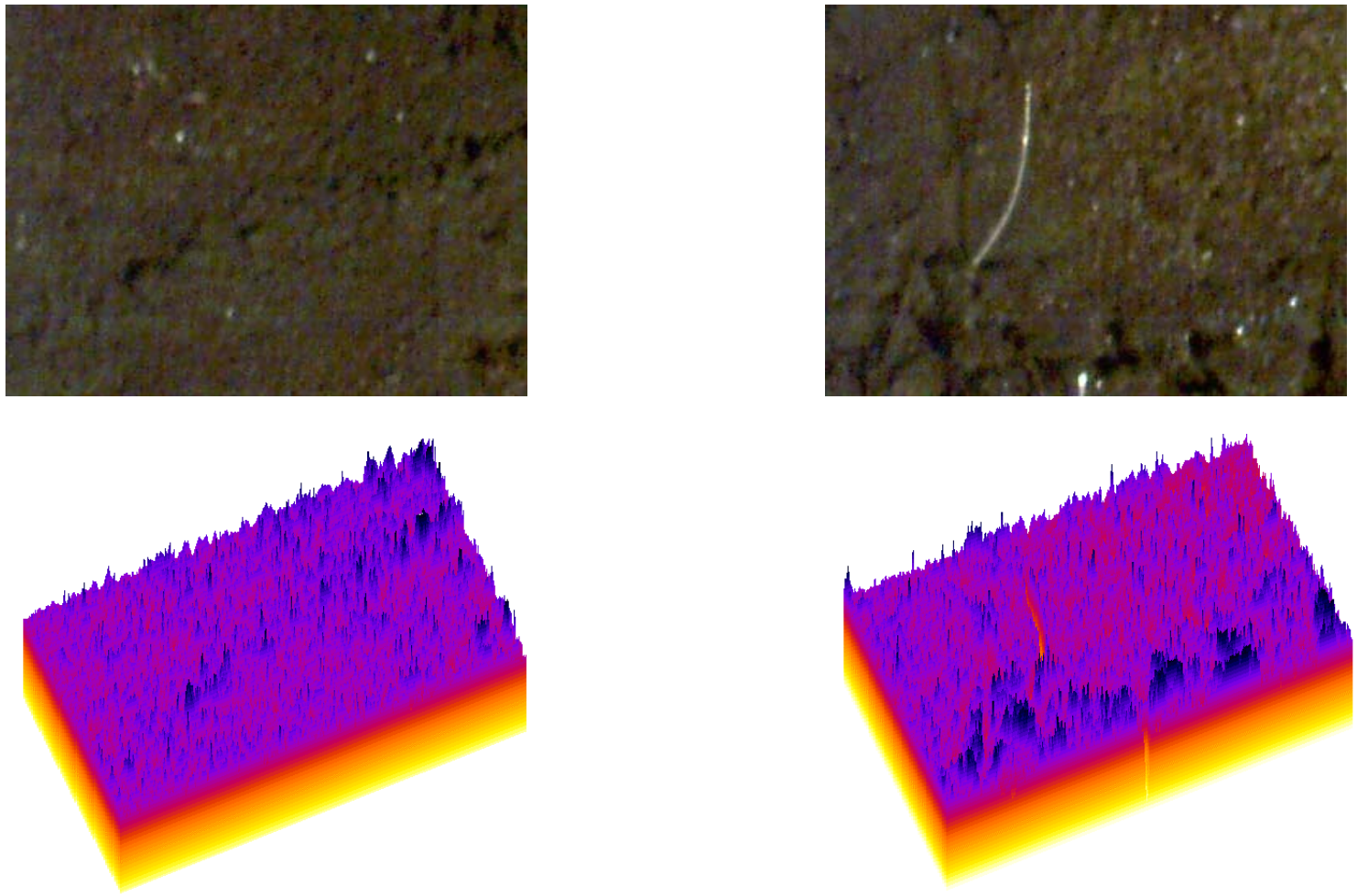

Figure 46c

Positive plate (PbO_2), 40Ah, 50 cycles (with pulses)

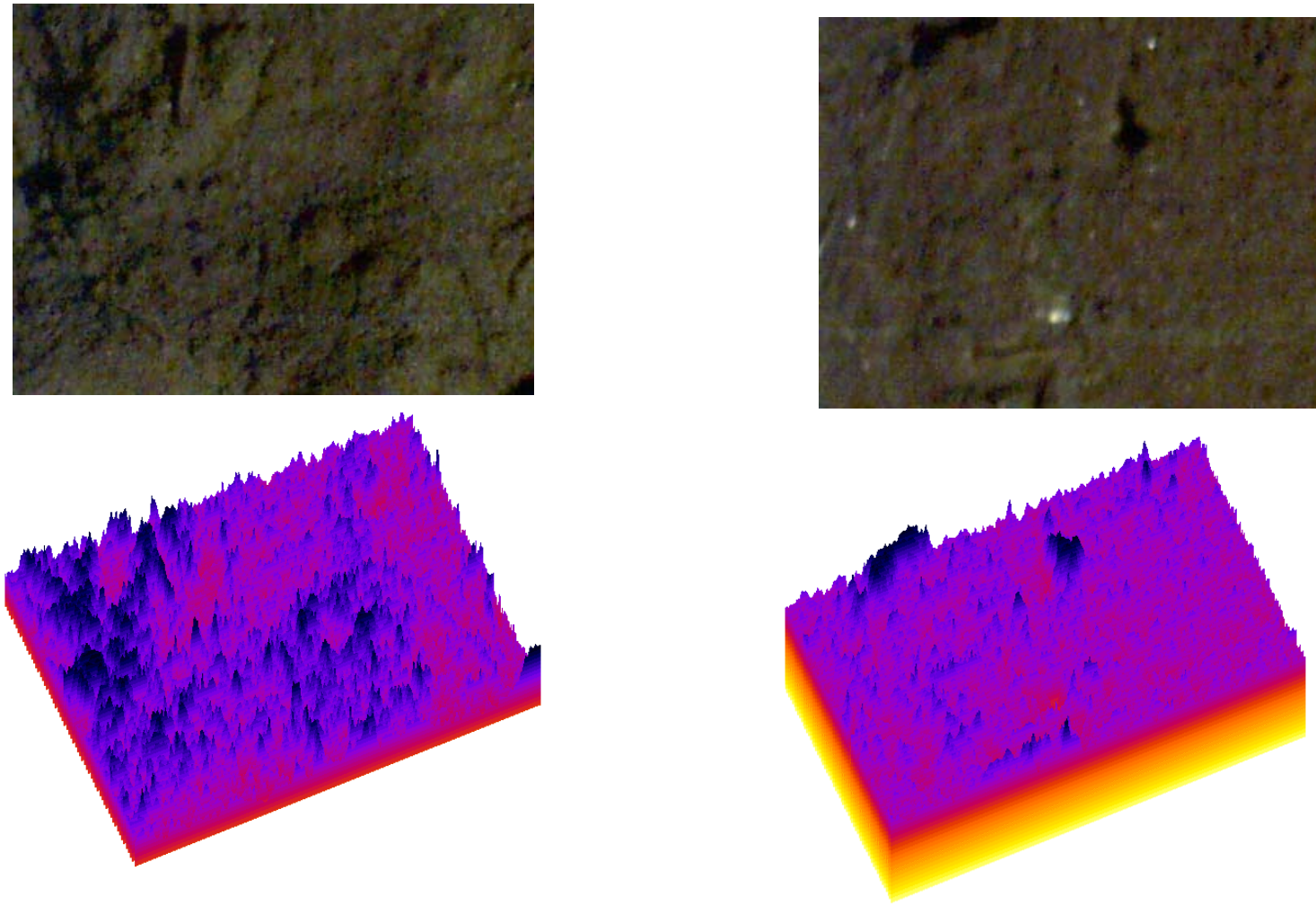

Figure 46d

a)

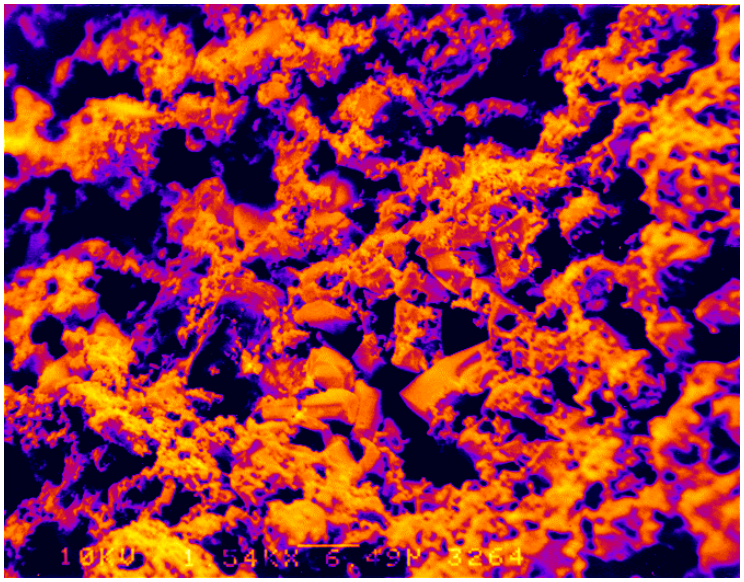

Positive electrode, no pulses, 20Ah,
after 50 cycles, magnification: 1500x

b)

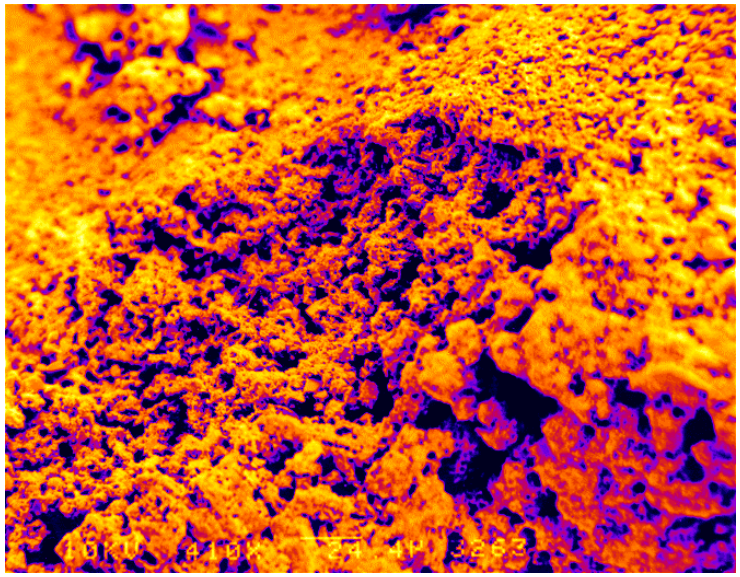

Positive electrode, no pulses, 20Ah,
after 50 cycles, magnification: 400x

Figure 47

a)

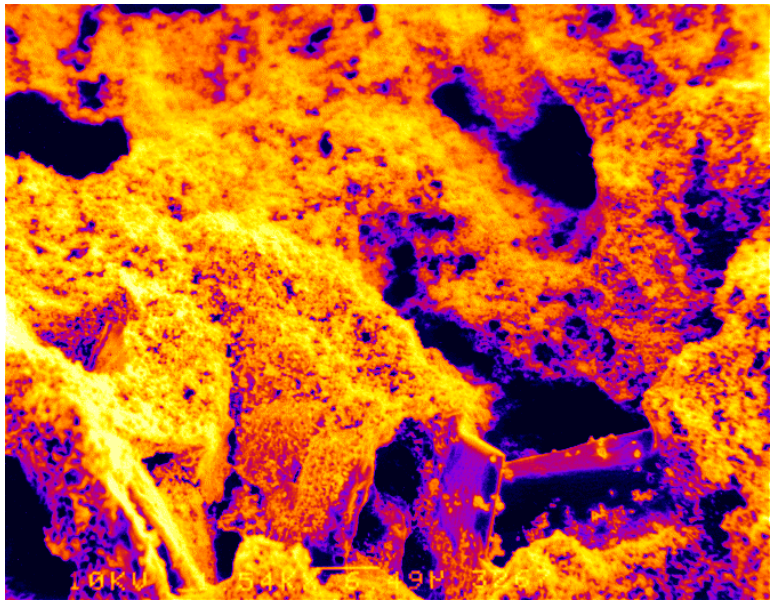

Positive electrode, with pulses, 20Ah, after 56 cycles, magnification: 1500x

b)

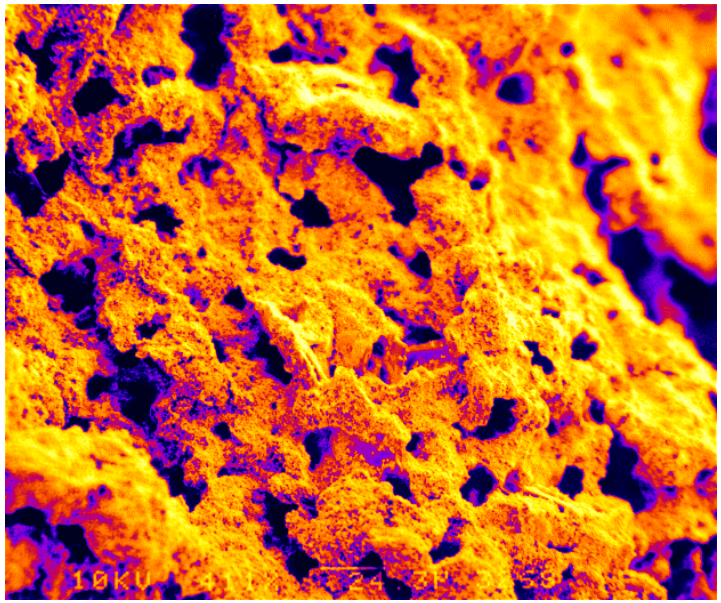

Positive electrode, with pulses, 20Ah, after 56 cycles, magnification: 400x

Figure 48

a)

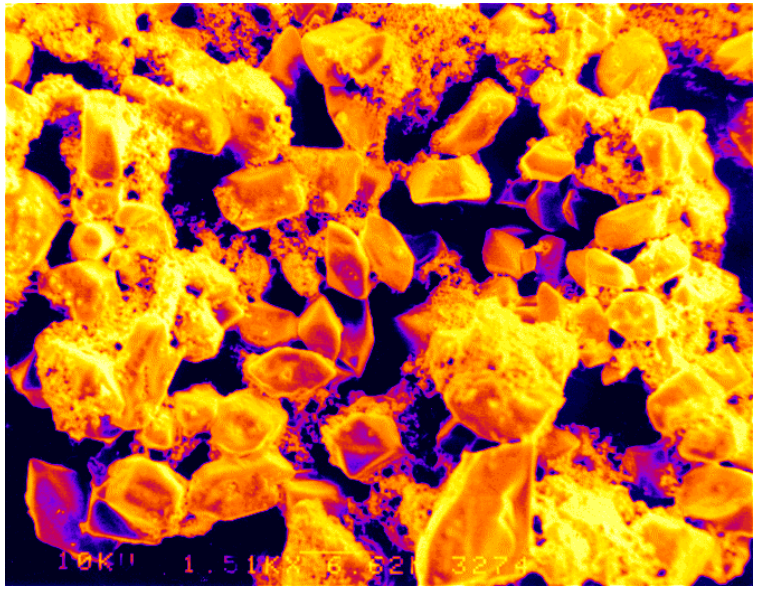

Positive electrode, no pulses, 40Ah, after 41 cycles, magnification: 1500x

b)

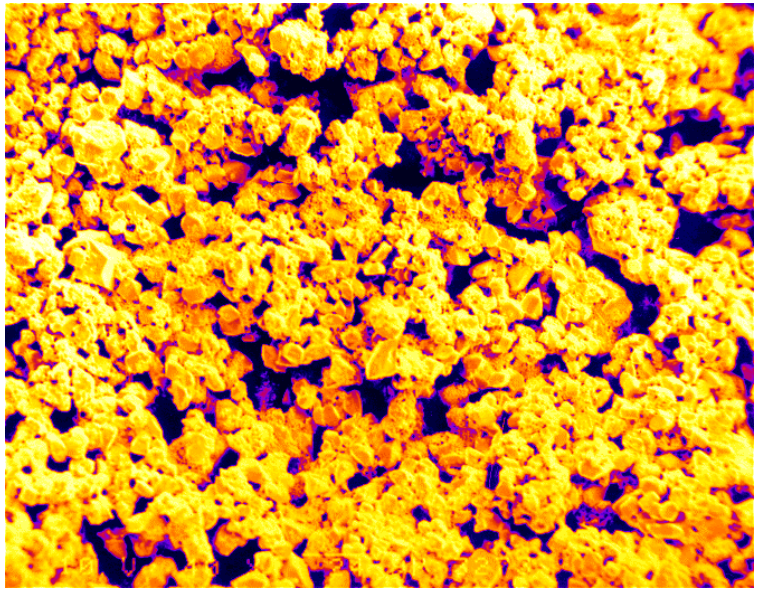

Positive electrode, no pulses, 40Ah, after 41 cycles, magnification: 400x

Figure 49ab

c)

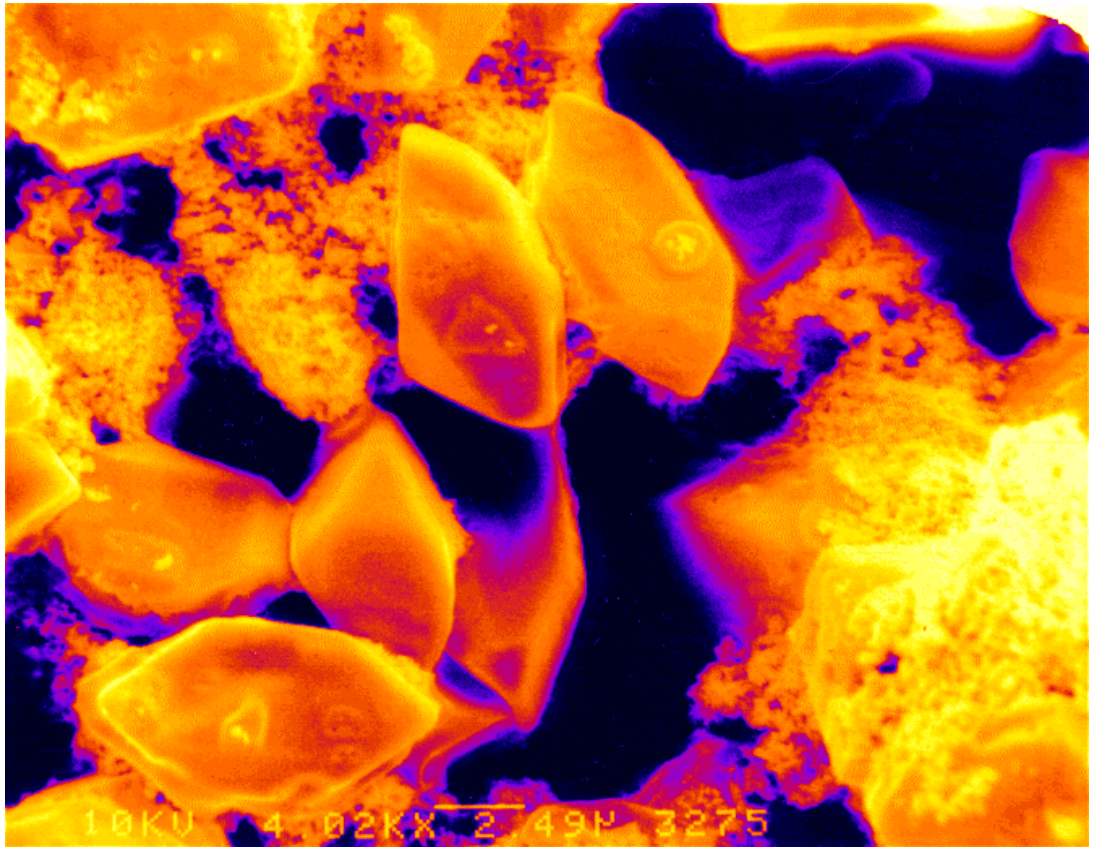

Positive electrode, no pulses, 40Ah, after 41 cycles,
magnification: 4000x

Figure 49c

a)

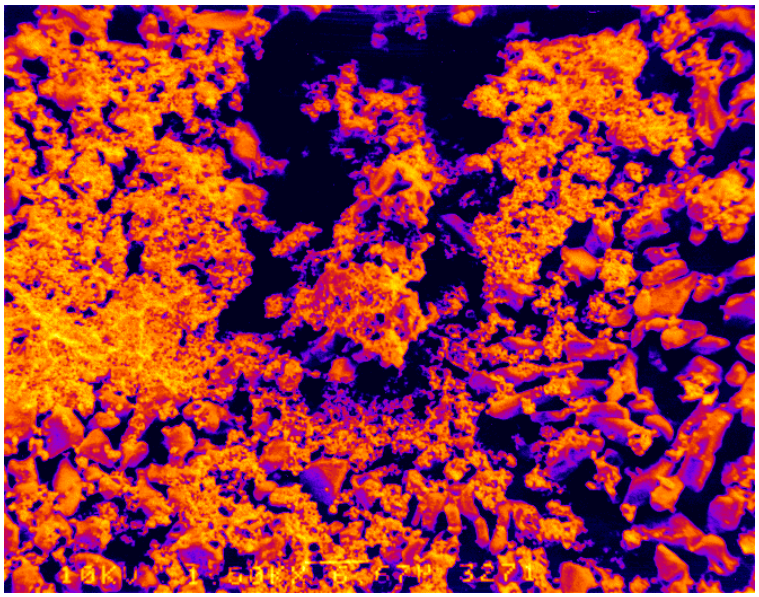

Positive electrode, with pulses, 40Ah, after 46 cycles, magnification: 1500x

b)

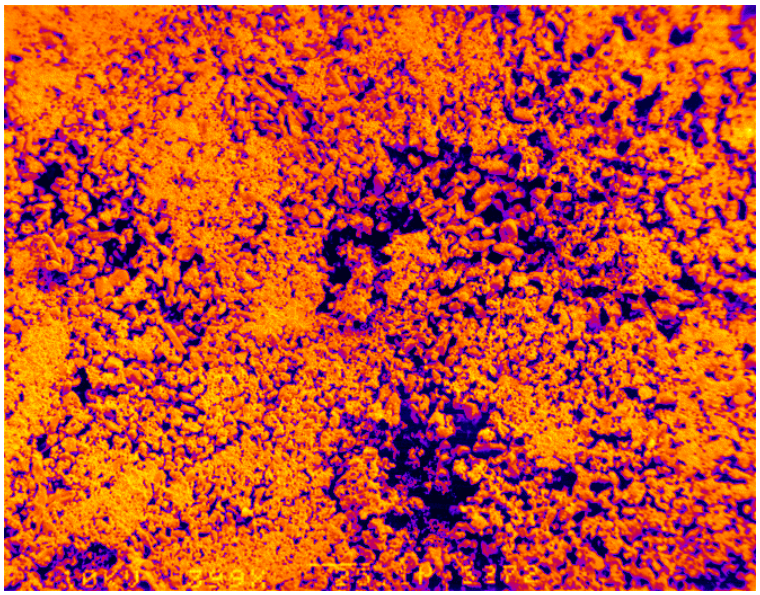

Positive electrode, with pulses, 40Ah, after 46 cycles, magnification: 400x

Figure 50

X-ray diffraction spectroscopy

The determination of components by means of x-ray diffraction is subject to several limitations. Usually constituents present in amounts of more than 5% are recognizable. Only highly symmetrical, well-crystallized compounds are detected at lower concentrations. Chemically prepared samples of α-PbO_2 and β-PbO_2, as well as samples taken during the formation of commercial lead-acid plates, nearly always show the same trend in intensities. For the determination of the amounts of dioxide modification the intensities of adjacent reflections can be measured. In modifications of the same substance mass absorption coefficients and equal densities are assumed. In a formed active material with an analytical determined content of 90% PbO_2 the crystalline constituents are placed at 23% α-PbO_2 and 43% β-PbO_2. The remaining 34% is usually considered amorphous. The x-ray diffraction was used in these studies to identify a proportion between PbO_2 and $PbSO_4$ crystallographic structure in the positive plates of lead-acid battery after the charge/discharge cycles without pulses. Figure 51 shows typical low resolution x-ray diffraction spectrum obtained for the positive plate of lead-acid battery (20 Ah) (lattice spacing in Å are listed for each major diffraction peak). High resolution spectra were used for computer assisted quantitative and qualitative analysis of PbO_2 electrode (Figure 52).

Positive plate (20Ah), without pulses

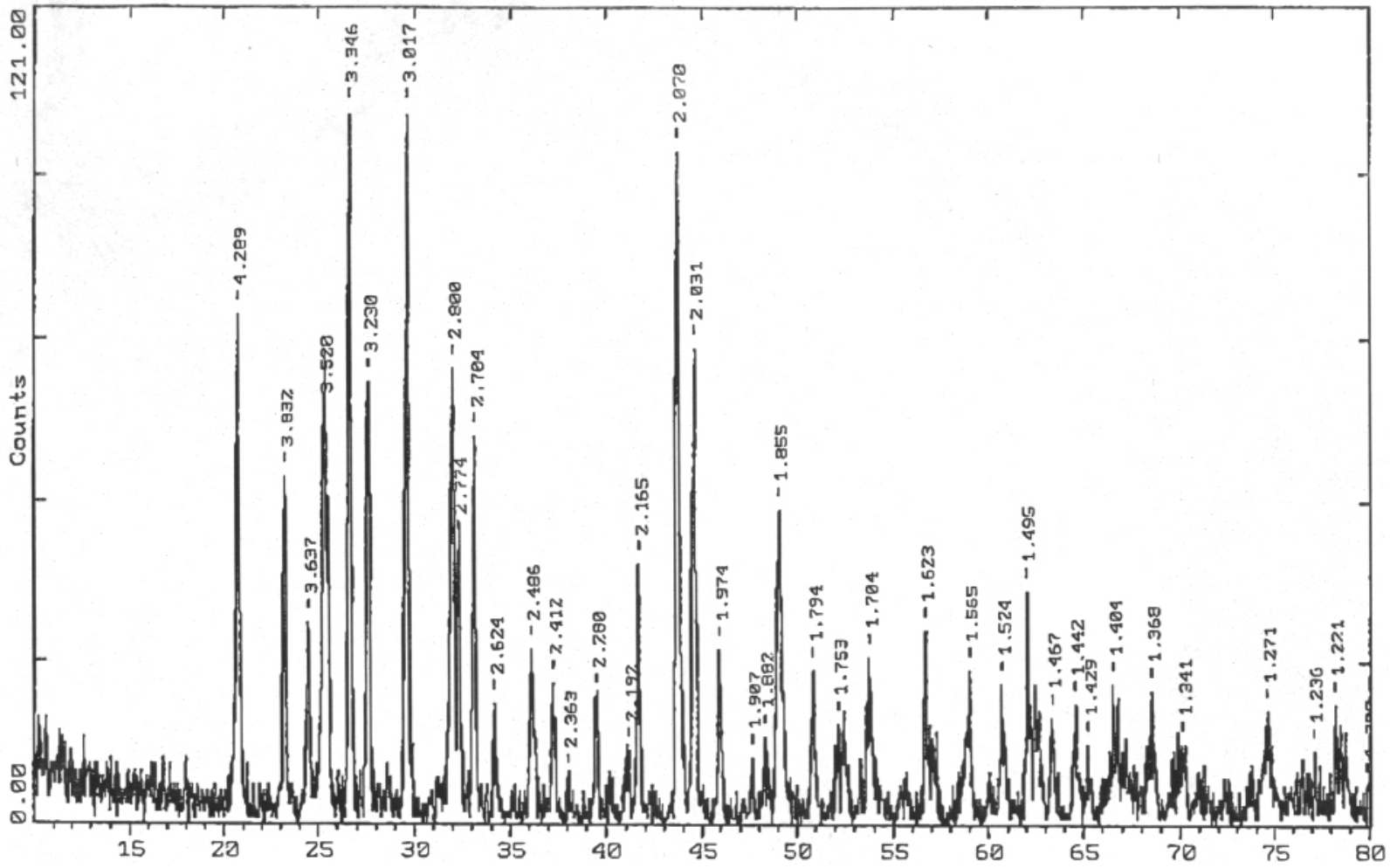

Figure 51

Positive plate (20Ah), without pulses, (range: 15-45)

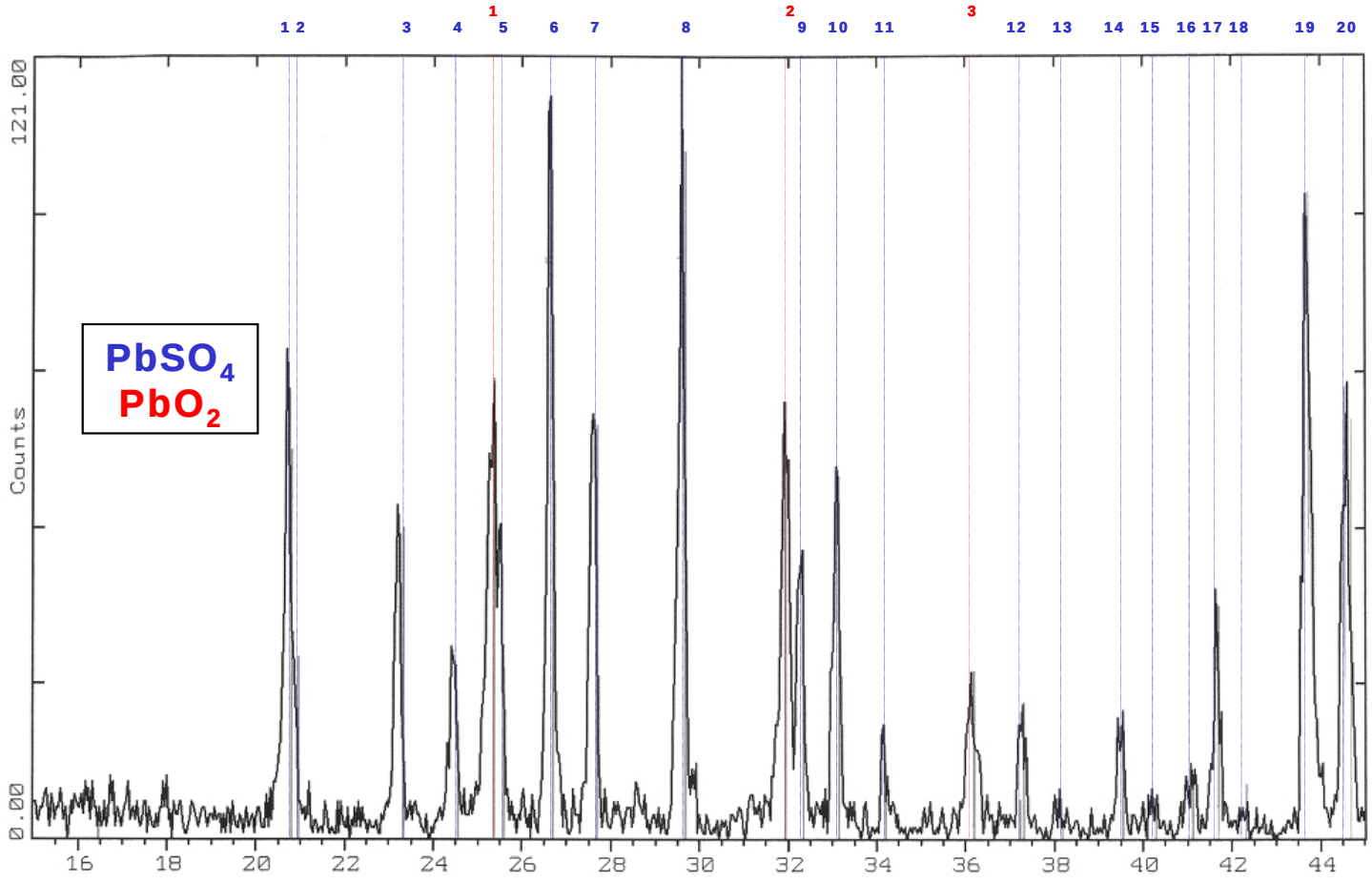

Figure 52a

Positive plate (20Ah), without pulses (range: 45-80)

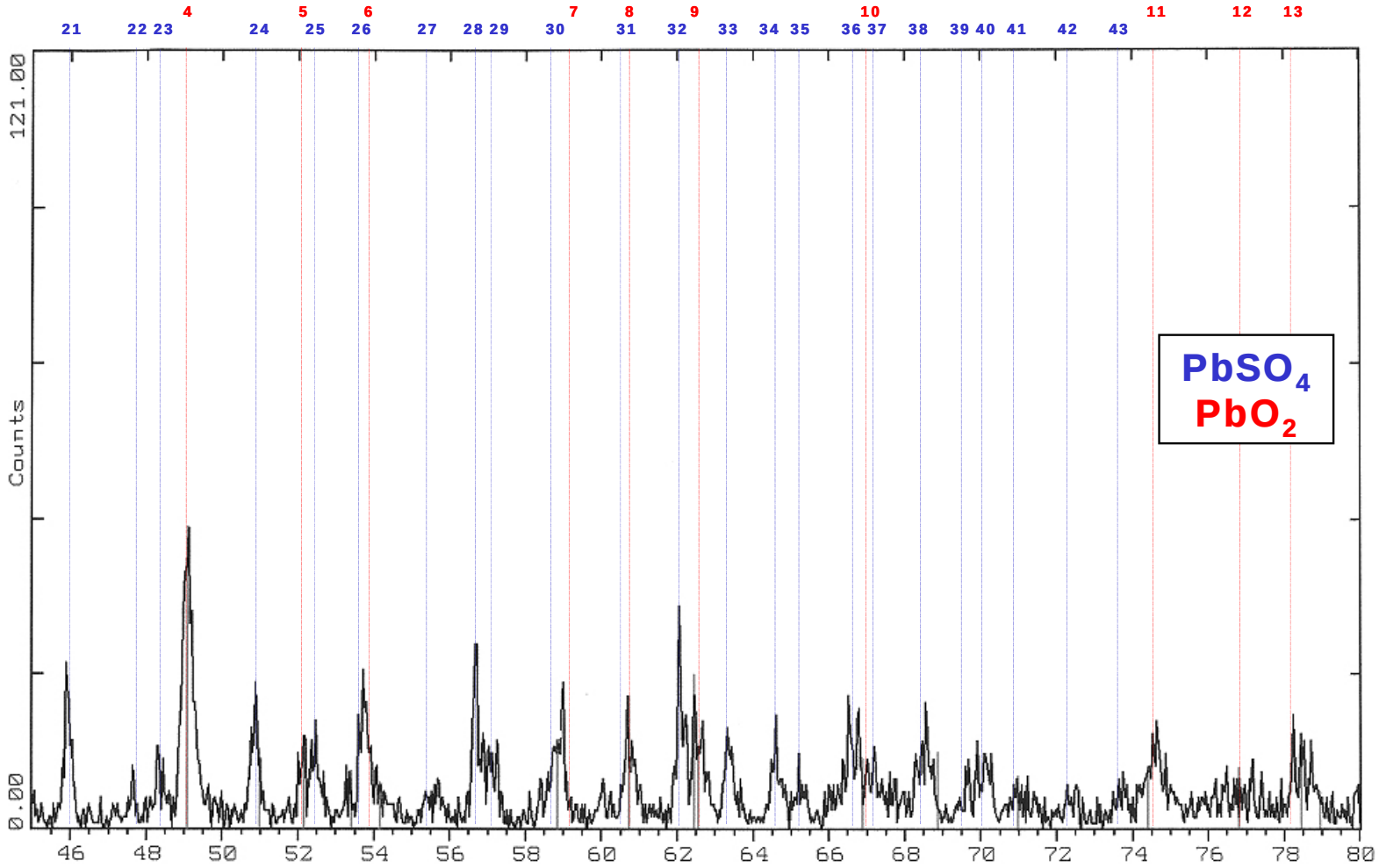

Figure 52b

Positive plate (20Ah), with pulses

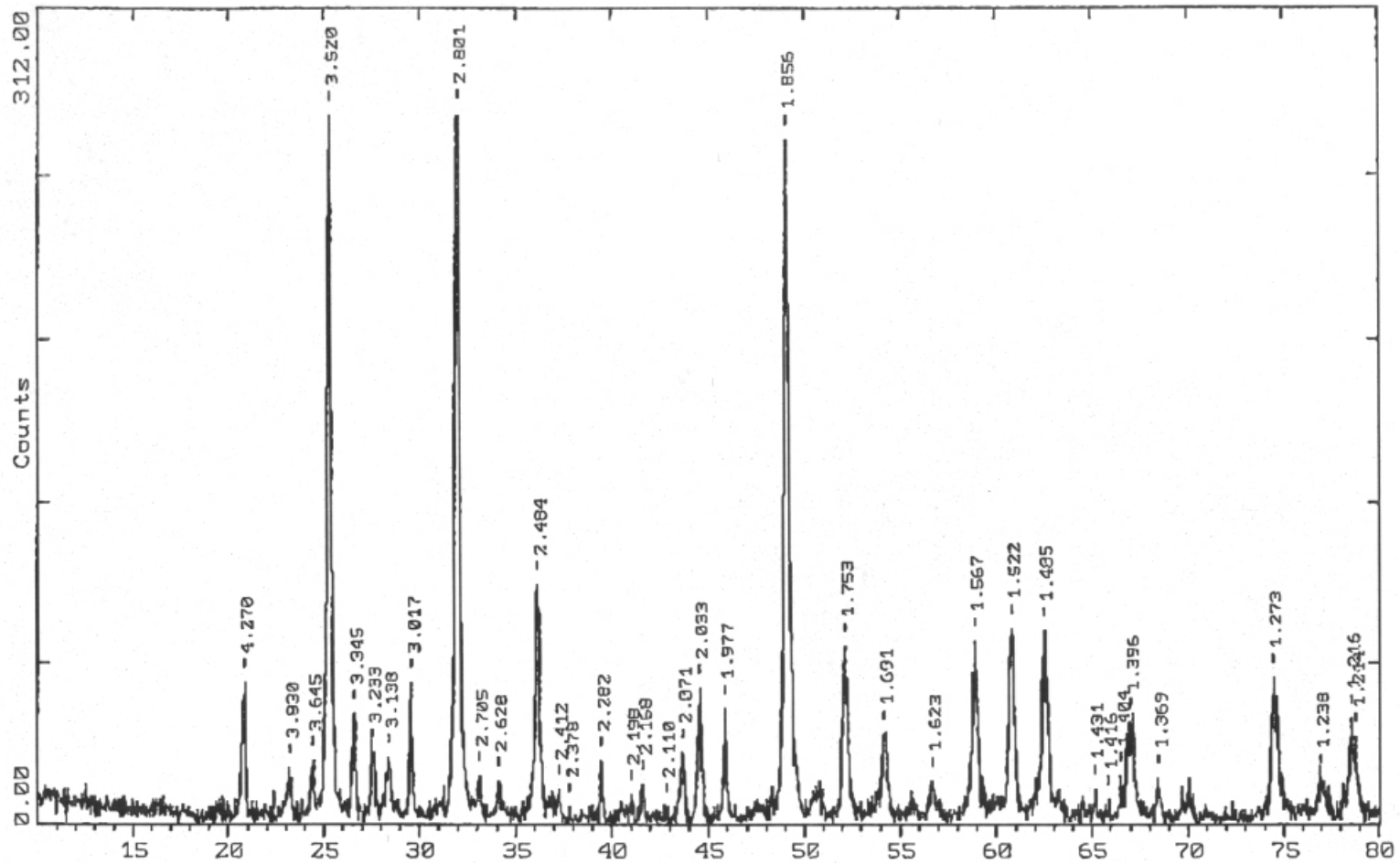

Figure 53

Positive plate (20Ah), with pulses (range: 15-45)

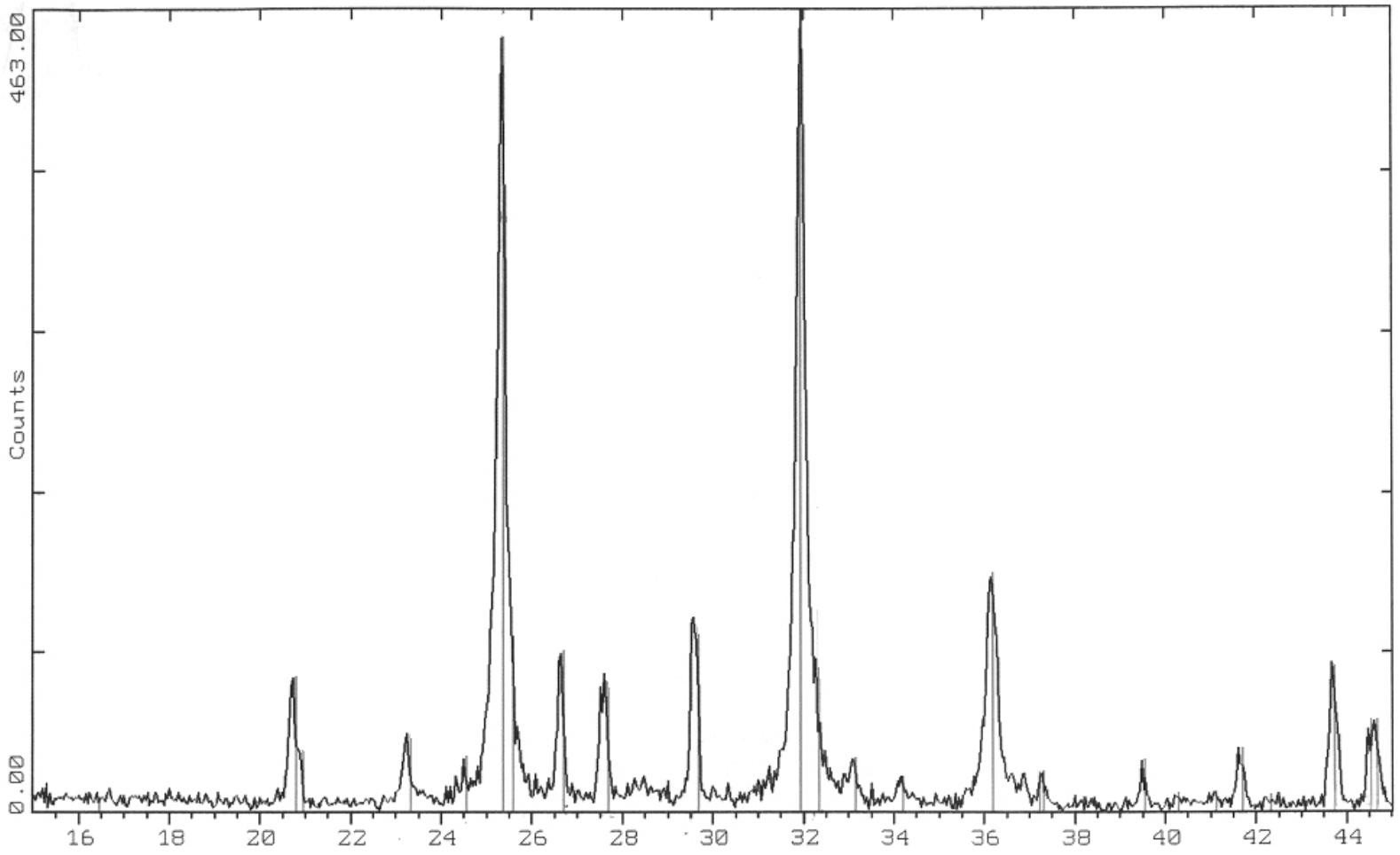

Figure 54a

Positive plate (20Ah), with pulses (range: 45-80)

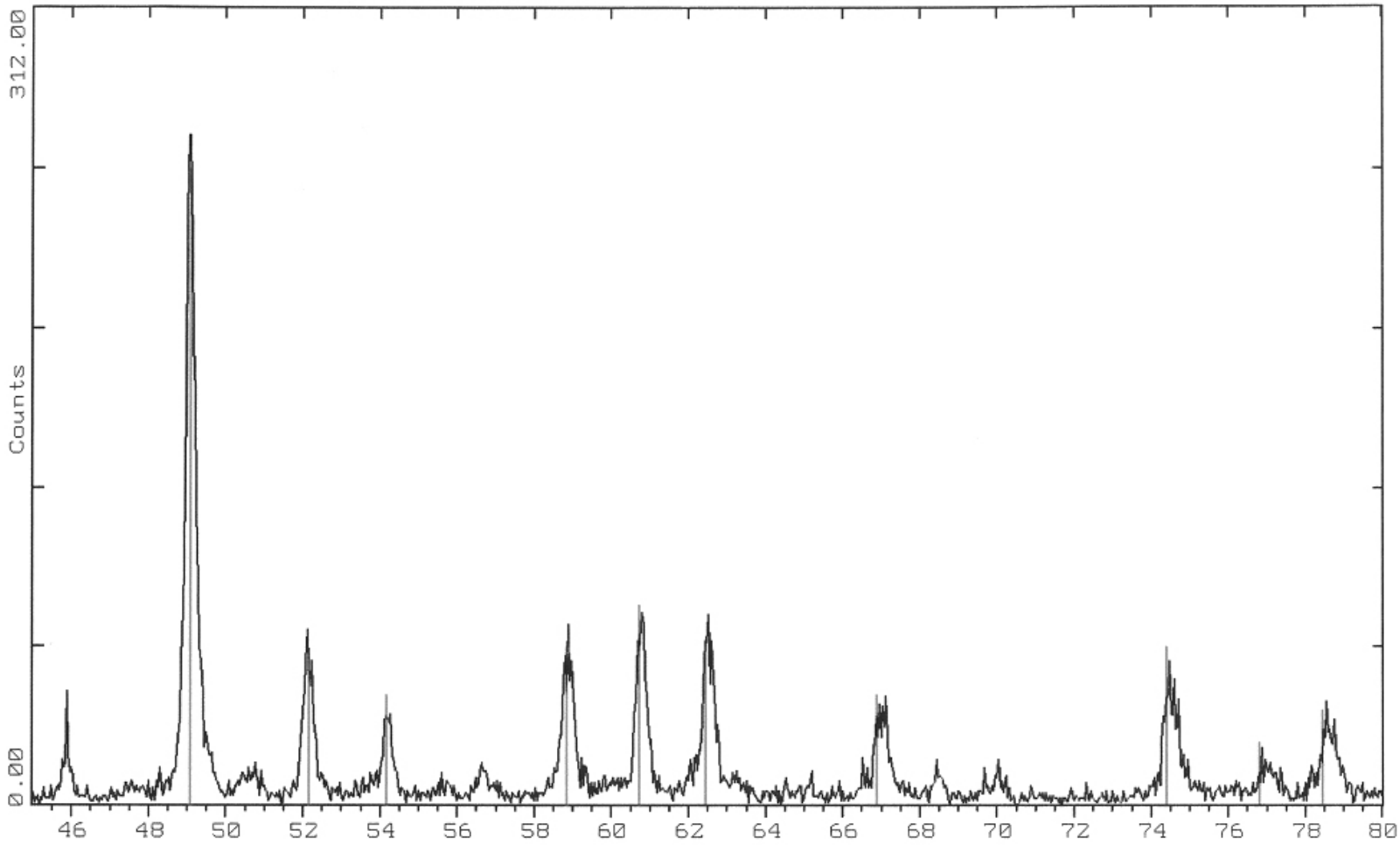

Figure 54b

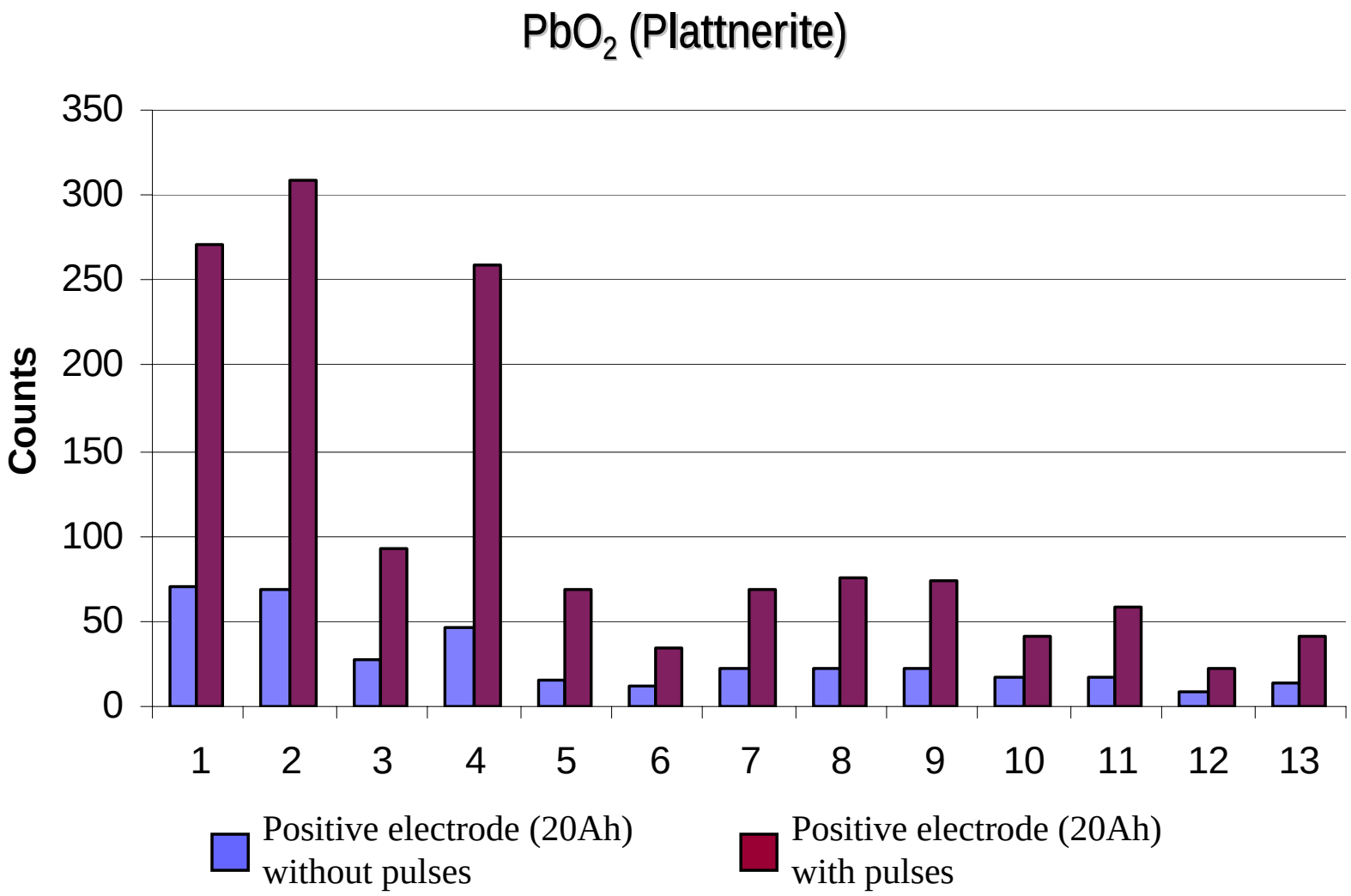
PbO2 (Plattnerite)
Counts
350
300
250
200
150
100
50
0
1
2
3
4
5
6
7
8
9
10
11
12
13
Positive electrode (20Ah) without pulses
Positive electrode (20Ah) with pulses

Figure 55

Similar x-ray spectra recorded for a positive plate (20 Ah battery) charged/discharged (50 cycles) with pulses are shown in Figure 53 and 54. Figure 55 lists intensity of major peaks assigned generally to different form of PbO_2 (platteneritte). After 50 charge/discharge cycles the amount of crystallographic form(s) of PbO_2 in the electrodes charged/discharged with pulses is significantly higher than in material without pulse treatment. Contrary, the amount of $PbSO_4$ (anglesite) is much higher in positive electrodes not treated with pulses than in electrodes treated with pulses (Figure 56). The same pattern of increasing/decreasing content of $PbSO_4$ and of PbO_2 respectively with an increasing number of charge/discharge cycles was alsoobserved also for 40 Ah and 60 Ah batteries (Figures 57 and 61).

Pulsation effect on the stored batteries

Batteries were stored at a constant temperature of 25°C up to 14 weeks, with or without the Solargizer connected to the batteries. After a designated period of storage the batteries were tested for charge capacity and after that electrodes were removed and analyzed. Figure 62 shows a galvanostatic curve obtained after discharge of a 15 Ah battery stored for 14 weeks and Figure 63 also depicts a galvanostatic curve recorded after a 15 Ah battery was stored for 14 weeks with a Solargizer attached. There is a distinctive difference in the charge capacity between

these two batteries. A battery stored under the influence of pulsation retained its original capacity while the capacity of the battery stored without pulsation lost a considerable amount of charge. The decrease of charge capacity of batteries stored without pulsation decreased linearly with time (Figure 64). After 14 weeks the decrease of charge capacity accounted for about 25% of the battery's original capacity. In this same period of time the charge of the battery attached to the Solargizer slightly increased. This is probably due to a reconditioning (reforming) process of the battery plates by continuous pulsation. A ratio of charge capacity R, measured after pulsation Q_p to charge capacity measured without pulsation is shown in Figure 65. After 12 weeks of storage R=~1.5. The coefficient R is an excellent indicator of the beneficial effect of pulsation in preserving the charge in lead-acid battery. Electron scanning microscopy as well as x-ray spectroscopy clearly underline reasons for the preservation process. During the storage of a battery without pulsation, a formation of large crystallographic domains is observed on the surface of positive electrodes (Figure 66). This is in contrast to the morphology of the battery stored with pulses (Figure 68). A smooth, homogeneous surface with significantly smaller crystals was formed during the storage process due to the pulsation effect (Figure 67). X-ray diffraction shows no statistically significant difference in the amount of platternite

PbO_2 found in the new battery and the battery stored for 14 weeks under the influence of pulsation (Figure 68).

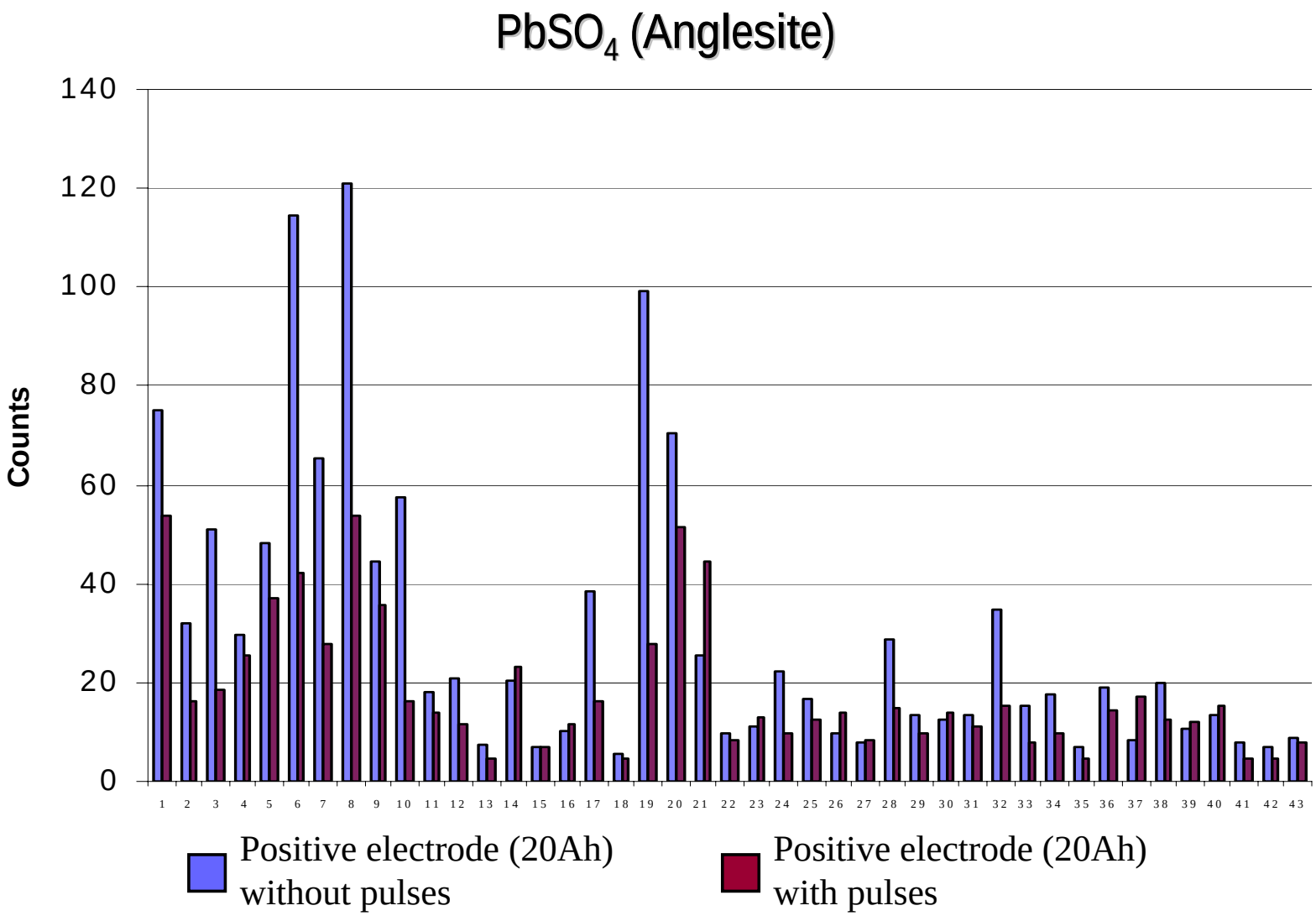
PbSO4 (Anglesite)
Counts
140
120
100
80
60
40
20
0
1 2 3 4 5 6 7 8 9 10 11 12 13 14 15 16 17 18 19 20 21 22 23 24 25 26 27 28 29 30 31 32 33 34 35 36 37 38 39 40 41 42 43
Positive electrode (20Ah) without pulses
Positive electrode (20Ah) with pulses

Figure 56

Positive plate (60Ah), without pulses

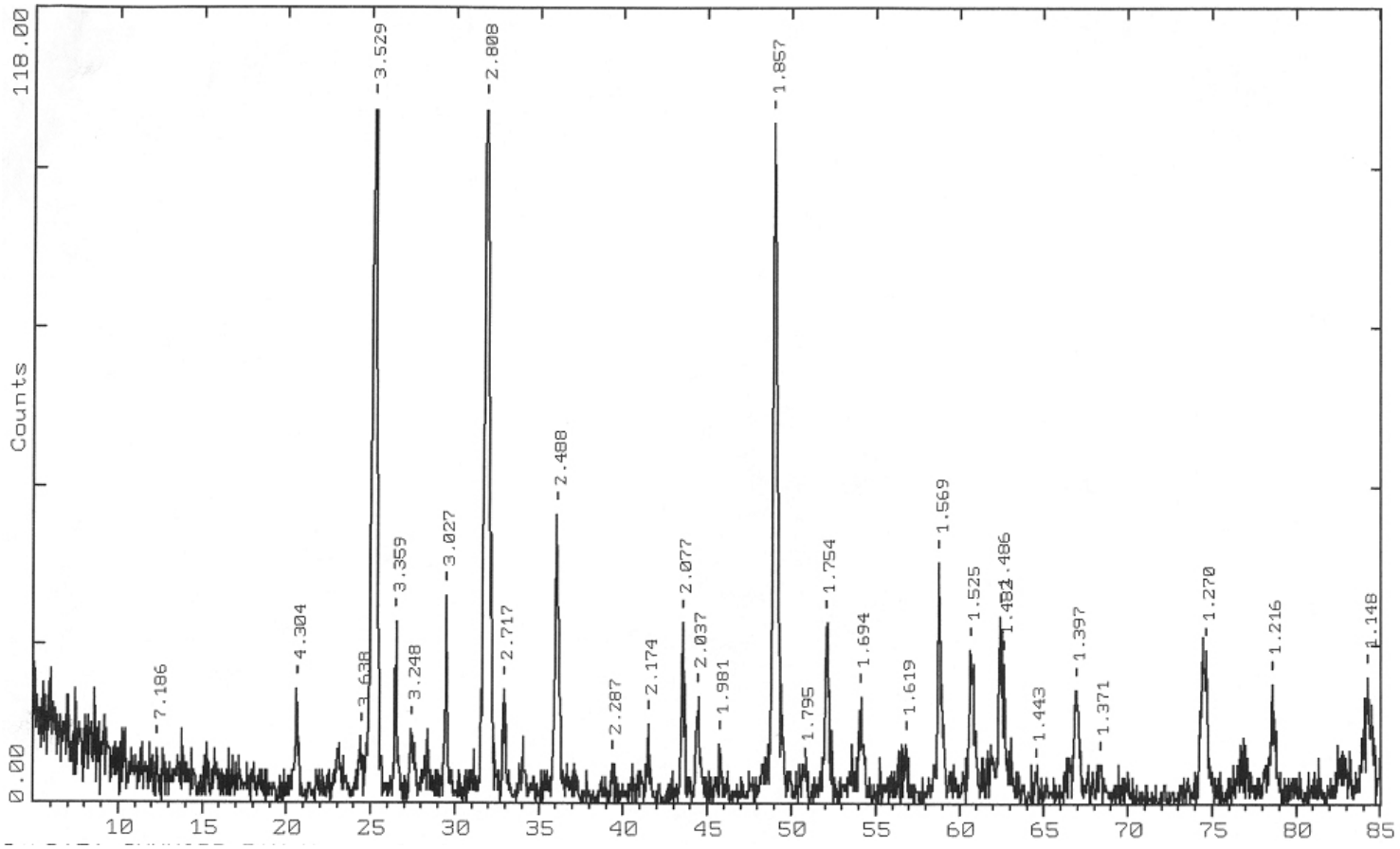

Figure 57

Positive plate (60Ah), without pulses (range: 15-45)

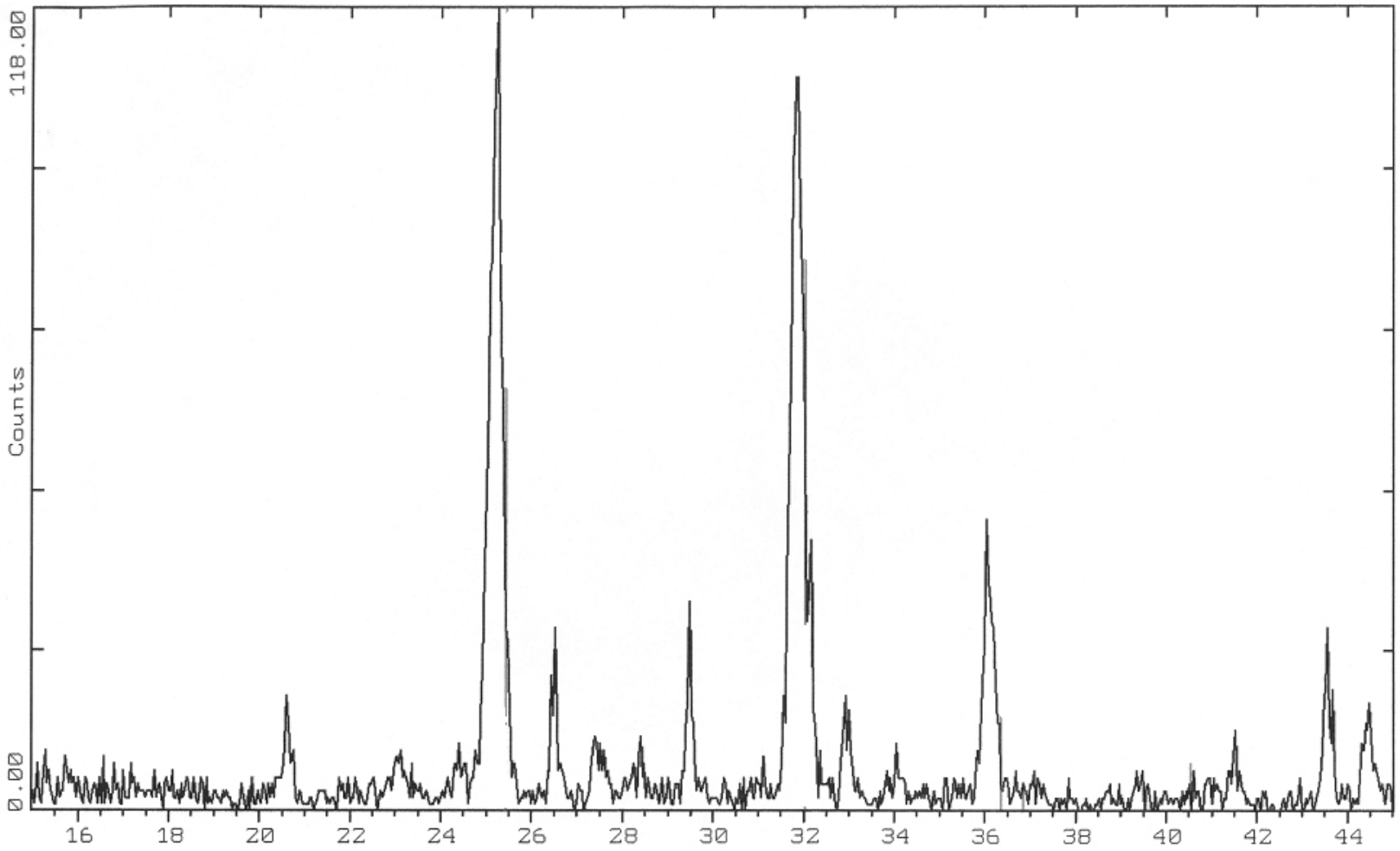

Figure 58a

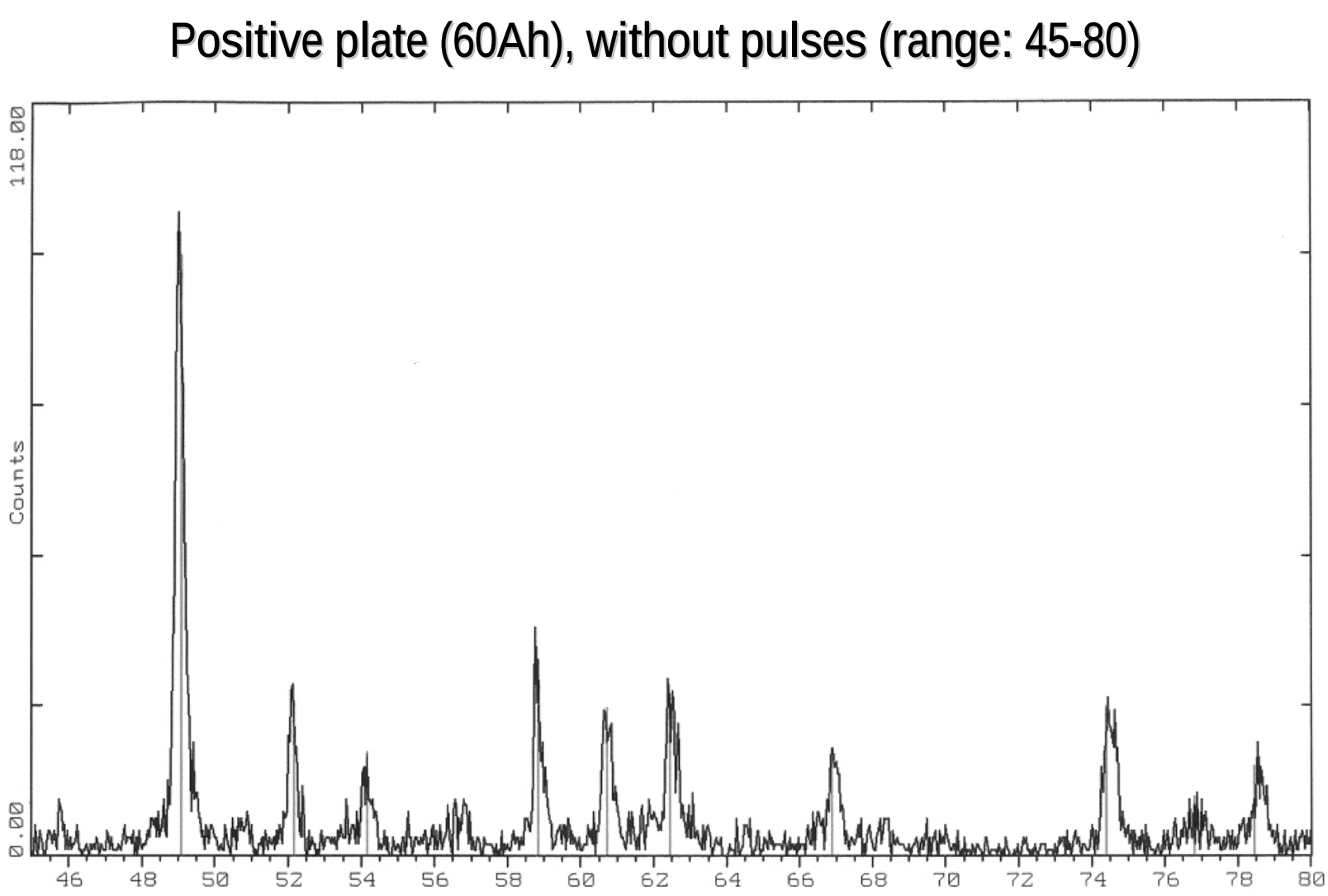
Positive plate (60Ah), without pulses (range: 45-80)
118.00
Counts
0.00
46
48
50
52
54
56
58
60
62
64
66
68
70
72
74
76
78
80

Figure 58b

Positive plate (40Ah), with pulses

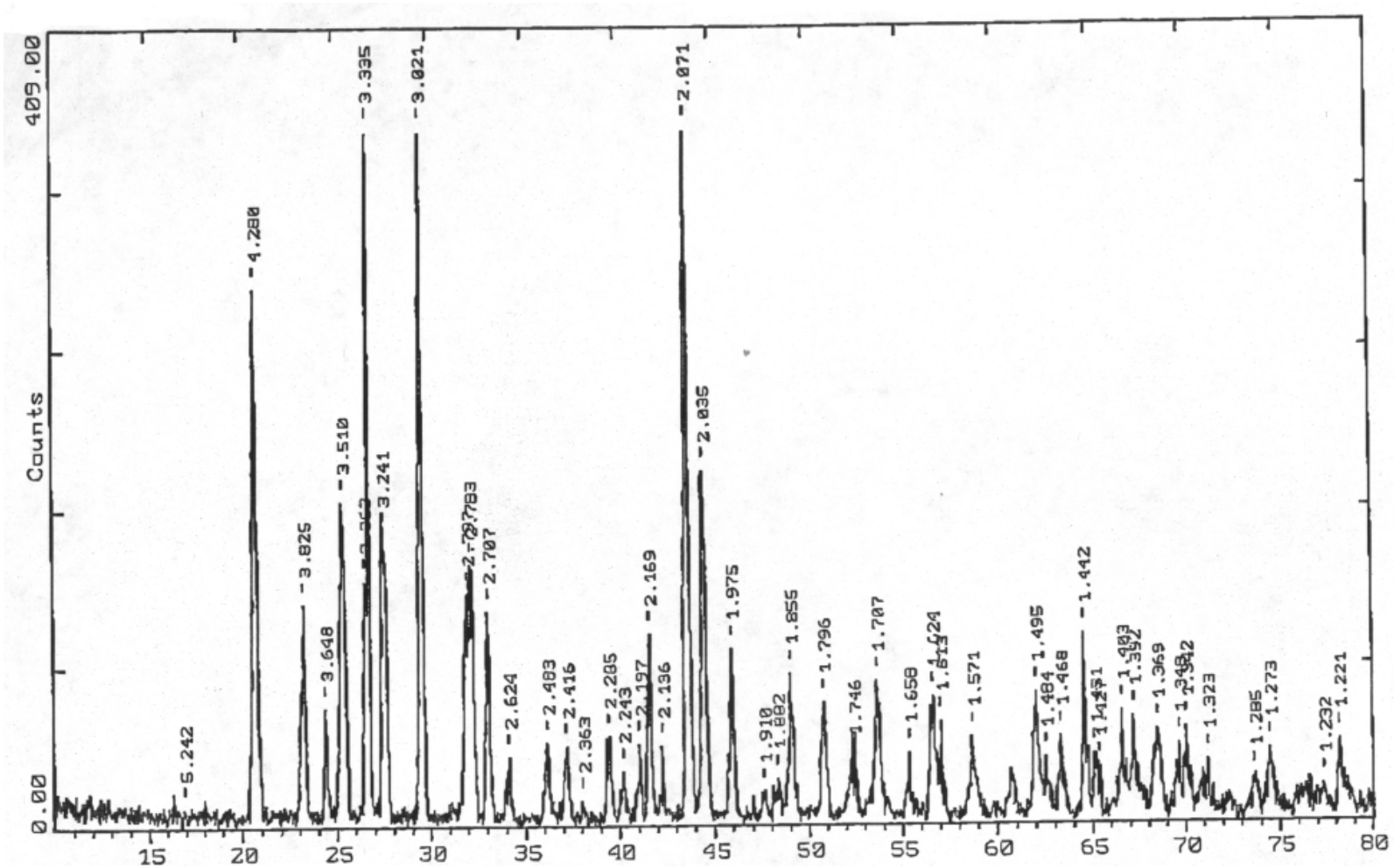

Figure 59

Positive plate (40Ah), with pulses (range: 15-45)

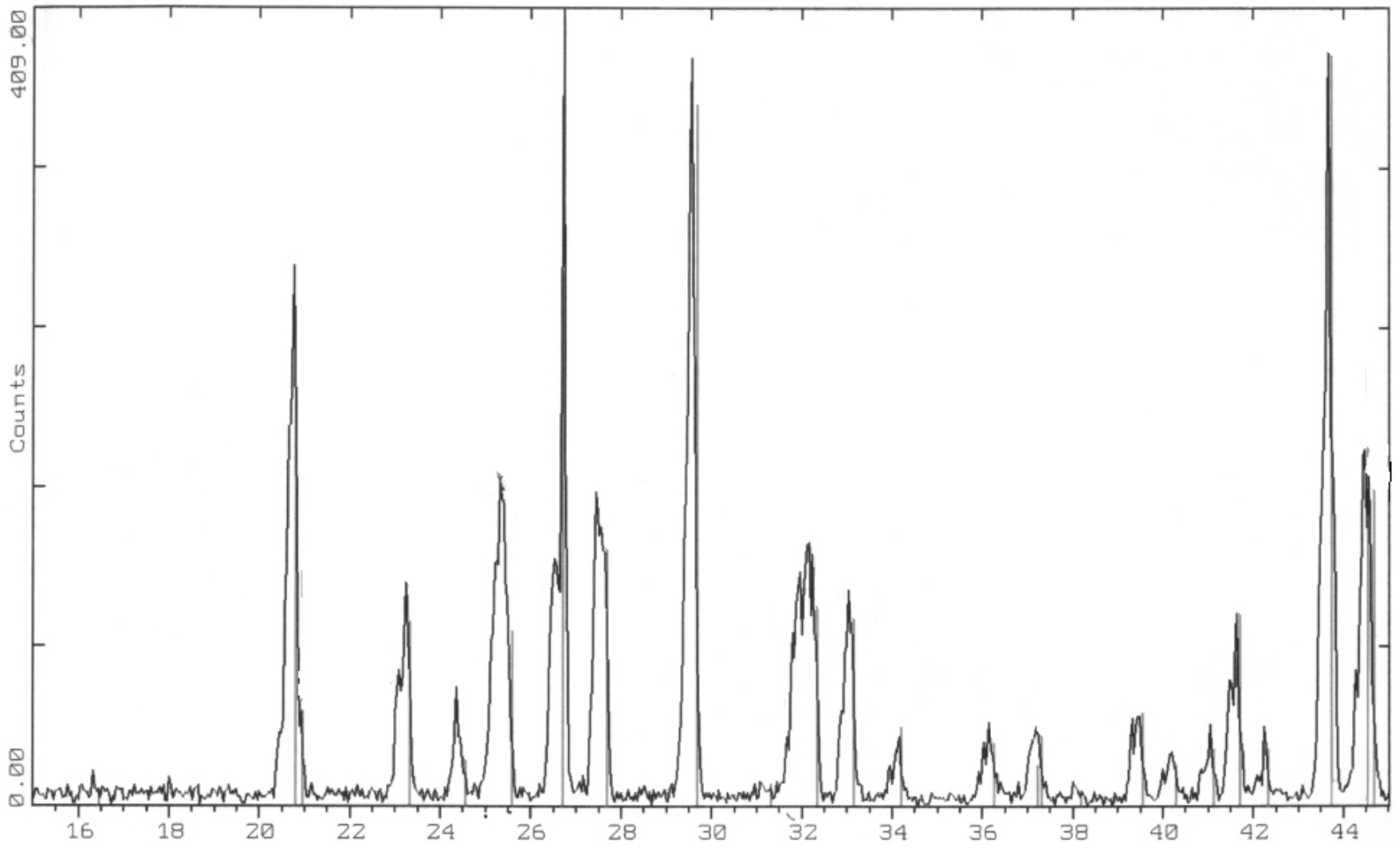

Figure 60a

Positive plate (40Ah), with pulses (range: 45-80)

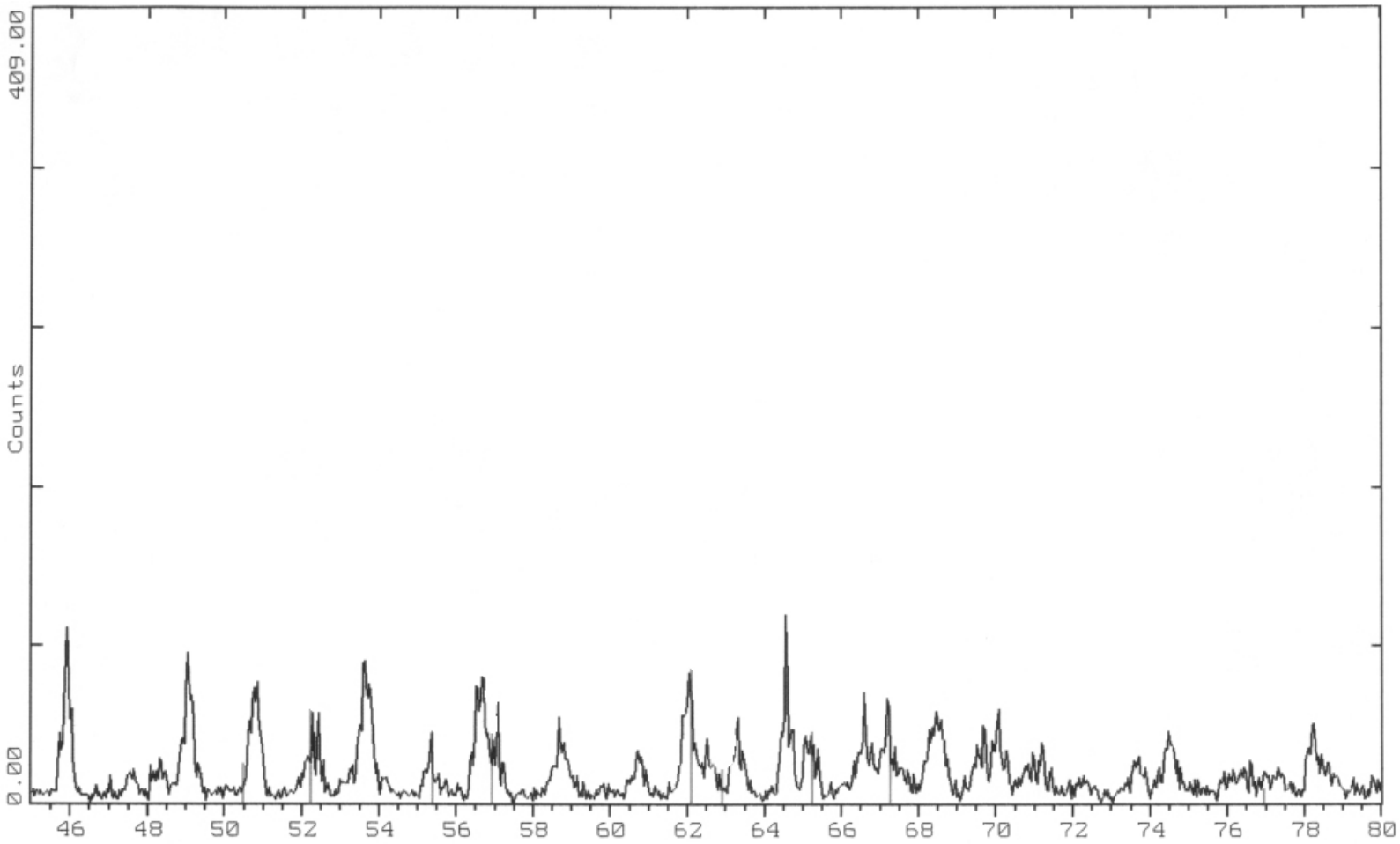

Figure 60b

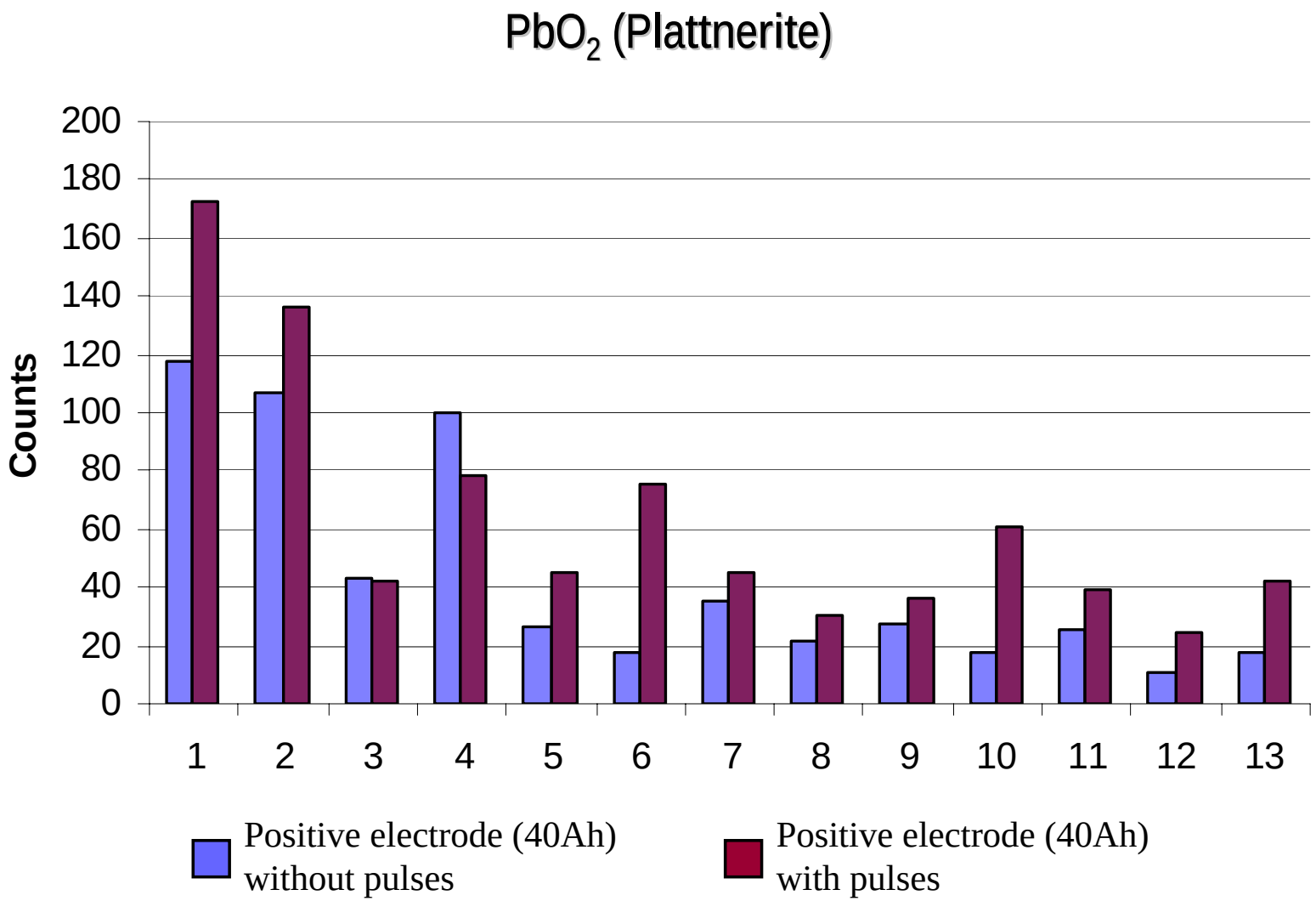
PbO2 (Plattnerite)
Counts
200
180
160
140
120
100
80
60
40
20
0
1
2
3
4
5
6
7
8
9
10
11
12
13
Positive electrode (40Ah) without pulses
Positive electrode (40Ah) with pulses

Figure 61

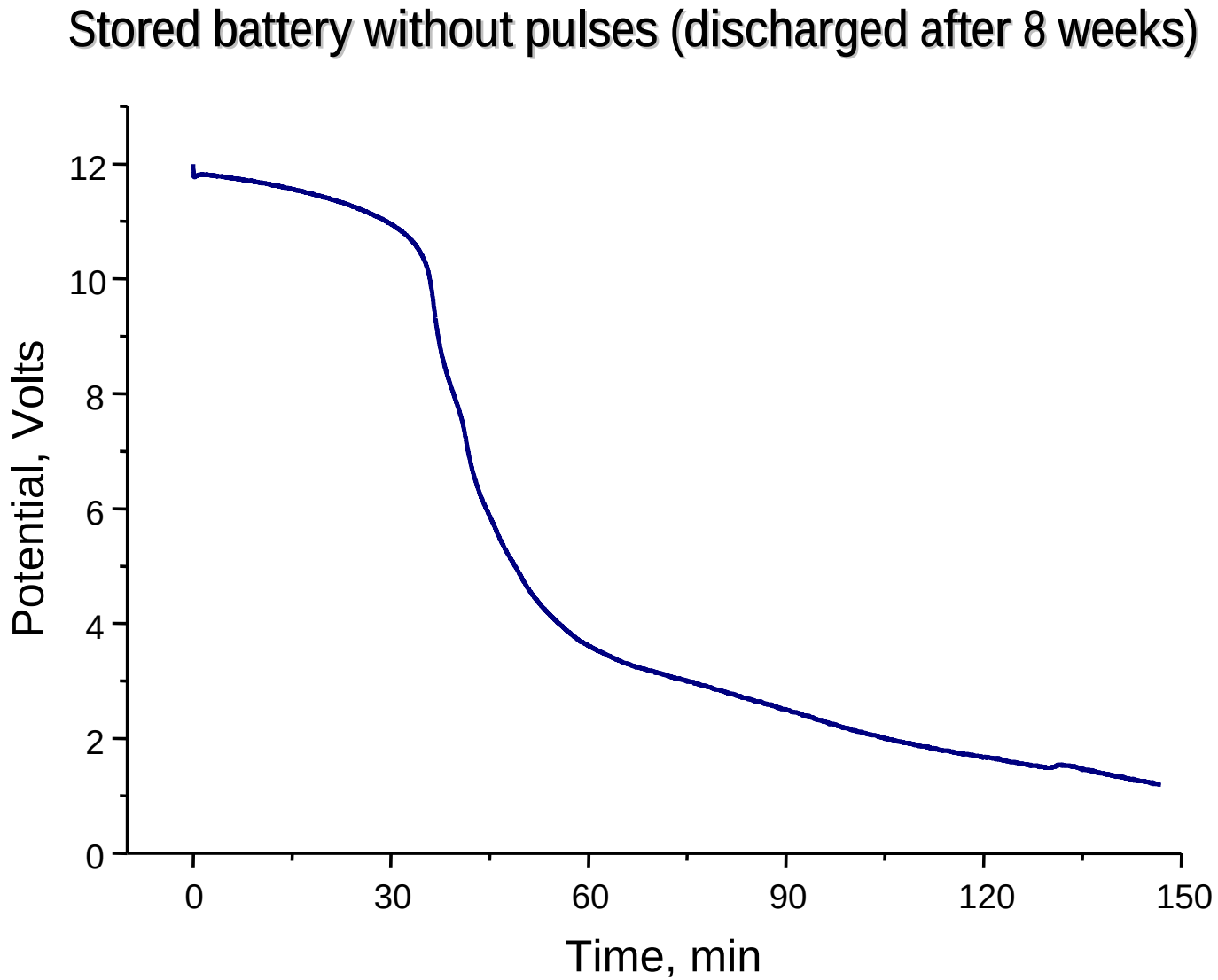
Stored battery without pulses (discharged after 8 weeks)
Potential, Volts
0
2
4
6
8
10
12
0
30
60
90
120
150
Time, min

Figure 62

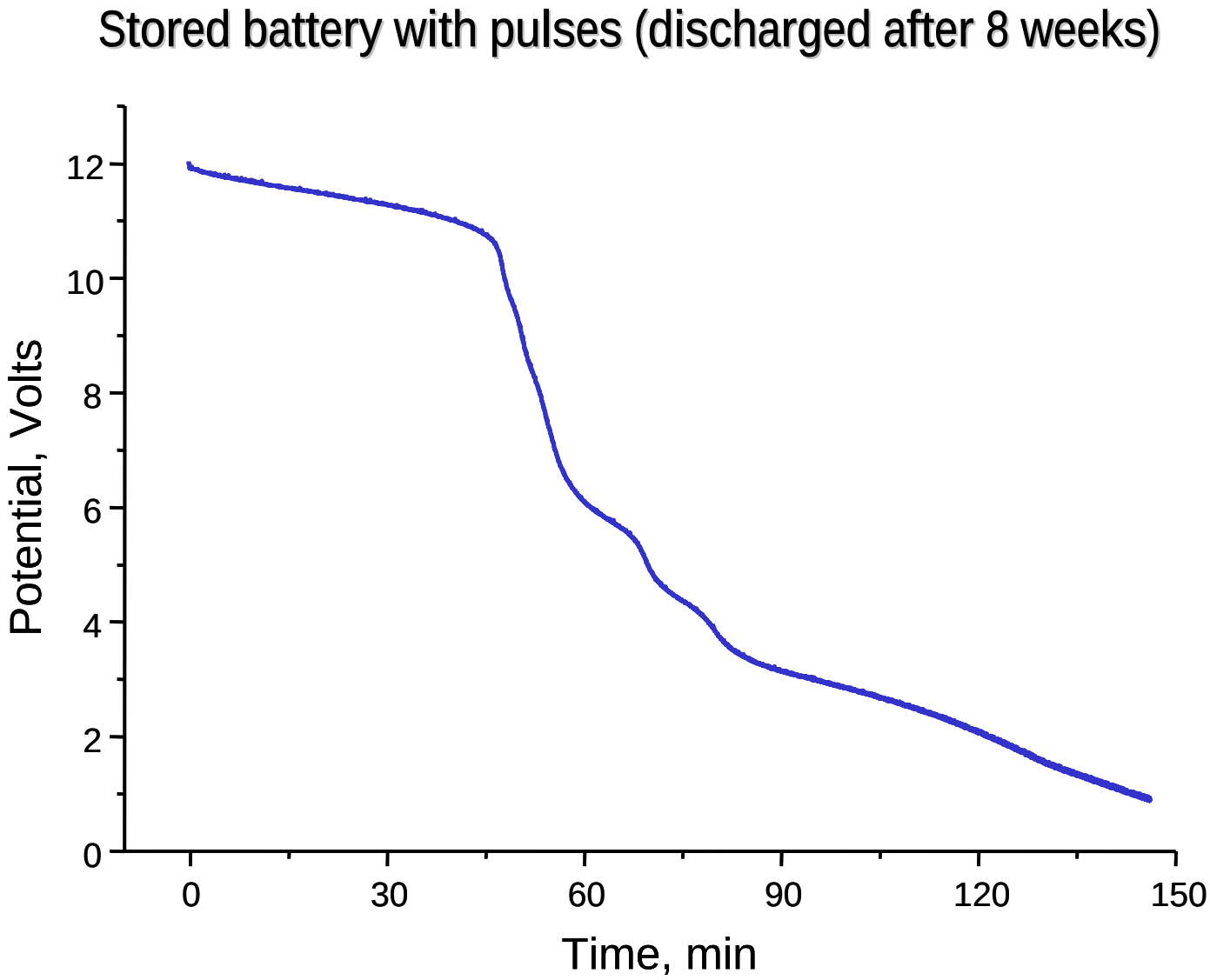
Stored battery with pulses (discharged after 8 weeks)
Potential, Volts
0
2
4
6
8
10
12
0
30
60
90
120
150
Time, min

Figure 63

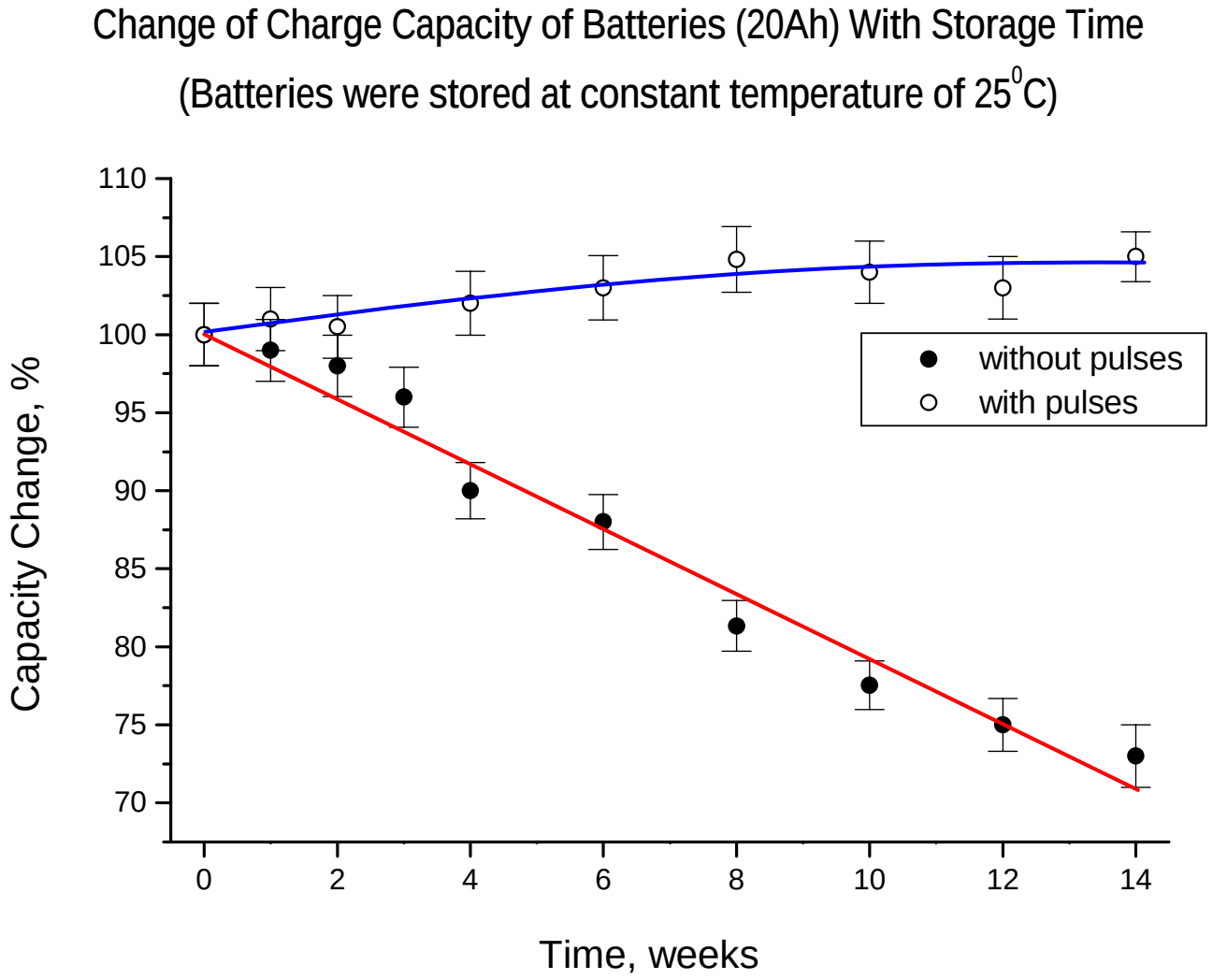
Change of Charge Capacity of Batteries (20Ah) With Storage Time
(Batteries were stored at constant temperature of 25^{0}C)
Capacity Change, %
Time, weeks
without pulses
with pulses
110
105
100
95
90
85
80
75
70
0
2
4
6
8
10
12
14

Figure 64

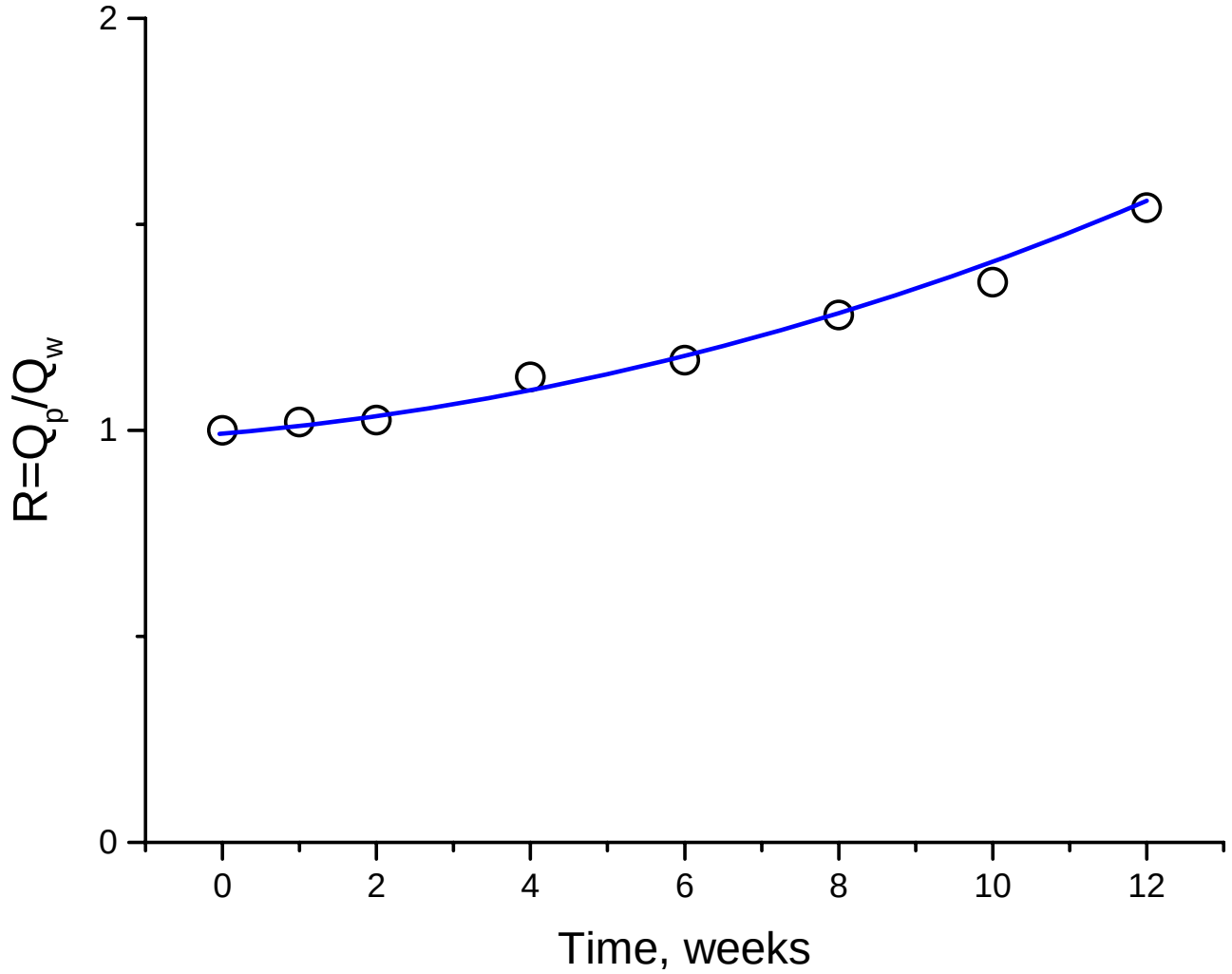

Figure 65

a)

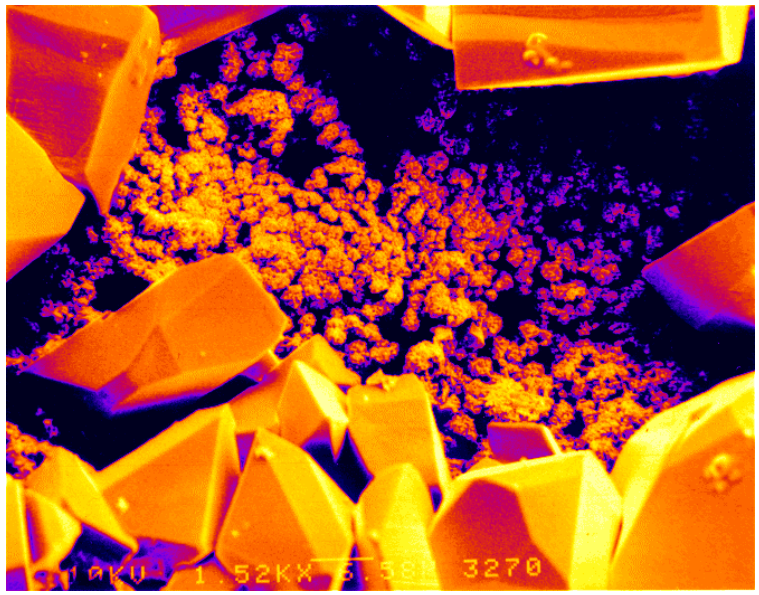

Positive electrode, without pulses, 20Ah, stored 8 weeks, magnification: 1500x

b)

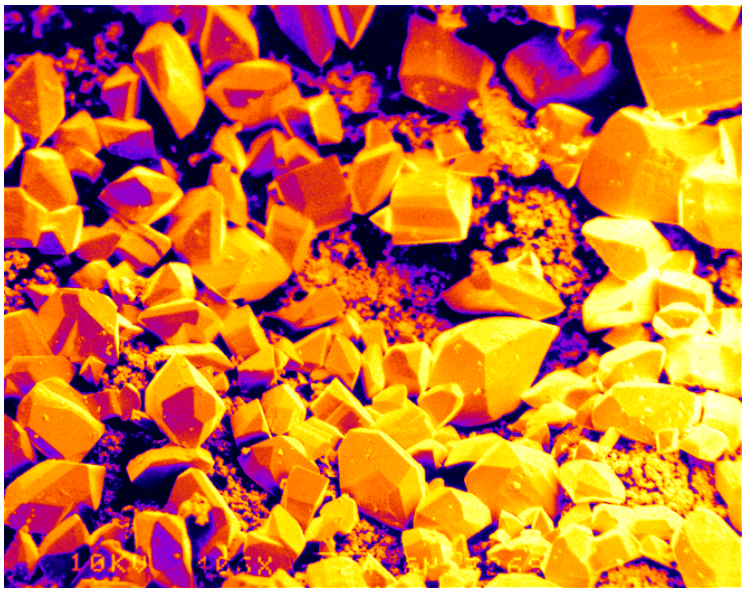

Positive electrode, without pulses, 20Ah, stored 8 weeks, magnification: 400x

Figure 66

a)

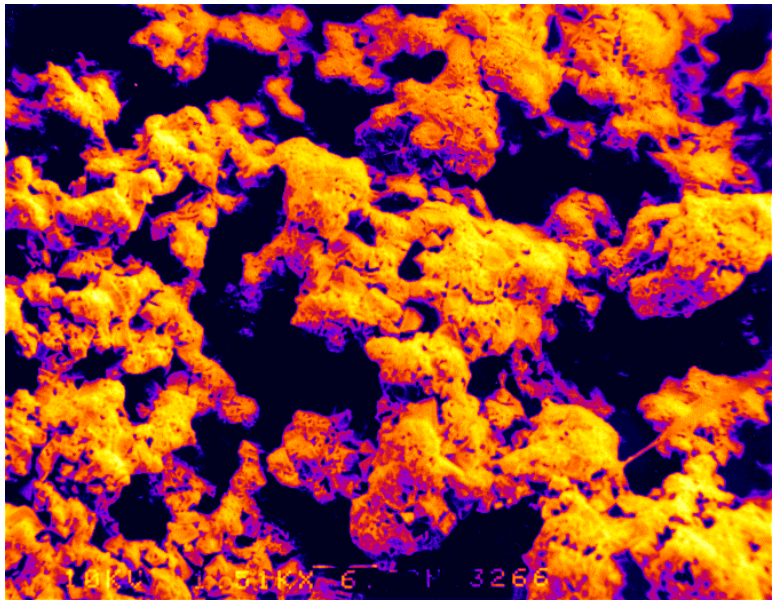

Positive electrode, with pulses, 20Ah, stored 8 weeks, magnification: 1500x

b)

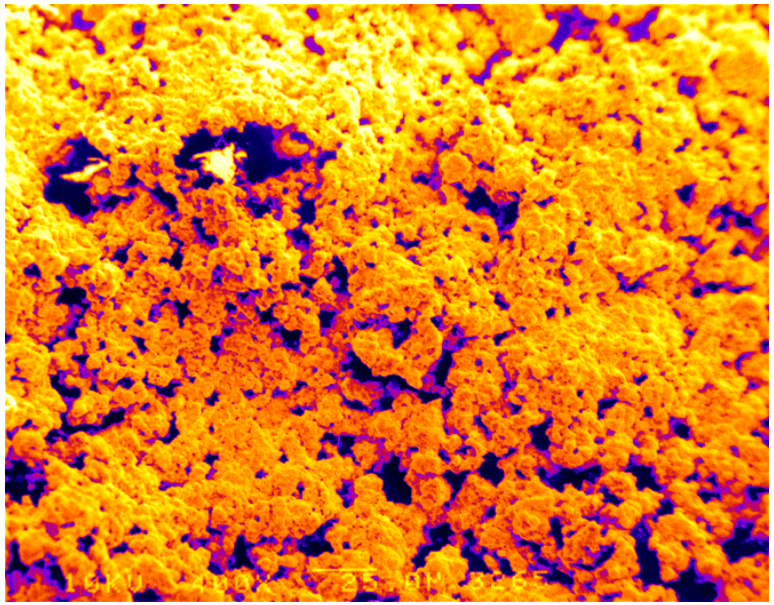

Positive electrode, with pulses, 20Ah, stored 8 weeks, magnification: 400x

Figure 67

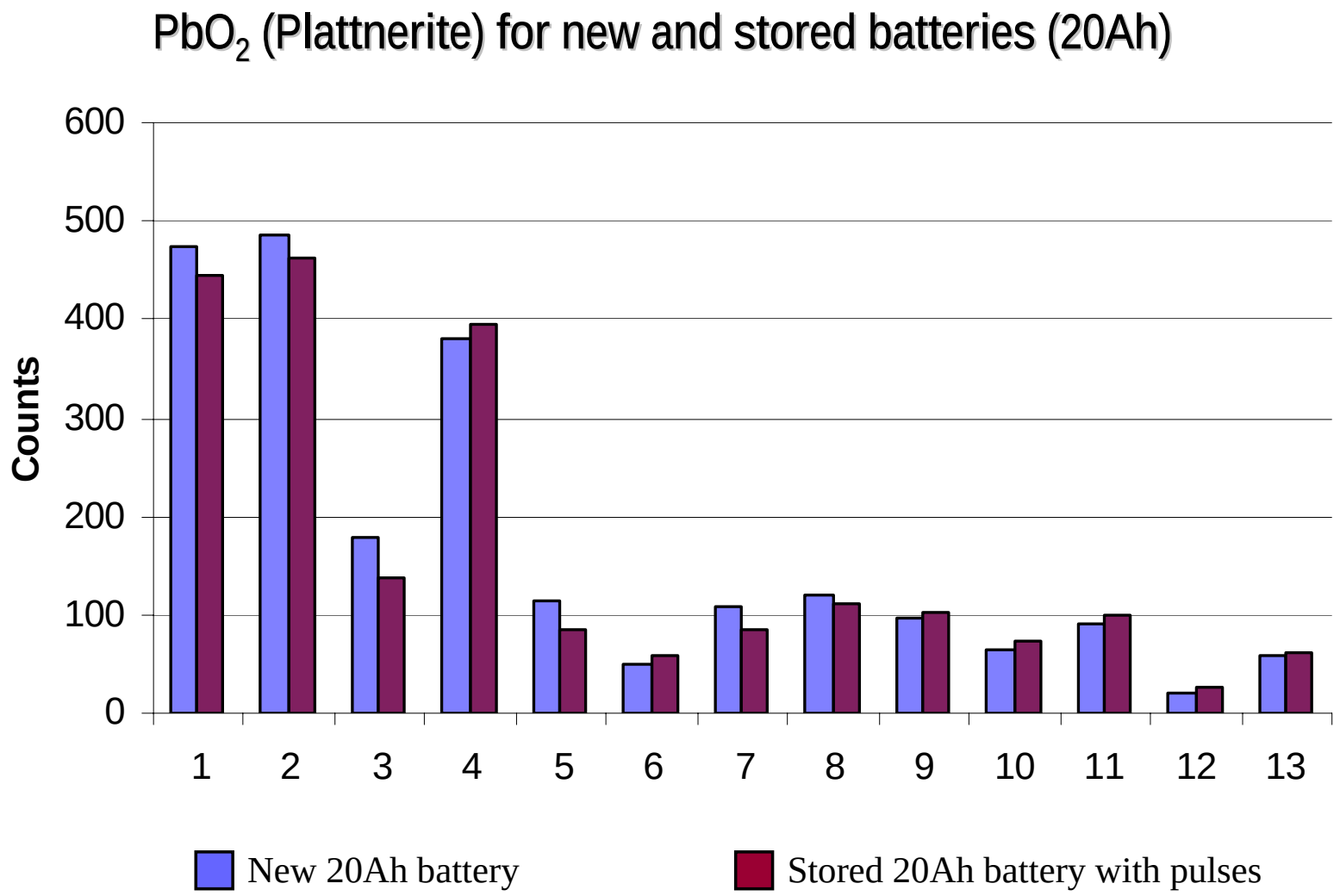
PbO2 (Plattnerite) for new and stored batteries (20Ah)
Counts
600
500
400
300
200
100
0
1
2
3
4
5
6
7
8
9
10
11
12
13
New 20Ah battery
Stored 20Ah battery with pulses

Figure 68

DISCUSSION

As in any technical device, the capability of the lead-acid battery to function is limited to a certain period called operating life. In order to judge the end of the capability to function we distinguish the following:

1. Sudden complete failure (random failure).
2. Slow decrease of the discharge capacity to a prescribed limit.

The data on operational life presented here, are based on a large number of tests of the batteries charged/discharged with and without pulses. Therefore, these data can be statistically evaluated with respect to life distribution and failure reasons. The depth of discharge of the batteries tested was about 100%. Under these conditions of discharge the operational life (also called second life) is about 40-55 cycles. A relative portion of sludge relative to original weight of electrode(s) after 50 cycles is estimated on the level of about 60%.

In spite of the different experimental background and uncertainties of temperature correction, a rule of thumb can be formulated:

$$N_2 \, \alpha = \text{constant} \qquad (6)$$

Where N_2 is the number of operational life cycles and α is the relative portion of sludge. The experimental data presented here for battery charged/discharged without pulses are in good agreement with these predicted values. However, the operational life cycle for battery charged/discharged with pulses does not follow this

rule. The operational life cycle for the battery charged/discharged with pulses is significantly longer than that for the battery charged without pulses. The relative portion of sludge generated during charge/discharge cycles with pulses is much lower. Therefore, based on equation 6 one can predict longer life cycles of the battery with lower sludge generation, and this effect was clearly observed in these studies during charge/discharge with pulses. The relative portion of sludge is about 50% lower for the battery charged with pulses than that for ones charged without pulses (Figure 69).

Batteries that have been tested in the laboratory forgoing special methods show a smaller spectrum of failure modes than the batteries in the field.
The most frequent failure reasons for batteries tested in the laboratory are sludging positive mass and shedding of the positive grid.

Sludging of the positive mass occurs especially in charge/discharge service. During the life of a battery a weight loss of the active mass parallel to the decrease of capacity is observed. A fine grain sediment that contains different portions of sulfate and lead dioxide is formed on the particle sides below 0.1 μm. Sludging occurs preferentially at the end of the charge and the beginning of the discharge.

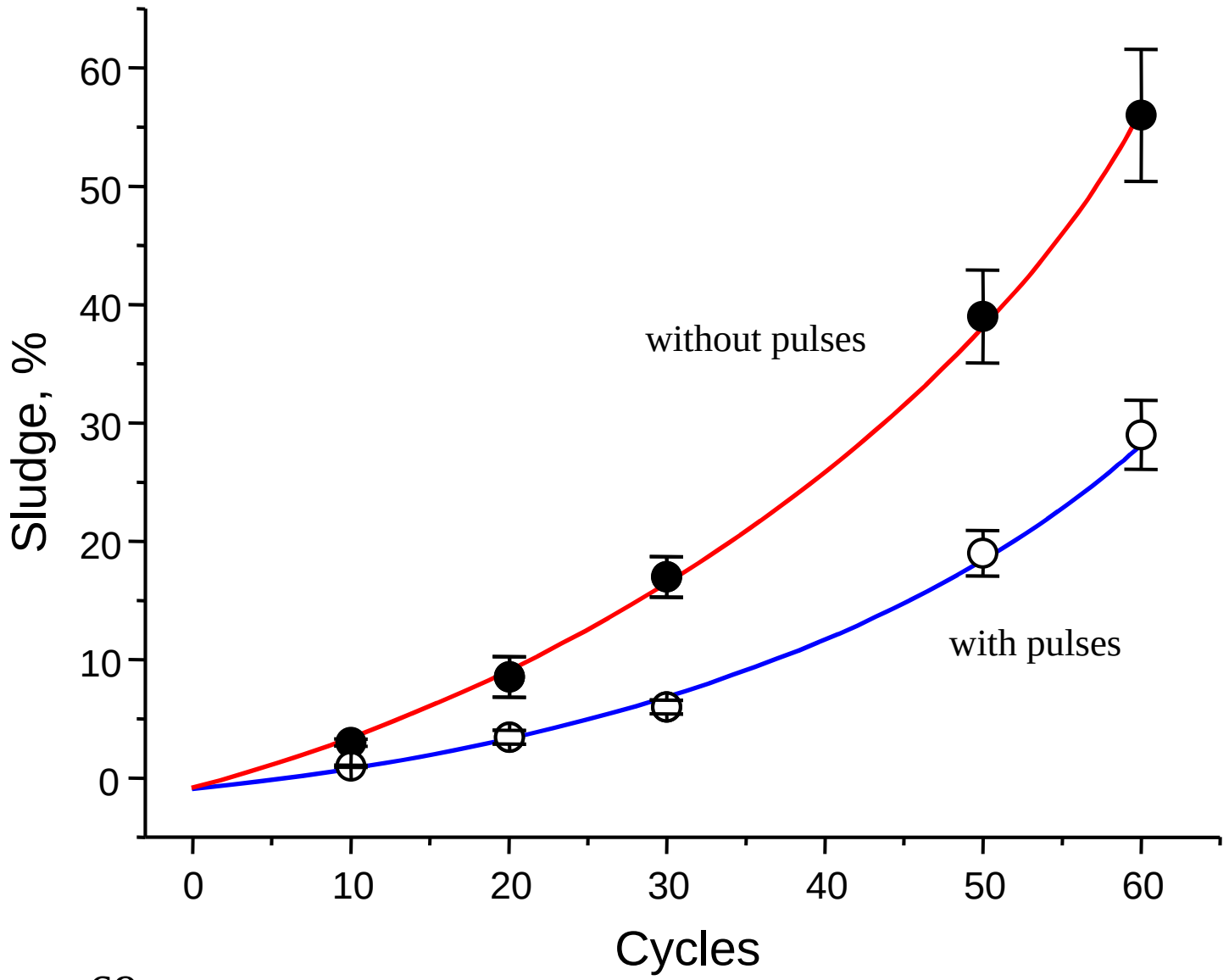

Figure 69

Strong gas evolutions during over-charge facilitates the sludging. The type of discharge and charge is important for sludging. Temperature and current density during charging has a lesser influence on the life cycle (sludging). At the beginning of discharge with a small current density only a few crystal seeds or nuclei of lead sulfates are formed, which grow during the process into larger coarse-grained crystals. During subsequent charge a solid mass of coarse-grained PbO_2 is formed, which is in good electronic contact with the base mass of the electrode collector. However, during discharge at a larger current density, many nuclei are formed first and from them a dense layer of lead sulfate builds up. During subsequent charge the lead dioxide precipitates in the form of dendrites in fissures and cracks of this cover layer. The dendrites continue to grow and may lose contact with the electrode as well as with the electrode collector at the end of charge and the beginning of discharge. This leads to sludging and shedding, respectively. Both sludging and shedding are significantly lower in PbO_2 electrodes treated with pulses compared to electrodes not treated with pulses.

It is well known that if the acid concentration is drastically reduced or the temperature increased or the current density decreased, the life of a battery is considerably increased. Data presented here indicate that this same or similar effect can be achieved just by applying the pulses during the charge/discharge of the battery. It is very interesting to note that the difference in the charge capacity between batteries charged/discharged with or without pulses at different current density remains approximately the same (Figure 71). This difference is about 20-

25% of the total capacity of the battery. For this same number of extensive cyclings the capacity of the battery will decrease for both charging/discharging with and without pulses. However, the decrease of capacity will always be 20-25% lower (based on total capacity) for the non-pulse charging/discharging process. It appears that the capacity difference of 20-25% does not depend significantly on the area of plates or density of the charging/discharging current. There is only about 5% difference in the capacity change between electrodes charged/discharged with a current density of 1 mA/cm^2 and 150 mA/cm^2. For this same number of cycles a ratio of $Q = Q_p/Q_w$ (capacity of battery charged with pulses Q_p to the capacity of battery charged without pulses Q_w) increases with the initial capacity of batteries (Figure 71).

It is well established that the lead acid battery PbO_2 active mass crystals have a nonhomogeneous mass distribution and contain some defects in their crystal lattice. By electron diffraction analysis of the active mass agglomerates and individual crystals, it was determined that β-PbO_2 is formed in the form of long and a needle-like crystals, while α-PbO_2 is formed in the form of short crystals often with a non-uniform shape. During plate discharge besides $PbSO_4$ crystals, fine orthorhombic PbO crystals are formed

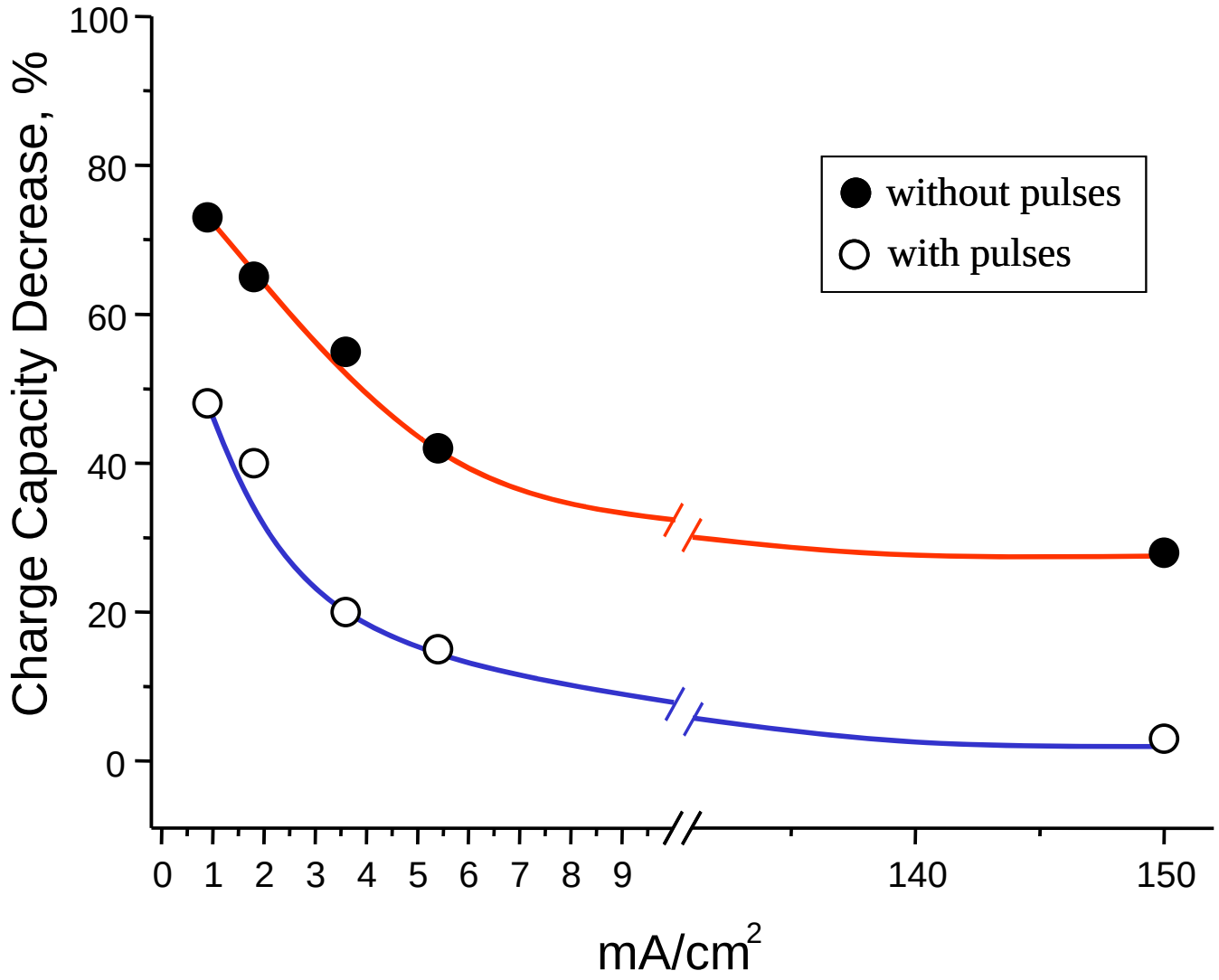
Charge Capacity Decrease, %
100
80
60
40
20
0
without pulses
with pulses
0 1 2 3 4 5 6 7 8 9
140
150
mA/cm2

Figure 70

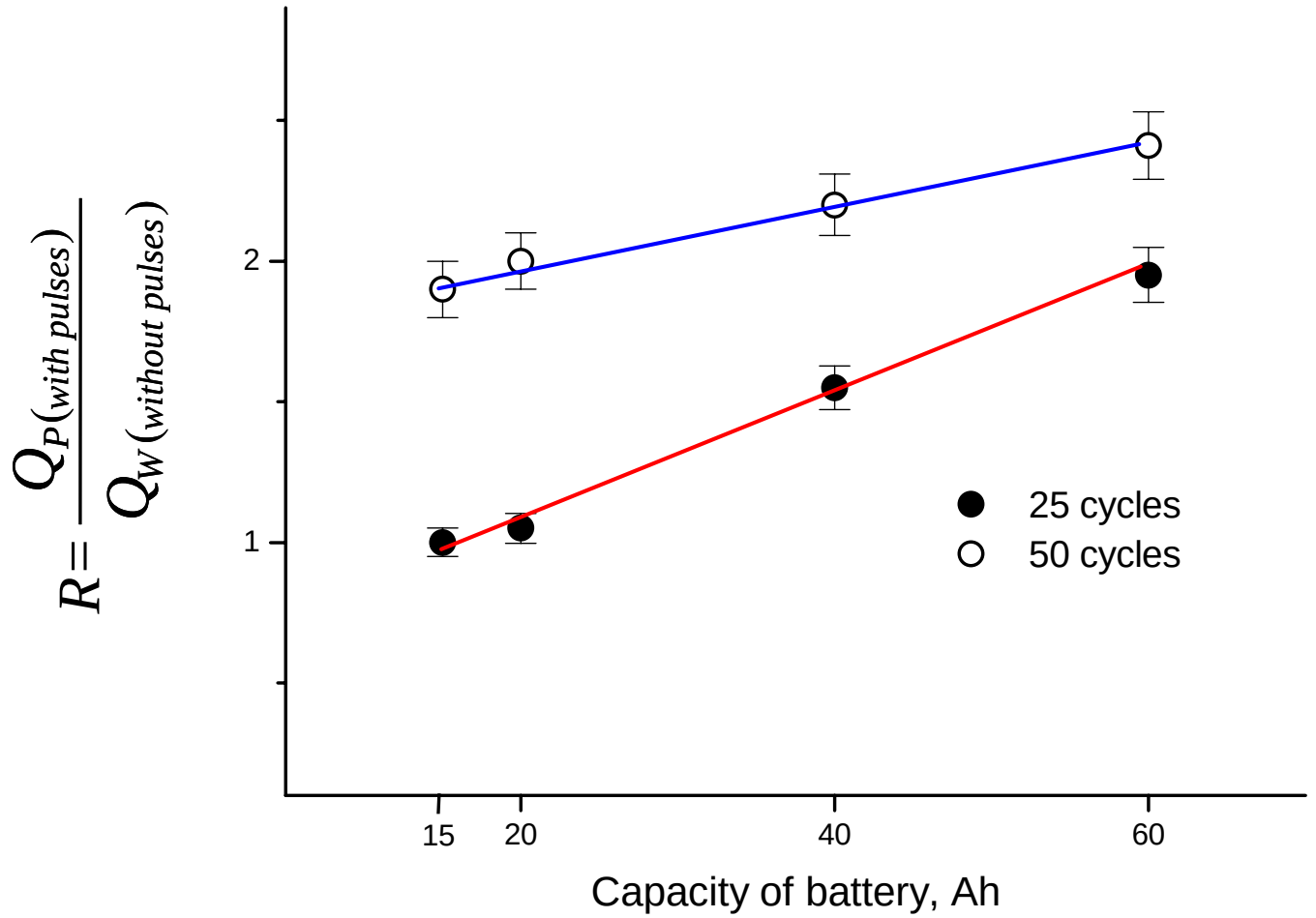
$R = \frac{Q_{P(with\ pulses)}}{Q_{W(without\ pulses)}}$
2
1
25 cycles
50 cycles
15
20
40
60
Capacity of battery, Ah

Figure 71

as well. This is explained by the proton-electron mechanism of PbO_2 reduction. The difficult penetration of SO_4^{2-} ions into the agglomerates micropores closes alkalization of the solution and creates conditions for the forming of PbO. Since the molar volumes of PbO and PbO_2 are almost equal the transport of proton ions and water along the agglomerates micropores is not impaired by the reduction of PbO_2 to PbO. This reaction allows the PbO_2 crystals into the agglomerates interior to take part in the discharge process. That high coefficient of active mass utilization is achieved when the discharge is stopped and PbO reacts with H_2SO_4 forming $PbSO_4$. The data presented in our study show that pulses generated by the Solargizer change sludging as well as shedding of the positive mass. The pulsation probably also improves transport of protons through the active mass system and this important feature contribute to the improvement of the charge capacity as well as the life span of positive electrodes.

The active mass structure is one of the basic factors determining the electrical characteristics of the lead-acid battery positive plate.

The electrochemical reaction could proceed at a spot situated deep in the active mass volume. This can occur only when free access to that spot of H^+, SO_4^{2-} ions, and H_2O is maintained. Also, an electron transfer from the plate grid through the corrosion layer and the active mass cannot be hindered. Both of these processes, ion transport and electron transfer, depend on the structure of the crystals of positive mass composition of crystals and their orientation and organization in the microstructure of active mass. It is evident from the data presented here that pulses

generated by the Solargizer influence crystal formation during charging as well as discharging processes. As a macro-effect of these crystallographic changes the morphology of the positive plate changed significantly.

The reflectance images of the macrostructure of the PbO_2 surface as well as electron scan microscopy images presented here, clearly show significant changes of crystallographic structure of the PbO_2 electrode during charge/discharge cycles with pulses**.**

The changes caused by pulsation are manifested by smooth surface, fine and well organized crystals, high homogeneity of the active mass, and high content of PbO_2 and low content of $PbSO_4$. Positive electrodes not treated with pulses during charge/discharge cycles show the domains of larger crystals, rough surface with craters, low content of PbO_2 and high content of $PbSO_4$. Also, X-ray diffraction spectra indicate that PbO_2 electrodes without pulse treatment show a much higher number of crystallographic phases $Pb_xO_y(PbSO_4)_n$ (shown as additional peaks on X-ray spectrum), which contribute to the diminishing charge capacity of these electrodes during deep discharge processes.

In the discharging process of the positive electrode, H^+ ions take part in the current transfer from the negative plate maintaining the electrochemical reaction while H_2SO_4 participates in the $PbSO_4$ formation. When the discharge of the PbO_2 electrode is started, the solution in the micropores of the positive plate (having usually a radius bigger than 0.1 μm) has a H_2SO_4 concentration equal to that of the bulk of the electrolyte. During the discharge process, H_2SO_4 in the macropores of the

PbO_2 solid material takes part in this reaction, and the concentration of H^+ decreases leading to microalkalization in the pore. H_2SO_4 is involved in the charge transport system and macropores are striving to maintain the H_2SO_4 concentration. During the $PbSO_4$ crystal growth, the macropore cross-section decreases to such an extent that the movement of SO_4^{2-} ions is impeded. In order to maintain the proper mass transport of H^+ and SO_4^{2-} not only the morphology of the crystals of $PbO_2/PbSO_4$ has to be optimal, but also the mass transport of both of these ions has to be as rapid as possible. Under normal static conditions present in any lead-acid battery, the mass transport of those ions in the reaction layer is maintained based on the pure diffusion only (a battery has a minimal mass transport based on convection).

However, when the charging/discharging process is carried out in the presence of pulses, a microstirring of the diffusion layer (Nernst diffusion layer) of the positive electrode can be observed. The stirring of the diffusion layer reduces its thickness (Figure 72) and increases the mass transport of ions, which increases the current and also makes the alkalization of the micropore structure of the PbO_2 electrodes less probable.

The charge supply to the electrode due to pulsation generated by the Solargizer is a small fraction (much lower than 1% of the total charge capacity of the battery) of the charge needed to recharge the battery. Therefore, under normal circumstances (large battery) the Solargizer cannot be considered as a battery charger. However, the small pulses generated by the Solargizer when superimposed on a charging current or potential make significant changes in the structure of the

electrodes in a lead-acid battery and these changes are especially noticeable in the positive electrodes. Therefore a beneficial effect of pulse charging has to be considered based on the favorable changes in microstructure of the energy storage system and not based on the total energy delivered to the system.

An electrochemical relaxation technique involving the application of repetitive pulses of potential to an electrode has been developed and used in the electroplating processes, electroanalytical chemistry and also to study the kinetics of electrode reactions. In the electroplating processes repetitive pulses of high frequency and low amplitude are applied to obtain a smooth homogeneous surface. In this process the energy of pulsation is much smaller than the total energy needed for deposition of the material. It is well

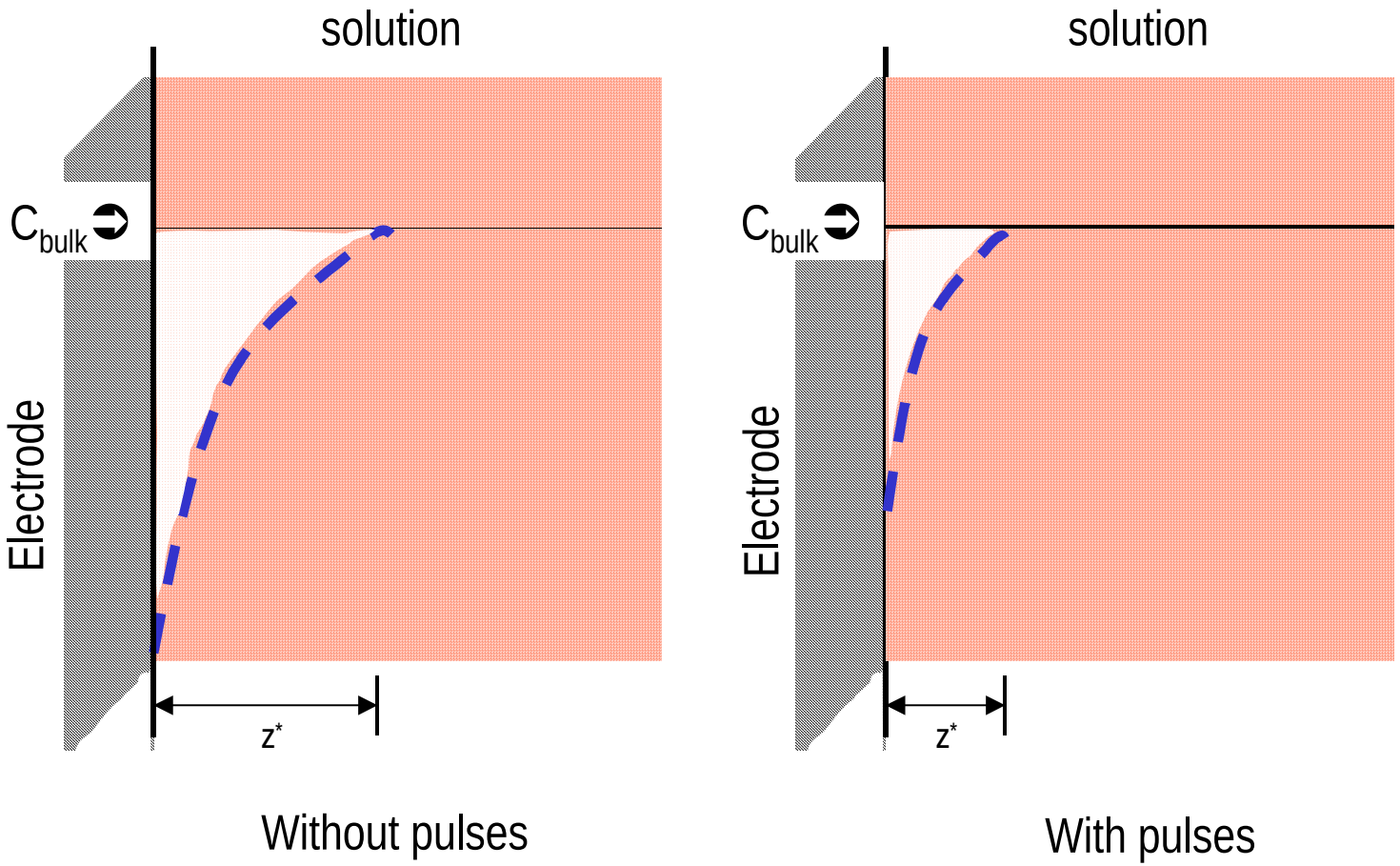
solution
C_{bulk}
Electrode
z^*
Without pulses
solution
C_{bulk}
Electrode
z^*
With pulses

Figure 72

established that pulses change mass transport rate, slow down the crystallization rate and reduce the process of occlusion of crystals which disturb the crystallographic patterns. As a final effect, a smooth surface of the deposit is produced. The repetitive pulsation changes mass transport to the electrode and thickness of the diffusion layer (Nernst diffusion layer). Mass transport can also be affected by all movements of the electrolyte, whether from natural convection produced by changes in density, from thermal gradients, or from enforced convection by stirring or flow of electrolyte. The flow or the stirring require a supply of additional energy therefore are neither practical nor economical. It appears from these studies that by applying small energy in the form of pulses generated by the Solargizer a similar effect to that observed in the stirred electrolyte can be achieved.

In all cases of improved mass transport (convection, flow, stirring, sonication, pulsation) the thickness of the Nernst diffusion layer is decreased and the concentration gradient increased.

A current generated during electrochemical process is proportional to the mass transport:

$$i = \frac{nFD^{1/2}c}{z} \qquad (7)$$

where i – current density, n– charge, F- Faraday constant, z- thickness of diffusion layer and c – concentration of electroactive species, D- diffusion coefficient.

If needle crystals are formed at random, the crystallization overvoltage at the assumed spherical peaks will drop sharply if the crystals diameter is appreciably smaller than the diffusion layer. For an unstirred electrolyte the diffusion layer thickness is about $z<0.1$ mm. This means that needle shaped crystals will branch out specially, preferably in the direction of the needle axis. On the inside of a porous electrode under these conditions, a growth of dendrites will appear. Also, for the diffusion-controlled electrocrystallization the current density on protuberances will be greater than in the valleys of a rough surface. These processes lead to decreased conductivity (high impedance crystallographic domains slow electron transfer, and limited mass transport to and from the electroactive sites) and as a net effect the charge capacity of the battery will also decrease.

Therefore for the discharge of plates in lead-acid batteries two limiting cases are important:

1. The formation of coherent $PbSO_4$ precipitate to form insulating coating layers, decreases the uncoated active surface, and raises the specific current density and over-voltage.
2. The formation of fewer large coarse-grained $PbSO_4$ crystals that possess only a small covering effect but fall away easily.

As documented in these studies pulsation at least limits the first process and decreases/eliminates the second by limiting the formation of large $PbSO_4$ crystals.

The effect of microstirring of the diffusion layer of the electrode under pulse conditions can be similar to the microstirring effect of the diffusion layer by ultrasound. The influence of ultrasound upon mass transport of electrochemical processes is well known. Ultrasound not only increases the rate of mass transport but also decreases the diffusion layer thickness and increases limiting current. Ultrasound is also used to improve properties of the deposited materials on the electrode. Electrosonication (electrochemistry in the presence of ultrasound) is used to improve electroplating processes, to improve morphology and adhesion of deposited films and also to increase

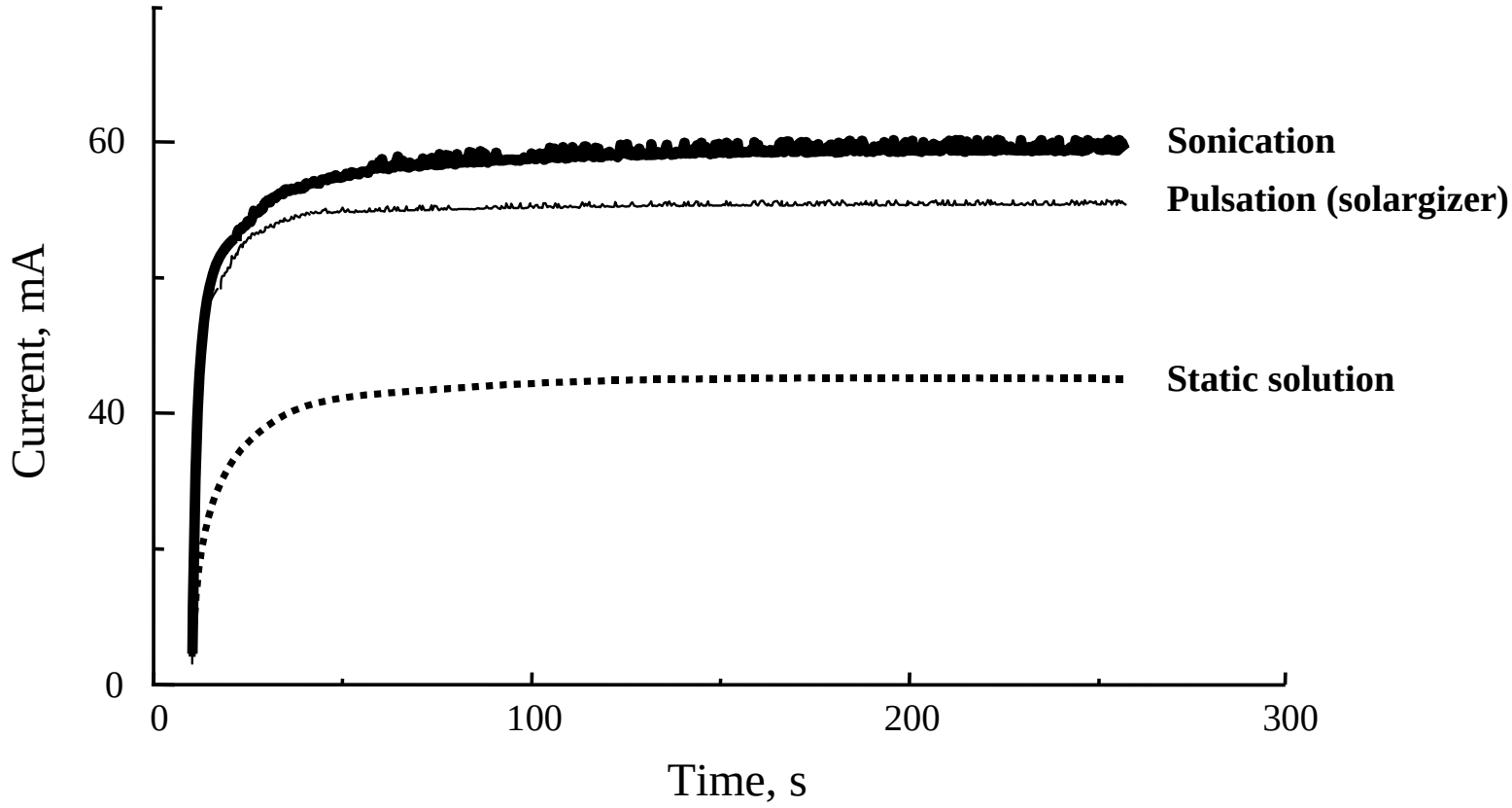
60
40
0
Current, mA
0
100
200
300
Time, s
Sonication
Pulsation (solargizer)
Static solution

Figure 73

brightness of deposited materials. Our studies have shown that the pulsation generated by the Solargizer as well as the electrosonication treatment of the PbO_2 electrode, leads to the increase of current (Figure 73). As can be seen from this figure the increase of current due to the ultrasound treatment or due to the pulse treatment with the Solargizer is very similar. Therefore, it is safe to assume that ultrasound treatment or pulse treatment decreases the diffusion layer thickness and increases current. The change of diffusion layer thickness and microstirring of this diffusion layer lead to significant changes of the mass transport. An improvement of mass transport is followed by desirable changes of the morphological structure of deposited crystals on the electrode surface. The process of pulsation contributes significantly to deposition of fine crystals of PbO_2, and limits occlusion of impurities and deformation of crystallographic structure.

Data presented here also indicates that pulsation generated by the Solargizer is very efficient in preventing self-discharge of lead-acid batteries. Both electrodes in a lead-acid battery are soluble in sulfuric acid. Therefore, regardless of the self-discharge mechanism, a decrease in sulfuric acid density takes place. The instability of the active masses of both electrodes are most important during self-discharge. The decomposition of the active mass occurs with gas evolution and formation of lead sulfate on both electrodes. Data presented here clearly indicate that pulsation generated by the Solargizer abolishes the process of self-discharge for batteries tested up to $3^1/_2$ months at temperature 25°C. Therefore, pulsation appears to be useful in the charge maintenance of lead-acid batteries. To compensate for capacity loss the

batteries are usually placed on maintenance charge. A constant current of 0.04 to 0.1 A/100 Ah is used which corresponds to a self-discharge coefficient of 0.4 – 1 x 10^{-3}/hr. The small current generated by the Solargizer can partially contribute to the maintenance charge. However, significant change in morphology and crystallographic structure strongly indicate that the pulsation contribution to charge maintenance is much more than just a simple supply of additional charge. It appears that pulsation not only preserves the battery charge but also conditions the positive electrode

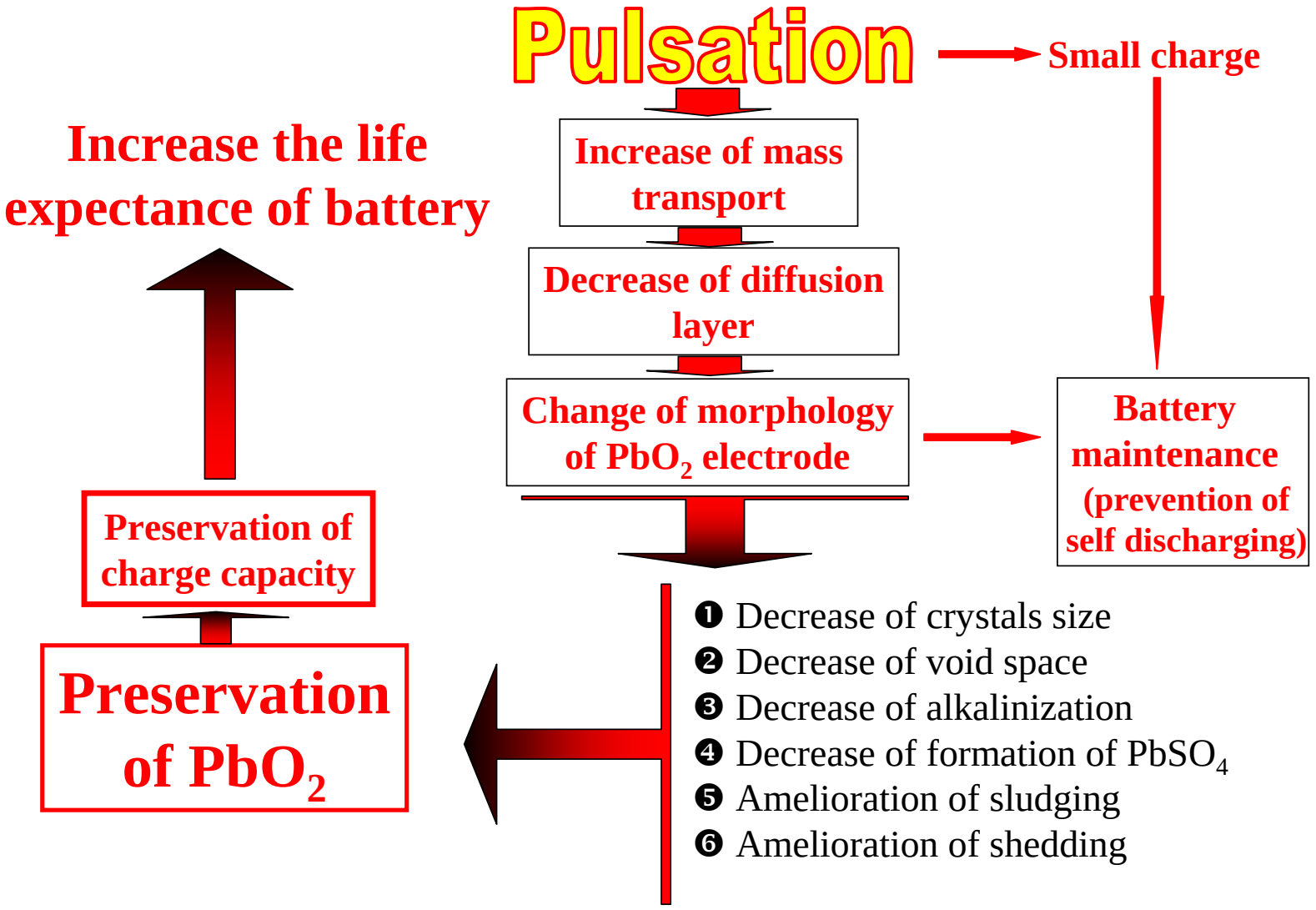
Pulsation
Small charge
Increase the life expectance of battery
Increase of mass transport
Decrease of diffusion layer
Change of morphology of PbO_2 electrode
Battery maintenance (prevention of self discharging)
Preservation of charge capacity
Preservation of PbO_2
❶ Decrease of crystals size
❷ Decrease of void space
❸ Decrease of alkalinization
❹ Decrease of formation of $PbSO_4$
❺ Amelioration of sludging
❻ Amelioration of shedding

Figure 74

CONCLUSIONS

The objective of these studies has been to evaluate the effect(s) of pulsation generated by the Solargizer on the charge/discharge process and cycle-life performance of lead-acid batteries. The major findings of these studies can be summarized as follows:

1. Pulsation extends the operating life (charge/deep discharge) of lead-acid batteries.
2. The rate of charge capacity loss with number of cycles is significantly slower for batteries charged/discharged with pulses.
3. Beneficial effect of pulsation on lead-acid battery is mostly due to the preservation of the active mass (PbO_2) of the positive electrode during charging/discharging processes.
4. Pulsation changes mass transport to electrodes, thickness of the diffusion layer and micromorphology of electrodes by slowing down the crystallization process. This in turn prevents sludging and shedding.
5. Pulsation minimizes the development of nonactive/nonconductive crystallographic domains of $PbSO_4$ and preserves (PbO_2) in the positive electrodes.
6. Pulsation contributes to charge maintenance and abolishes or decreases the process of self-discharge of batteries (tested up to $3^1/_2$ months)

Figure Captions

Figure 1. Concentration changes and chemical reactions during the charge/discharge of the electrodes of a lead-acid storage battery.

Figure 2. Electrochemical set-up for galvanostatic, coulometric and amperometric measurements of lead oxide (PbO_2) electrode.

Figure 3. Typical pulse produced by the Solargizer. The amplitude of potential is 130-150 mV and frequency 10-15 kHz.

Figure 4. A typical charge/discharge galvanostatic curve for the PbO_2 electrode (first cycle).

Figure 5. Continuous charge/discharge galvanostatic cycles (i = 150 mA/cm^2) for the PbO_2 electrode (no pulsation was applied during cycles).

Figure 6. Typical galvanostatic curve (i = 150 mA/cm^2) showing a) 25^{th} and b) 50^{th} charge/discharge cycle recorded during continuous charge/discharge process of the PbO_2 electrode (no pulses were applied during the charging/discharging process).

Figure 7. Typical galvanostatic curve (i = 150 mA/cm^2) showing 25^{th} charge/discharge cycle of the PbO_2 electrode (pulses were applied during the charge/discharge process).

Figure 8. Typical galvanostatic curve (i = 150 mA/cm^2) showing 50th charge/discharge cycle recorded during continuous charge/discharge process of the PbO_2 electrode (pulses were applied during cycles).

Figure 9. Continuous charge/discharge galvanostatic (i = 150 mA/cm^2) cycles for the PbO_2 electrode (pulsation was applied during cycles).

Figure 10. The decrease of charge capacity of the PbO_2 electrode during continuous charge/discharge cycles with (●) and without (○) applied pulses.

Figure 11. Photographic images of the PbO_2 electrodes after continuous charge/discharge cycling (i = 150 mA/cm^2) with and without pulses.

Figure 12. Micromorphology of the PbO_2 electrodes after continuous charge/discharge cycling (i = 150 mA/cm^2) with and without pulses.

Figure 13. UV-visible specular reflectance image of the surface of the PbO_2 electrode after continuous charge/discharge cycles (35 cycles, i = 150 mA/cm^2) without pulses.

Figure 14. UV-visible specular reflectance image of the surface of the PbO_2 electrode after continuous charge/discharge cycles (35 cycles, i = 150 mA/cm^2) with pulses.

Figure 15. X-ray spectrum (range 0-85°) of the PbO_2 electrode after 50 cycles of charge/discharge (150 mA/cm^2) without pulses (numbers above the peaks indicate the lattice plane distance in A°)

Figure 16. High resolution x-ray spectrum a) range 15-45° and b) range 45-80° of the PbO_2 electrode after 50 cycles of charge/discharge cycles (150 mA/cm^2) without pulses (PbO_2 platternite or $PbSO_4$ anglesite peaks are indicated)

Figure 17. X-ray spectrum (range 0-85°) of the PbO_2 electrode after 50 cycles of charge/discharge (150 mA/cm^2) with pulses.

Figure 18. High-resolution x-ray spectrum a) range 15-45° and b) 15-80° of charged PbO_2 electrode after 50 cycles of charge/discharge (150 mA/cm^2) with pulses.

Figure 19. The change of intensity of selected x-ray peaks ($PbSO_4$ peaks) of charged PbO_2 electrode after 50 charge/discharge cycles (150 mA/cm^2) with and without pulses.

Figure 20. The change of intensity of x-ray peaks (PbO_2 peaks) of charged PbO_2 electrode after 50 charge/discharge cycles (150 mA/cm^2) with and without pulses.

Figure 21. An average change of selected x-ray diffraction peaks of PbO_2 crystals and $PbSO_4$ crystals in the PbO_2 electrode as a function of the number of charge/discharge cycles without pulses.

Figure 22. An average change of selected x-ray diffraction peaks of PbO_2 crystals and $PbSO_4$ crystals in the PbO_2 electrode as a function of the number of charge/discharge cycles with pulses.